Assurance, Provision, Management and Enhancement of QoS in 5G Communication Networks

by

Basim Khalaf Jarullah Al-Shammari

Supervisor: ***Professor Hamed Al-Raweshidy***

Department of Electronic and Computer Engineering
College of Engineering, Design and Physical Sciences
Brunel University London
United Kingdom

This thesis is submitted for the degree of
Doctor of Philosophy (PhD) in Communication Engineering

October 2018

Abstract

Enhancement of QoS in PS network as 5G communication network is non trivial endeavour which faces a host of new challenges beyond 3G and 4G communication networks. The number of nodes, the homogeneity of the access technologies, the conflicting network management objectives, resource usage minimization, and the division between limited physical resources and elastic virtual resources is driving a complete change in the vision and methodologies for efficient management of the available network resources. QoS is the measure of the reliability and performance of the networks' nodes and links, particularly as perceived by the end users of the services and application that are transported via PS network. Furthermore, QoS is a composite metric as it based on a number of multiple factors, which indicate the E2E characteristics and performance of the network condition, applications and services. Hence, reductions or improvements in the QoS level can brought about through a number of combined factors. This thesis tries to introduce a vision of Quality of Service (QoS) enhancement and management based on the 5^{th} generation network requirements and solutions by:

Firstly: Proposing a traffic flow management policy, which allocates and organises Machine Type Communication (MTC) traffic flow's network resources sharing within Evolved Packet System (EPS), with an access element as a Wireless Sensor Network (WSN) gateway for providing an overlaying access channel between the Machine Type Devices (MTDs) and EPS. This proposal addresses the effect and interaction in the heterogeneity of applications, services and terminal devices and the related QoS issues among them. The introduced work in this proposal overcomes the problems of network resource starvation by preventing deterioration of network performance. The scheme is validated through simulation, which indicates the proposed traffic flow management policy outperforms the current traffic management policy. Specifically, simulation results show that the proposed model achieves an enhancement in QoS performance for the MTC traffic flows, including a decrease of 99.45% in Packet Loss Rate (PLR), a decrease of 99.89% in packet End to End (E2E) delay, a decrease of 99.21% in Packet Delay Variation (PDV). Furthermore, it retains the perceived Quality of Experience (QoE) of the real time application users within high satisfaction levels, such as the Voice over Long Term Evolution (VoLTE) service possessing a Mean Opinion Score

(MOS) of 4.349 and enhancing the QoS of a video conference service within the standardised values of a 3GPP body, with a decrease of 85.28% in PLR, a decrease of 85% in packet E2E delay and a decrease of 88.5% in PDV.

Secondly: Proposing an approach for allocating existing 4G installed network radio access nodes to multiple Base Band Unit (BBU) pools, which is proposed to deploy 5G Cloud-Radio Access Network (C-RAN) and improve the offered Network QoS (NQoS). The proposed approach involves performing radio access nodes clustering based on the Particle Swarm Optimization (PSO) algorithm, model selection Bayesian Information Criterion (BIC), Measure of spread technique and Voronoi tessellation. The proposed scheme is used to consider a Dynamic C-RAN (DC-RAN) operation, that adaptively adjusts the main Radio Remote Head (RRH) coverage range according to the traffic load requirement as well as considering energy saving. The numerical results of the approach show that the optimized partition of the proposed network model is 41 BBU pools, with an average density of RRHs per pool area, which matches the primary average density of the radio access nodes per network area.

Thirdly: Developing mathematical framework that investigates the Power Consumption (PC) profile for the interaction of Internet of Thing (IoT) Application QoS (AQoS) with NQoS in wireless Software Defined Network (SDN) as SDN for WIreless SEnsor network (SDN-WISE). This profile model offers flexibility for managing the structure of the Machine to Machine (M2M) system in IoT. It enables controlling the provided NQoS, precisely the achieved PHY layer transmission link throughput, combined with the AQoS, represented by IoT data stream payload size. The investigation is composed of two essential SDN traffic parts, they are control plane signalling and data plane traffic PCs and their relevance with QoS. The results show that 98% PC in data plane companion with a control plane PC of 2% in overall of the proposed system power, these figures were achieved with control plane signalling Transmission Time Interval (TTI) of 5 sec and a maximum data plane payload size of 92 Bytes as a worst case scenario.

Declaration

I hereby declare that except where specific reference is made to the work of others, the contents of this dissertation are original and have not been submitted in whole or as a part for consideration of any other degree or qualification in this, or any other university. This thesis is my own work and contains nothing which is the outcome of work done in collaboration with others, except as specified in the text and Acknowledgements. This thesis contains fewer than 65,000 words including appendices, bibliography, footnotes, tables and equations and has fewer than 150 figures.

by
Basim Khalaf Jarullah Al-Shammari
October 2018

Acknowledgements

My gratefulness and appreciation would go to the Ministry of Higher Education and Scientific Research (MOHESR), Cultural Attache and University of Wasit in Iraq for funding and supporting this study. I also would like to give my sincere thankfulness to Professor Hamed Al-Raweshidy for his useful advices, guidance, and encouragement. His unstopping belief, enthusiastic, support and beneficial discussions with him are very precious and helpful. Most appreciated thing is his understanding and patience while allowing me enough room to chose the study topics on my own. Also, I value the role of my family, for their moral support, love, inspiration and encouragement during the years of my study. Finally, deep gratefulness for my friends and colleagues who always encourage me to complete this study.

Table of contents

List of figures

List of tables

List of Acronyms

3G, 4G, 5G	3^{rd}, 4^{th}, 5^{th} **G**eneration
Adapt	**Adap**tation
AC	**A**dmission **C**ontrol
ARP	**A**llocation and **R**etention **P**riority
AQoS	**A**pplication **QoS**
BEC	**BE**a**C**on
BIC	**B**ayesian **I**nformation **C**riterion
BS	**B**ase **S**tation
BBU	**B**ase **B**and **U**nit
CN	**C**ore **N**etwork
CO	**C**entral **O**ffice
CoAP	**Co**nstrained **A**pplication **P**rotocol
Config	**Config**uration
C-RAN	**C**loud **R**adio **A**ccess **N**etwork
CRE	**C**overage **R**ange **E**xtension
CTR	**C**on**T**rolle**R**
CP	**C**ontrol **P**lane
DAT	**DAT**a
DC-RAN	**D**ynamic **C-RAN**
DL	**D**own**l**ink
DP	**D**ata **P**lane
DSCP	**D**ifferentiated **S**ervices **C**ode **P**oint
E2E	**E**nd To **E**nd
eNB	**e**volved **N**ode**B**
EPS	**E**volved **P**acket **S**ystem
E_{th}	**Eth**ernet
FTP	**F**ile **T**ransfer **P**rotocol
FWD	**F**or**W**ar**D**

GBR	**G**uaranteed **B**it **R**ate
H2H	**H**uman-to-**H**uman
HTC	**H**uman **T**ype **C**ommunication
HTD	**H**uman **T**ype **D**evice
INPP	**I**n-**N**etwork **P**acket **P**rocessing
IoT	**I**nternet **o**f **T**hings
IP	**I**nternet **P**rotocol
KPI	**K**ey **P**erformance **I**ndicator
KQIs	**K**ey **Q**uality **I**ndicator**s**
LPWAN	**L**ow **P**ower **WAN**
LTE	**L**ong **T**erm **E**volution
LTE-A	**LTE A**dvanced
LTE-APro	**LTE-A P**roximity
M2M	**M**achine to **M**achine
MAC	**M**edium **A**ccess **C**ontrol
MBR	**M**aximum **B**it **R**ate
MBSFN	**M**ultimedia **B**roadcast **S**ingle **F**requency **N**etwork
MC	Mission Critical
MCN	**M**obile **C**ellular **N**etworks
MOS	**M**ean **O**pinion **S**core
MTC	**M**achine **T**ype **C**ommunication
MTD	**M**achine **T**ype **D**evices
NAS	**N**on **A**ccess **S**tratum
NB-IoT	**N**arrow **B**and **IoT**
NFV	**N**etwork **F**unctions **V**irtualization
NGBR	**N**on- **G**uaranteed **B**it **R**ate
NGN	**N**ext **G**eneration **N**etwork
NOS	**N**etwork **O**perating **S**ystem
NQoS	**N**etwork **QoS**
PC	**P**ower **C**osumption
PCEF	**P**olicy **C**ontrol **E**nforcement **F**unction
PCC	**P**olicy **C**harging and **C**ontrol
PCRF	**P**olicy and **C**harging **R**ule **F**unction
PDB	**P**acket **D**elay **B**udget
PDCCH	**P**hysical **D**ownlink **C**ontrol **CH**annel
PDV	**P**acket **D**elay **V**ariation
PDN	**P**acket **D**ata **N**etwork
PDU	**P**acket **D**ata **U**nit

PLR	**P**acket **L**oss **R**ate
PPS	**P**ackets **P**er **S**econds
PRACH	**P**hysical **R**andom **A**ccess **C**hannel
PS	**P**acket **S**witching
PSO	**P**article **S**warm **O**ptimization
PUSCH	**P**hysical **U**plink **S**hared **CH**annel
QCI	**Q**oS **C**lass **I**dentifier
QoE	**Q**uality of **E**xperience
QoS	**Q**uality of **S**ervice
RAN	**R**adio **A**ccess **N**etwork
REP	**REP**ort
REQ	**REQ**uest
RES	**RES**ponse
RRH	**R**adio **R**emote **H**ead
RSSI	**R**eceived **S**ignal **S**trength **I**ndication
SDF	**S**ervice **D**ata **F**low
SDN	**S**oftware **D**efined **N**etwork
SDN-WISE	**SDN** for **WI**reless **SE**nsor
SDU	**S**ervice **D**ata **U**nit
SN	**S**ensor **N**ode
SNK	**SiNK**
Stdv	**St**andard **de**viation
TD	**T**opology **D**iscovery
TFT	**T**raffic **F**low **T**emplate
TM	**T**opology **M**anager
TTI	**T**ransmission **T**ime **I**nterval
UE	**U**ser **E**quipment
UL	**Up**link
VD	**V**oronoi **D**iagram
VoLTE	**V**oice over **LTE**
WAN	**W**ide **A**rea **N**etwork
WSN	**W**ireless **S**ensor **N**etwork

Chapter 1

Introduction

QoS has attracted a lot of attention by both academia and industry since it was proposed to represent the achieved network levels of Key Performance Indicators (KPIs) as well as the minimum required applications' levels of different Key Quality Indicators (KQIs) in PS network.
The vision of QoS in Next Generation Network (NGN) as 5G wireless communication network lies in providing very high PHY layer throughput as link data rates (typically of Gbps order) with an extremely low latency as MAC layer Packet Data Unit (PDU) delay. NGN with a manifold increase in radio access node capacity and a significant improvement in users' perceived QoS, compared to current and previous generations [1].
Today with ever increasing proliferation of Human Type Communication (HTC), Machine Type Communication (MTC) and introduction of new emerging IoT applications and services, together with an exponential rise in wireless data (multimedia) demand and usage are already creating a significant burden on available network ecosystem. NGNs and systems, with improved performance such as data rates, capacity, latency and enhanced QoS are expected to be the panacea of most networks' problems [2].

Enhancement of QoS in Packet Switching (PS) network as 5G communication network is non trivial endeavour which faces a host of new challenges beyond 3G and 4G communication networks. The number of nodes, the homogeneity of the access technologies, the conflicting network management objectives, resource usage minimization, and the division between limited physical resources and elastic virtual resources is driving a complete change in the vision and methodologies for efficient management of the available network resources. QoS is the measure of the reliability and performance of the networks' nodes and links, particularly as perceived by the end users of the services and application that are transported via PS network. Furthermore, QoS is a composite metric as it based on a number of multiple

factors, which indicate the E2E characteristics and performance of the network condition, applications and services. Hence, reductions or improvements in the QoS level can brought about through a number of combined factors.

This thesis is focused on introducing a mechanisms for improving QoS in the NGN. Specifically, It conceives and analyses newly emerging applications, services and network architectures as well as considers energy efficiency. Let's commence by outlining the motivation of this research efforts, the problems to be solved as well as the contributions made by the thesis.

1.1 Motivation

Nowadays wireless communication has been perceived in every part of our daily lives. Future networks will gradually be converted into integrated entities with high broadband and large-scale traffic due to the interconnection of social medias, virtual systems, and physical networks [3]. As a result, the world has witnessed a tremendous increase in global mobile traffic and subscribers.

Mobile cellular networks are evolving rapidly in order to meet these massive demands that imposed for communication network and the required KQIs. Thus, this will produce in an interaction between AQoS and NQoS [4]. This interaction could result in a serious issues if it's not controlled in such a way. The steering of the control has to be aimed to overcome the problems of network resource starvation and enhance NQoS in order to meet the required AQoS and terms of E2E transmission link throughput, latency and IP layer PDU (delay, loss & jitter) [5, 6]. Further more, the aforementioned enhancement in QoS introduces a new functions and architectures in the future networks' infrastructures. Therefore, the consideration of energy efficient goal is one of the important feature of environmental awareness and economic awareness [7].

Based on the facts as mentioned above, the primary motivation for this PhD work is to assure and to provision the requirement/demand represented by the KQI of current and future applications and services, as an AQoS, by exploiting:

(a) Traffic differentiation feature at the application layers levels.

(b) Traffic policy.

(c) Network deployment architecture.

(d) Applications, services and network protocols' layers and traffic streams.

(e) Interaction among different PS network applications, protocols and elements.

to achieve an enhancement in NQoS with higher levels of network KPIs and investigate the cost from PC point of view.

1.2 Research challenges

Support, assurance and provision the QoS are a challenging research areas. The communication network transports, as examples, the traffic of real-time application, high-quality services and delay-sensitive data. In turn network must provide predictable, measurable, guaranteed QoS and supports QoE, by controlling bandwidth, delay, jitter and loss parameters on the network elements. This controlling process of these network resources will pose a cost from energy efficiency point of view. Therefore this energy figure has to be considered carefully [7]. The supportive tools and elements can be employed to provide an optimal way to exploit the available network resources and provide saving in energy as well. Some of the challenges addressed by this thesis are highlighted in the following facts:

(a) Proactive topics as follows:

(i) Application QoS (AQoS).
Deals with AQoS design of various application-class QoS requirements. First of all marking and classification of application traffic is the key element of exploiting the network resources usage in optimal manner. Fig. 1.1 demonstrates an example of 5 classes AQoS model; it can be extended to meet the current applications and the future ones. The classification including the following AQoS:

(A) Types of traffic, such as Guaranteed Bit Rate (GBR) & Non-GBR (NGBR).

(B) Level of priority, such as Universal Datagram Protocol (UDP) & Transport control Protocol (TCP).

(C) Level of importance, such as Real time, Delay sensitive application & Non Real time.

(D) QoS Models, such as Integrated Service (IntServ) or Differentiated Service (DiffServ).

Fig. 1.1 Five class AQoS model

(ii) Network QoS (NQoS).
Deals with E2E NQoS in three parts of the network, which are source, transportation part and destination. Via a set of local and global polices of NQoS rules and functions. They are:

(A) Optimised network deployment.

(B) Scheduling.

(C) Queuing management.

(D) Dropping policies.

(E) Traffic shaping.

(F) IPv4 & IPv6.

Fig. 1.2 shows an example of IP Queuing management over the network nodes [8].

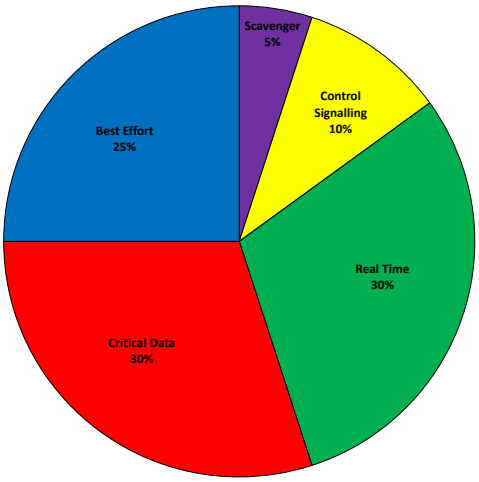

Fig. 1.2 Example of IP Queuing management

(b) Reactive and active topics. QoS and QoE management, which deals with global vision of the overall QoS of application and network in an end to end framework. This provides a method or way to overcome any issue regarding AQoS and NQoS. Its main parts are:

(i) Monitoring AQoS and NQoS (using probes in specific points over the network nodes).

(ii) Analyse data of NQoS (using a specific application set on a server).

(iii) Introduce action based on specific rules set by network operator or introduced by a specific policier engine.

(iv) Feedback and set action on network elements, which is driven by main network central controller, such as Core Network (CN).

1.3 Aim and objectives

The main aim of this study is to address the effect of the heterogeneity of future applications traffic and related QoS performance of present applications when the network ecosystem resources have to be shared in such a way. The following objectives address the research aim;

(a) Formulating an E2E QoS model as an AQoS and NQoS matching problem as well as representing it as a level of network E2E performance metric. This includes the following sub-objectives:

(i) Proposing an access WSN gateway to provide access and connectivity for MTD traffic within an LTE-A Proximity (LTE-APro) eNB license spectrum radio interface.

(ii) Proposing a traffic flow management policy to define the existence of IoT traffic with Human to Human (H2H) traffic over an EPS network and provide an acceptable level of NQoS for MTC traffic flows, whilst preserving a good QoE of HTCs.

(iii) Introducing specific QoS Class Identifiers (QCIs), which are elected to classify the MTC traffic flows, whilst taking into account the heterogeneity of IoT services and applications, over an EPS network, in order to discriminate the treatment of EPS from the NQoS point of view from the standard QCIs of HTC traffic flows.

(b) Applying optimisation algorithms at C-RAN deployment process in order to achieve an optimum value for NQoS by:

(i) Introducing an approach for solving the multiple BBU pools planning problem over DC-RAN architecture.

(ii) Ensuring that the C-RAN planning achieves high NQoS by optimizing the placement and the number of BBU pools as well as the number of RHHs in each BBU pool across the whole network.

(c) Investigating and modelling the impact of the integration of IoT applications and services with wireless SDN architecture, among control plane signalling streams and data plane traffic streams according to the Power Consumption (PC) point of view that related to the required AQoS and offered NQoS.

(i) Decomposing SDN PC components as a data plane traffic PC and control plane signalling PC with their triggered collaboration effort in order to tackle their interaction complexity in a simplified manner.

(ii) Profiling of the SDN PC in order to assess how it will be the efficient use of the network resources, when the WSN united with SDN, from different point of views as:

(A) Data plane traffic point of view.

(B) Control plane signalling point of view.

This allow the network administrators and end users to consider the PC effectiveness in both planes.

(iii) Estimating the effect of interaction among the control plane signalling header regarding TTI with data plane traffic regarding IoT applications such as data PDU size and the achieved transmission link throughput, which has adopted related to PHY layer and transmission media conditions, in order to meet IoT AQoS requirements.

These are essential and required to evaluate the overall cost and figure out any extra demand caused by extra control signalling that are required to achieve .

1.4 Thesis scope

This thesis consolidates different research areas and has a multidisciplinary nature; it includes a blend of concepts for QoS, QoE, traffic policies, protocols designs, network deployment design optimisation, central management, mathematical modelling and networking among others.

(a) Regarding E2E QoS as a composite metrics, redefine QoS requirements and needs among current applications, services and networks as well as future ones as

(i) KQI to define AQoS needs.

(ii) KPI to define NQoS offered levels.

(b) Regarding QoE as a subjective matter, promoting AQoS and NQoS concept to satisfy applications and services needs, instead of utilising human user sanctification.

(c) Regarding traffic policies and central management, organising the network resources shares among real time and non real time application and services as well as HTC and MTC traffic flows.

(d) Regarding network deployment optimisation, a C-RAN is considered, solving the multiple BBU pools planning problem architectures and providing a methodological framework for converting a single network to a multiple BBU pools, in order to simplify network management and enhance the NQoS.

(e) Regarding mathematical modelling, investigating a wireless SDN and modelling of the interaction among KQI, KPI and consumed energy in the network.

1.5 Thesis outline and contributions

This thesis is organised into five chapters. Every chapter begins with a concise introduction highlighting the contributions made in the chapter. Towards the end of every chapter, a brief conclusion is presented.

Chapter 2: Presents an introduction and a brief overview of the essential background materials relevant to the works presented in this thesis.

Chapter 3: In this chapter, the work addressed the challenges of integrating HTC and IoT traffic flow management in the QoS supported network. It is proposed an access WSN gateway to provide E2E connectivity for MTCs traffic flow. The effect and interaction in the heterogeneity of applications, services and terminal devices and the related QoS issues were addressed. Furthermore, the work in chapter 3 is supported by introducing a simulation study, using Riverbed software [9] to verify the performance of the proposed scheme.

Chapter 4: This chapter provides a proposal of a new approach for solving the multiple BBU pools planning problem over DC-RAN architectures. In particular, it provides a methodological framework for converting a single network to a multiple BBU pools, in order to simplify network management and enhance the NQoS. Basically, the novelty of this chapter is about combining different very well-known approaches, like PSO algorithm, BIC, measure of spread technique and Voronoi tessellation, to obtain the optimal number of BBU pools, the coordinates of the optimal position of each BBU pool and the optimal number of connected RRH in each BBU pool area.

Chapter 5: The work in this chapter proposes a mathematical framework to investigate the interaction among the AQoS, NQoS and PC of IoT application and SDN. This framework is based on the SDN in WSNs. It presents the PC models for the Sensor Nodes (SNs), SiNK (SNK) node and SDN controller. The performed evaluations have been done on both control plane and data plane.

1.6 Publications

1.6.1 Published

- **B. K. J. Al-Shammari**, N. Al-Aboody, and H. S. Al-Raweshidy, "Iot traffic management and integration in the qos supported network," *IEEE Internet of Things Journal*, vol. 5, no. 1, pp. 352–370, Feb 2018.
  This journal article is related to the work presented in **Chapter 3**.

1.6.2 Submitted

- **B. K. J. Al-Shammari**, W. H. Al-Zubaedi, and H. S. Al-Raweshidy, "Heterogeneous dynamic C-RAN deployment based on a multiple BBU pools approach for 5G network," *IEEE Transactions on Network and Service Management*, vol. X, no. X, pp. XXX–XXX, Month X Year X.
  This journal article is related to the work presented in **Chapter 4**.

- **B. K. J. Al-Shammari**, W. Twayej, and H. S. Al-Raweshidy "Profiling Power Model for SDN-WISE Based on IoT Application QoS," *IEEE Internet of Things Journal*, vol. X, no. X, pp. XXX–XXX, Month X Year X.
  This journal article is related to the work presented in **Chapter 5**

Chapter 2

Background and Fundamentals

2.1 Introduction

QoS in PS system means different things to different people from different points of view as well. QoS can be defined from the end-user perspective as a good network service quality for the end users. More specifically, it can say that the network has QoS or provides QoS when the network is able to meet the need of the end users' applications in a satisfactory way. With this definition, QoS has a broad scope. Anything that can affect end user's perception on network service quality, for example, reliability, security, routing policy, traffic engineering, all fall into the scope of QoS.
This chapter is going to illustrate the QoS concept in the context of this thesis by introducing the composite factors that determine the end users' QoS perception. Furthermore, it explains the QoS requirements of applications and services among different part of PS communication network as in the following topics.

The ***first*** topic in Section 2.1.1 provides an introduction of the aspect of AQoS and NQoS. What's more, Section 2.2.1 provides a background of the work introduced in Chapter 3.

The ***second*** topic in Section 2.1.2 introduces an introduction of an approach that tries to overcome the limitations in network resource during the deployment phase in order to improve the offered NQoS. The RAN planning prior to the network deployment phase is an important concept in terms of designing optimized KPIs networks in order to meet customers' QoE satisfaction levels and AQoS requirements by providing high NQoS. Additionally Section 2.2.2 highlights the background materials used in Chapter 4.

The ***third*** topic established in Section 2.1.3 is an introduction about the mathematical framework that investigates the Power Consumption resulting from the interaction of AQoS with NQoS. Whereas, Section 2.2.3 provides the an overview and background about about

afromentioned model and the materials used in Chapter 5.
After all, QoS itself is not the goal. The goal is to make sure that the end users' applications work satisfactorily. Therefore, the service providers (and or) network operators need to know the factors that determine the end users' QoS perception, and the applications' requirements regarding the composite QoS metrics and their driven factors.

Section 2.3 presents the state of the art related to the work and contributions presented in this thesis from some highlighted points of view as seen within the time of doing this work.

2.1.1 AQoS into QoS supported network

The key issue in providing Applications and Services over the wireless network is the QoS support in the presence of changing wireless link connectivity due to the variable link characteristics and its limited resources. Furthermore, the available wireless link resources will be shared, noisy [10].

2.1.1.1 M2M communication

MTC or M2M communication introduces the concept of enabling networked devices (wireless and/or wired), electronic devices, dubbed MTC devices and/or communication from MTC devices to a central MTC server or a set of MTC servers, for exchanging data or control without human interference. This includes the mechanisms, algorithms and the technologies used to enable MTC communication. Which involves connecting large number of devices or piece of software with the creation of the IoT. MTC developments are driven by the unlimited potential of IoT everyday applications, as a result from the connected objects to grow more intelligent. These applications presented in the form of smart grids, healthcare systems, smart cities, building automation, and many other. Such systems can be implemented through the use of WSN, within which the utilisation of cooperating devices can achieve intelligent monitoring and management.

2.1.1.2 IoT ecosystem

IoT presents a massive ecosystem of new elements, applications, functions and services. Existing transmits of MTC traffic flows for IoT devices run over wireless Wide Area Network (WAN), 3G and 4G networks. However, 5G is expected to become the main platform for meeting the requirements of IoT traffic demand in the very near future. EPS protocols and architectures were aimed and enhanced to handle HTC traffic flows. With the anticipated mass deployment of MTDs, there are concerns from the network operator's side, the service

provider side and from the application consumer's perspective. The fear is that the network ecosystem may become exhausted and/or the available network resources will not be able to meet AQoS traffic flow requirements for both HTC and MTC traffic flows simultaneously. Moreover, MTC traffic characteristics of IoT devices are different from those of HTC and can augment the risk of network performance deterioration.

2.1.1.3 Future of cellular wireless networks

Future networks will gradually be converted into integrated entities with high broadband and large-scale traffic due to the interconnection of social medias, virtual systems and physical networks [3]. It is estimated that between 50 to 100 billion MTC devices will be connected to the internet by 2020 [11] [12] and that the majority of these devices will be run through cellular wireless networks and WSNs. However, cellular networks were mainly designed for H2H communication, where the UpLink (UL) resource allocation is less than the DownLink (DL). In contrast, the M2M traffic could produce more data in the UL channels, which can lead to a deterioration of the human QoE or could overload the network. To overcome this challenge, an efficient resource allocation model can be used to take full advantage of the opportunities created by a global MTC market over cellular networks. The 3GPP and the Institute of Electrical and Electronics Engineering (IEEE) standardisation bodies have initiated their working groups for facilitating such applications through various releases of their standards [13]. LTE-A is very close to reach the technologically possible efficiency limits in the currently available bands, according to 3GPP, hence, it is expected that LTE will remain as the baseline technology for wide area broadband coverage also in the 5G era. However, integrating M2M communication with LTE-A can have a dramatic negative impact on LTE network performance in terms of QoS and throughput [14]. Consequently, 3GPP will continue working on enhancing LTE to make it more suitable for M2M communication from a radio perspective as well as from a service delivery one and hence, mobile M2M traffic must not be neglected.

2.1.2 RAN deployment planning and QoS

RAN planning prior to the network deployment phase is an important concept in terms of designing optimized KPIs cellular networks in order to meet customers' QoE satisfaction levels and AQoS requirements by providing high NQoS [4] [15]. Such planning includes the deployment of radio access nodes by optimizing their KPI configurations and their site locations allocation with respect to the users' traffic demands[16].

2.1.2.1 NGN and C-RAN deployment

The Fifth Generation (5G) of cellular network requires new architectures and concepts in order to increase its deployment flexibility, to improve the offered performance, and to reduce its cost [17]. The innovation of C-RAN architecture is one of the candidates for NGN deployment as the 5G, which provides simplified network management architecture for mobile RAN [18].

2.1.2.2 Issues of C-RAN deployment

Issues associated with this innovation include BBU pool position allocation, with respect to its RRHs and the maximum number of BBU pools in a specified network area with the number of RRHs connected to their driver BBU pool. C-RAN can be defined as the traditional eNB separated into three main elements, which are BBU, RRH and fronthaul link, with the required interfaces among them [19]. BBUs are located at the Central Office (CO), which is called the BBU pool as well [20]. Each RRH is located at its cell site coordinates, which represents a single radio access node as part of the RAN to provide wireless connectivity to the Users' Equipment (UEs). The BBUs consist of parts of the digital signal processing units of the preceding eNB's PHY layer, with a specific interface to provide connectivity with the RRH, along with all the functions and protocols of all the other layers and interfaces among other BBUs and with the CN. Whilst the RRH contains the remaining parts of the preceding eNB's PHY layer, to provide a radio interface to all UEs. In addition, the RRH has another interface with a fronthaul link to provide connectivity with its associated BBU [21]. This connectivity can be provided by one of the following interfaces [22] [23] [24]

(a) Open Radio Interface (ORI).

(b) Open Base Station Architecture Initiative (OBSAI).

(c) Common Public Radio Interface (CPRI).

2.1.2.3 C-RAN deployment and NQoS

The C-RAN architecture requires precise BBU pool placement and number in each particular C-RAN to ensure a high NQoS. BBU pool positions in the network need to be set in the optimal locations with respect to its related RRHs. Hence, the fronthaul link propagation delay and BBU processing have to be considered carefully. That is, the network operator cannot allocate BBU pools in an arbitrary fashion. Currently, the adopted approach is by

considering any random group of radio access nodes' locations and choosing one as a feasible position to allocate their BBU pool, as proposed by Zainab et al.[25], based on radio access nodes' traffic capacity limits. In sum, multiple pool configuration allocation is essential for achieving effective network resource management.

2.1.2.4 Multi BBU pools and RRHs clustering

In chapter 4, an approach for solving the multiple BBU pools planning problem over DC-RAN architecture using optimization processes is proposed. The aim is that the C-RAN planning achieves high NQoS by optimizing the placement and the number of BBU pools as well as the number of RHHs in each BBU pool across the whole network. The clustering concept has been used to determine the best pre-configuration of pools in the architecture. Actual LTE network deployment has been used to represent and model the problem. The clustering has been applied using the PSO algorithm to group the RRHs (i.e. pooling the RRHs) of the network as well as to determine the BBU pool position for each pool. The BIC has been successfully applied to the problem of determining the optimized number of BBU pools in the network by ascertaining its minimum value [26]. The measure of spread of the radio access nodes presented by Range, Variance and standard deviation (Stdv) have been used to verify and support the BIC criterion in the optimized pooling concept. This can determine the differences between the maximum and minimum number of RRHs among all BBU pools in the network area. Furthermore, Voronoi tessellation of the main RRHs as the requisite of the DC-RAN concept for the proposed deployment has been utilised to simplify the network management and can be used to improve energy saving. That is, it switches off a number of RRHs at low traffic load demand and serves the UEs by the main RRH.

2.1.3 Relation among IoT AQoS, SDN NQoS and PC

Over recent years, telecommunication and data communication are collaborating with each other define the Internet of Things (IoT). As the development of the Internet continues in large strides, it is forecasted that ultimately billions of Appliances will be linked using this technology. Countless applications, such as the employment of IoT for environmental condition monitoring, will rise in popularity. Due to the quick high-tech expansion of sensors, WSNs will become a crucial technology in the IoT industry [27] [28].

2.1.3.1 SDN in WSNs

Recently, SDN solutions for WIreless SEnsor networks such as SDN-WISE have merged to allow the complexity of massive networks to be reduced [29]. This makes SDN-WISE a suitable approach for a huge number of applications as a solution for the abovementioned complication issue [30, 31]. However, little is known about the PC of SDN-WISE. Specifically, the integration of control plane signalling as an SDN header with data plane traffic.

Modelling the usage and integration of the SDN with WSNs has been studied in different research studies. These studies have considered various categories of WSNs and their essential differences in comparison with the SDN in wired network. The integration enables ease usage of real time network resources monitoring with reconfigurable adaptive routing path. All these fashioned the network elements communications in a more stable and more efficient manner, which are done by providing a centralised controller [32, 33]. Thus, it will provide a dynamic support to maintain the offered NQoS in high level, which is definitely will improve the energy efficiency in the whole network.

The requirements for utilizing the SDN architecture in WSNs have already been analysed in [34]. Since, the WSN characterized as a low capability in terms of energy, processing and memory, compared by wired network point of view. Hence, SDN-WISE supports an efficient use of network resources, specifically of the SNs as network elements.

The main efforts of chapter 5 is investigating and modelling the impact of the integration between WSNs and SDN, among control plane signalling streams and data plane traffic streams. According to the PC point of view related to the offered NQoS such as achieved or offered physical layer throughput, as well as AQoS such as IoT application data stream payload packet size. This could be done by profiling a PC model for wireless SDN platform as an essential requirement to evaluate the overall cost and figure out any extra demand caused by control signalling.

2.1.3.2 Interaction of SDN elements and IoT application

Having a clear view of these contributed factors when modelling a PC is an essential part of the IoT system architecture. The proposed PM provides a clear perspective about additional control signalling that support SDN in WSNs as in SDN-WISE scheme, and the effects of this in the proposed system model.

This shapes the objectives of the work introduced in chapter 5 as follows:

(a) Decomposing SDN PC components as a data plane traffic PC and control plane signalling PC with their triggered collaboration effort in order to tackle their interaction complexity in a simplified manner.

(b) Profiling of the SDN PC in order to assess how it will be the efficient use of the network resources, when the WSN united with SDN, from different point of views.

(i) Data plane traffic point of view.

(ii) Control plane signalling point of view.

It will allow the network administrators and end users to consider the PC effectiveness in both planes. Furthermore, the proposed model can provide one of the important building blocks to introduce an optimised QoS combined with energy-saving approach in IoT applications based SDN.

(c) Provides estimate of the interaction among the control plane signalling header regarding TTI with data plane traffic regarding IoT applications such as data payload packet size and the achieved link throughput, which has adopted related to physical layer and transmission media conditions, in order to meet IoT AQoS requirements.

The work presented in Chapter 5 is supported through a case study of SDN-WISE infrastructure, that has been introduced by [29], for evaluating the impact of enhancing the NQoS in profiling a generic PC model. The investigation takes into consideration PC, performance and the effects of extra control signalling on the total energy consumption for the whole system.

2.2 Background

2.2.1 IoT AQoS and NQoS

2.2.1.1 MTC traffic characteristics:

MTC terminals or SNs can communicate with one or many servers and their traffic characteristics have been discussed in detail in [35]. They can be considered as data centric communication for sending constant size packets toward server [36] [29]. Their traffic main characteristics are as follows:

(a) Service Data Flow (SDF) of MTC traffic is typically from the SN towards Packet Data Network (PDN), which will be more dominant in the UL direction. Whereas HTC's SDF traffic depends on the service type and its AQoS demands during the call session or service request.

(b) In much of MTC applications traffic, the SN harvests a small amount of information. This can be transferred at a specific data rate, which matches the application's needs.

(c) In the NGN, the MTC traffic has a share of the network resources and they will be not limited just for HTC. The MTC are going to join the use of licensed spectrum and take a share of the mobile broadband network access resources.

(d) In general, MTC traffic is delay tolerant and for the most part, it can be considered as having low priority. 3GPP in release 10 introduces Delay Tolerant Access in the Random Access Procedure (RAP) as part of Control Plane Signalling to provide a lower priority in the Physical Random Access Channel (PRACH) for MTC traffic than HTC traffic [37]. However, some MTC traffic is excluded from using this procedure, such as industrial control systems, fire alarms and live monitoring, as they are need to be transmitted with high priority. LTE-A release 13 introduces new QCI to provide a high priority SDF for emergency service application use cases [38] [39].

(e) SN data transmission is irregular and depends on many factors, which relate to the WSN type and deployment pattern. This irregularity in traffic generation can produce high traffic peaks, which could lead to starvation in the network resources, specifically in the wireless access part.

2.2.1.2 Future of MTC in NGN

The basic concern in MTC within the NGN is how to provide the required NQoS levels or KPIs, which will meet the AQoS of MTC traffic or KQIs, with a massive deployment of SNs, while guaranteeing high levels of expected and perceived quality or QoE of real time application users, simultaneously.
In order to integrate the IoT traffic in the LTE-A standard EPS resources need to be used. Consequently, it is necessary to provide a specific NQoS for MTCs applications traffic so as to avoid the substantial impact on the performance of HTC traffic, such as voice, video and file transfer and to keep the QoE at a satisfaction level.

2.2.1.3 Provision and assurance of QoS in EPS

Applications traffic, including that of HTC and MTC in PS networks has specific AQoS characteristics and demands. They require specific levels of NQoS parameters, which can be described in terms of:

(a) E2E IP layer PDUs as PLR [40],

$$PLR = \frac{(Traffic\ Transmitted) - (Traffic\ Received)}{(Traffic\ Transmitted)} \tag{2.1}$$

(b) Packet one-way IP layer E2E delay, time taken for the packet to reach its destination, in seconds. Measured as the difference between the time a packet arrives at its destination and the creation time of the packet. This statistic is collected separately for each source, destination pair [41, 9].

(c) Packet jitter at the end point at the IP layer [42, 43]. Packet jitter refers to the variation in the time change between two consecutive packets leaving the source node with time stamps $t1$ and $t2$; they are played back at the destination node at $t3$ and $t4$, with the jitter being calculated as [44, 9]:

$$Jitter = (t4 - t3) - (t2 - t1) \tag{2.2}$$

(d) Latency as the E2E delay of received MAC Layer PDU, which is called frame or transport block [45].

(e) PHY layer link throughput as achieved data rate between these two nodes[42, 43].

In EPS, these diverse NQoS quantitative performance parameters are provisioned via a standardised and effective mechanism, which is a class based EPS QoS concept [46]. This mechanism allows service providers to deliver service differentiation via NQoS control in the access and backhaul networks, thereby solving the issue of over-provisioning of the valuable network resources.

2.2.1.4 Management of QoS in EPS

NQoS control mechanism based service differentiation is performed on the EPS bearer level, with this bearer being a logical unidirectional connection between PDN-GW and UE as well as it being the core element of NQoS control treatment in EPS. The EPS bearer type and level define the SDF's QoS requirements among all the EPS nodes. EPS introduces two specified bearers:

(a) Default bearer.

(b) Dedicated bearer.

The former is initiated when the UE attaches to the network and remains activated until it detaches. The resource type of the default bearer is NGBR and it supports the best effort QoS level [38]. While the dedicated bearer is created dynamically on demand when the terminal device requests a service or access to services that require a higher QoS level than the default bearer, such as conversational voice or conversational video. The QoS of the EPS bearer is controlled by using a set of QoS's EPS parameters including:

- ***Resource Types***: define the bandwidth allocation for the bearer, there being two types, GBR bearer and NGBR. The GBR EPS bearer has a guaranteed minimum bandwidth (bit rate), while the NGBR EPS bearer's bandwidth is not assured. NGBR EPS bearer resource allocation depends only on the available resources remaining after the completion of the GBR EPS bearer resource assignment process.

- ***QCI***: The QoS level of the bearer is assigned to one and only one QCI, which is defined in (3GPP PCC architecture) as a reference between UE and the Policy Control Enforcement Function (PCEF), to indicate different IP packet QoS characteristics. It characterises the SDF in the UL and DL directions by resource type, packet priority handling, PLR and Packet Delay Budget (PDB). The QCI comes from the mapping process of the Differentiated Services Code Point (DSCP) values that are specified in the IP packet header. The nodes within EPS depend on the QCI value to translate

the demand for AQoS. This AQoS to NQoS mapping is to ensure that the packet flow carried on a specific bearer receives the minimum level of QoS in multiuser multiservice networks [46, 38]. In LTE the QCI is an integer value that varies from 0 to 255, the octet number 3 in EPS QoS information element [38]. While LTE Release 8 specifies nine standard QCI values varying from 1 to 9 [47], LTE-A Release 13 standardised thirteen different QoS levels, with four new QCI values having been added to be used in Mission Critical (MC) services for emergency services communication, as shown in Table 2.1 [38]. QCI value assignment is performed from the network side upon request from an application running on the terminal device.

- ***Allocation and Retention Priority (ARP)***: used for call Admission Control (AC), which is an integer value ranging from 1 (highest priority) to 15 (lowest priority) [48]. The ARP value, from the control plane perspective, sets the priority level and treatment for the EPS bearer. It permits the EPS control plane to exercise differentiation regarding control of the bearer's setting up and retention. Furthermore, it contains information about bearer pre-emption capability and bearer pre-emption vulnerability. The level of importance of resource request is defined by ARP and used for AC. Table 2.2 lists examples of ARP and related QCI values [49]. Whilst data plane traffic packets handling, among the EPS nodes and links, is carried by an associated bearer, as identified by QCI.

- ***GBR and Maximum Bit Rate (MBR)***: parameters are used for a GBR dedicated EPS bearer. GBR specifies the minimum provision and assured bit rate, while MBR sets the limit of the maximum bit rate allowed within the network. If the dedicated EPS bearer reaches the specified MBR, any new arriving packets will be discarded [48].

- ***Access Point Name - Available MBR (APN-AMBR)***: parameter is applied at UE for UL traffic only and it is utilised at PDN-GW for both DL and UL traffic. It controls the total bandwidth of all NGBR EPS bearers [48].

- ***UE - AMBR (UE-AMBR)***: is applied by eNB only, which specifies the maximum allowable bandwidth for all NGBR EPS bearers in the UL and DL directions [48].

Table 2.1 Standardised QCI characteristics

QCI	Resource Type	Priority	PDB msec	PLR	Service
0, 255	Reserved				
1	GBR	2	100	10^{-2}	Conversational Voice
2	GBR	4	150	10^{-3}	Conversational Video
3	GBR	3	50	10^{-3}	Real Time Gaming
4	GBR	5	300	10^{-6}	Non-Conversational Video (Buffered Streaming)
65	GBR	0.7	75	10^{-2}	Mission Critical user plane Push To Talk voice (MCPTT)
66	NGBR	2	100	10^{-2}	Non-Mission-Critical user plane Push To Talk voice
5	NGBR	1	100	10^{-6}	IMS Signalling
6	NGBR	6	300	10^{-6}	Video (Buffered Streaming) TCP-Based
7	NGBR	7	100	10^{-3}	Voice, Video (Live Streaming), Interactive Gaming
8	NGBR	8	300	10^{-6}	Video (Buffered Streaming) TCP-Based
9	NGBR	9	300	10^{-6}	Video (Buffered Streaming) TCP-Based, default bearer
69	NGBR	0.5	60	10^{-6}	Mission Critical delay sensitive signalling
70	NGBR	5.5	200	10^{-6}	Mission Critical Data
10-64, 67-68, 71-127	Spare				
128-254	Operator Specific				

Table 2.2 An example of QCI to ARP mapping

*ARP		*QCI		Pre-emption capability	Pre-emption vulnerability	Resource Type	Example Services	Typical Associated Protocols
Index	**Bearer Priority**	**Index**	**Packet Priority**					
1	1	1	2	Yes	No	GBR	Conversational Voice	UDP, SIP, VoIP
2	2	2	4	Yes	No	GBR	Conversational Video (live streaming)	UDP, RTSP
3	3	3	3	Yes	No	GBR	Real Time Gaming	UDP, RTP
4	4	4	5	Yes	No	GBR	Conversational Video (hi-definition)	UDP, RTSP
5	5	5	1	Yes	Yes	NGBR	IMS signalling	TCP, RTP
6	5	6	6	Yes	Yes	NGBR	Video (buffered streaming), TCP applications	TCP, FTP
7	6	7	7	Yes	Yes	NGBR	Voice, Video Live Streaming, Interactive Gaming	TCP, HTTP, VoIP
8	6	8	8	Yes	Yes	NGBR	Video (buffered streaming), TCP applications	TCP, SMTP, POP
9	8	9	9	Yes	Yes	NGBR	Video (buffered streaming), TCP applications	TCP, FTP, IMAP
10	15	5	9	No	Yes	NGBR	UDP based applications	UDP, SNMP
11	14	6	9	No	Yes	NGBR	UDP based applications	UDP, SNMP, POP
12	13	7	9	No	Yes	NGBR	UDP based applications	UDP, RTP
13	11	8	9	No	Yes	NGBR	UDP based applications	UDP
14	9	9	9	No	Yes	NGBR	UDP based applications	UDP, RTP
15	1	1	2	Yes	No	GBR	UDP based applications	UDP,SIP, VoIP
* ARP and QCI values from 1-9 are standardised in LTE R8 the rest are left for network operator setting.								

2.2.2 C-RAN deployment

For effective network deployment, the cells dimension and maximum capacity have to be related to the expected peak traffic load of the associated radio access nodes' coverage area span. Any traffic load fluctuates depending on the geographical area type, such as rural, suburban and urban as well as according to time, i.e. morning, rush hour, evening, night and off peak. For instance, in the daytime, the traffic load is heavy in office areas and light in residential ones, while the opposite happens in the evening [50]. Hence, static network deployment is not optimal owing to the varying traffic load. Therefore, the DC-RAN has been proposed in chapter 4 to deliver optimal network deployment as well as to enhance end users' QoE as future traffic demands grow and provides energy saving, when it adjusts the cell size according to the traffic demand.

2.2.2.1 DC-RAN action

DC-RAN can be defined as being when neighbouring cells can interact with others such that one cell can decrease its coverage area or switched off. Generally, the neighbouring cells will be able to increase its coverage area to prevent the creation of a gap in the radio coverage within the network area as shown in Fig.2.1. The interaction between cells will require techniques that can adapt the cell coverage area. Extension or contraction the radio access node coverage area span provides a potential capacity gain and enable the cells to modify their coverage area at any time for optimum configuration.

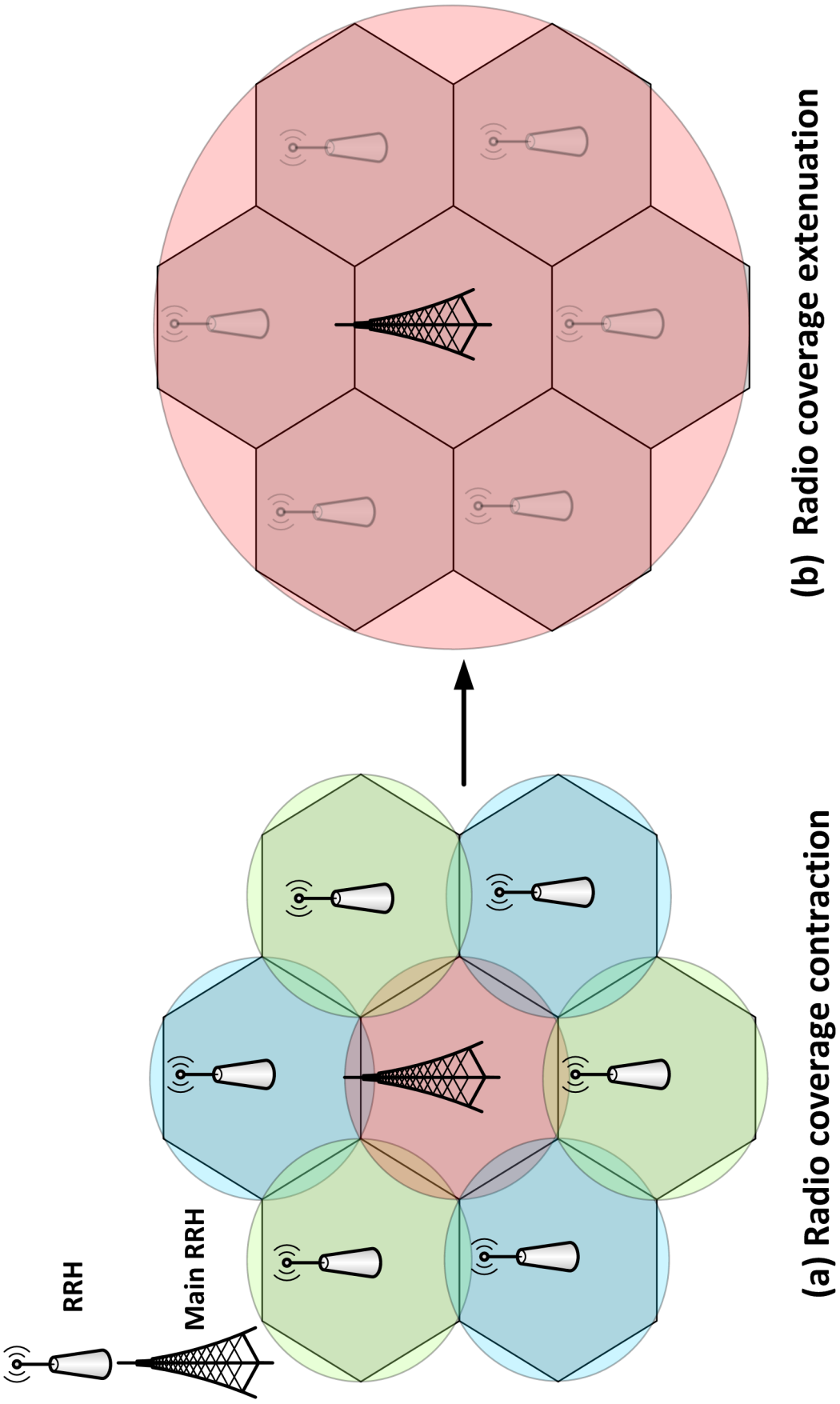

Fig. 2.1 DC-RAN concept

2.2.2.2 CRE mechanism

The main driver of the proposed DC-RAN is the Coverage Range Extension Mechanism (CRE) mechanism that is introduced by the 3GPP [51] [52], which is either cell coverage range expansion or contraction. It can be applied by the main RRH cell site within the BBU pool area to adjust the main RRH coverage range span. The CRE is used to change the coverage range of small and medium cell RRHs, such as femtocell, picocell, or microcell RRHs. Furthermore, CRE has been used to enhance Inter-Cell Interference Coordination (eICIC) in a heterogeneous network. CRE now can be applied in macro cell RRH, which is located at the main RRH site. In the Self Organising Network (SON) procedure that has been proposed to be used in the 4G network, there are three identified techniques to adopt CRE in the conventional radio access node [53] as:

(a) Mechanical and can be achieved by changing the antenna tilt angle and antenna height.

(b) Cell selection criteria, which can be done by instructing the UEs at the cell edge to select the second suitable cell. This will reduce the coverage range of the intended cell by ceasing its cell edge users, and increase the coverage range of the neighbours' cells by associate the abovementioned ceased users' to the neighbour cells.

(c) The technique of increasing or decreasing the main RRH Transmitted (Tx) power. This concept relies on changing of the Signal to Noise Ratio (SNR) level at the receiver in the UL and/or DL directions, where SNR is one of the important KPIs of the offered NQoS at the receiver PHY layer level.

2.2.3 Overview of SDN-WISE

This section provides a brief outline of the supportive solutions that provided by the SDN-WISE design with an overview of the SDN-WISE technical approach of the related protocols layers in order to justify the benefit of using SDN-WISE.

2.2.3.1 SDN-WISE supportive of QoS

The essential solutions provided by SDN in WSN will be characterised according to different applications. One of these solutions is that the SDN-WISE is considered an efficient usage of the network terminal elements resources represented by SNs and SNKs. which can be summarised as follows:

(a) The main objective of using SDN architecture in WSN is minimising the node state information exchange among the SNs, the proxy controller and the operation of SN programmable mechanism, such as Finite State Machines (FSM) enable them to run operations that cannot be supported by stateless solutions [29]. The SDN-WISE gives permission for each node to make decisions regarding incoming packets by taking into account the value of the recent state (stateful) [29].

(b) It provides flexibility for managing packet forwarding rules that fit WSN current topology. For instance, the report messages are used for updating the controller regarding the link state between nodes as well as the battery level information. The essential purpose of SDN-WISE is introducing simple network management by enhancing a novel application and investigating solutions for WSNs as a new type of networking [54].

(c) Duty cycles – switching off the radio is the most important technique for energy consumption reduction [32].

(d) Data aggregation technique is an initial part in SDN-WISE network. Removing the redundancy from the data in the network can reduce the energy that is used by adding a data aggregation technique. Consequently, that is made more possible by minimising the number of transmission packets in the network, as this has a positive effect on the PC efficiency [55].

(e) Data centric service is provided to make credentials for sensor nodes, particularly concerning their data as an alternative for their address. SDN-WISE has invented this

solution to specify the rules from the controller for packets with changed features [32] [29].

2.2.3.2 SDN-WISE data flow mechanism structure

There are three dynamic data structures that the SNs have to consider in SDN-WISE. The ***first*** one is the WISE State Array, where each SN in SDN-WISE has to consider different circumstances to specify the feature of the packets. In the WISE State Array the values of these situations (current state) are saved. This value is used to recognize the packet; this is related to the 802.15.4 standard [56] or to SDN-WISE.
The ***second*** one is the Accepted IDs Array. This makes it possible for SNs to only consent to packets that can be further processed. There is also an element in the SDN-WISE header of the packet that specifies an Accepted ID of the packet. The sensor node checks the packet to see whether it is included in the Accepted IDs Array – otherwise it will be ignored. The sensor node starts to find out the matching rule in the WISE Flow Table for the ID directly after checking that this ID is matched and need to be processed.
The ***third*** one is the WISE Flow table; each entry of the WISE Flow Table includes a section of Matching Rules, which specifies the conditions under which the entry used.
The Matching Rules may consider any part of the current packet as well as any bit of the current state. If the Matching Rules fulfil the needs, then the SN will achieve an action specified in the remaining section of the WISE Flow Table entry. The action may refer to how to manage the packet as well as how to change the current state. If no entry is recorded in the WISE Flow Table whose Matching Rules implement to the current packet/state, then sent a request to the controllers. The node needs to have a WISE Flow Table entry indicating its best next hop towards one of the sinks in order to contact the controllers. This entry is not set by the controller like the others because it is detected by each node in a distributed way. Depending on the Topology Discovery (TD) in the node to provide the information for choosing the next hop to the SNK. In addition, the remaining parts of the WISE Flow Table are used for the matching rule; in case of matching then it will perform the action related to the ID. If it is not included in the table, then it sends a request to the controller [57] [58]. The received packet processing flow is shown in Fig. 2.2.

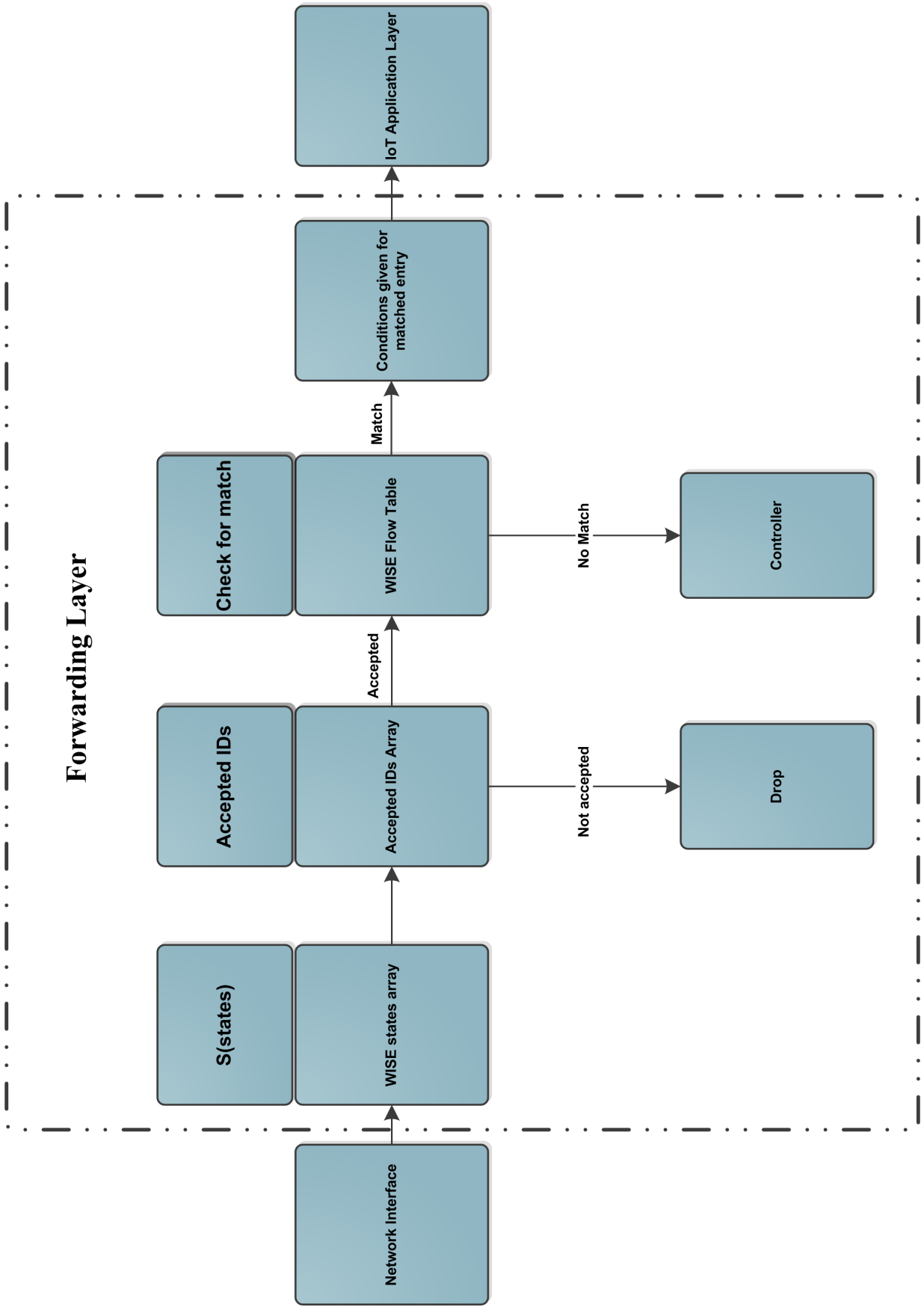

Fig. 2.2 Processing of packet arriving at SN in SDN-WISE

2.2.3.3 SDN-WISE protocol architecture

This section describes the details and features of the SDN-WISE protocol stack. Furthermore, it explains all the architecture of the layers and the responsibility of each one as shown in Fig. 2.3. Additionally, it will describe the SDN-WISE layers' packets in details.

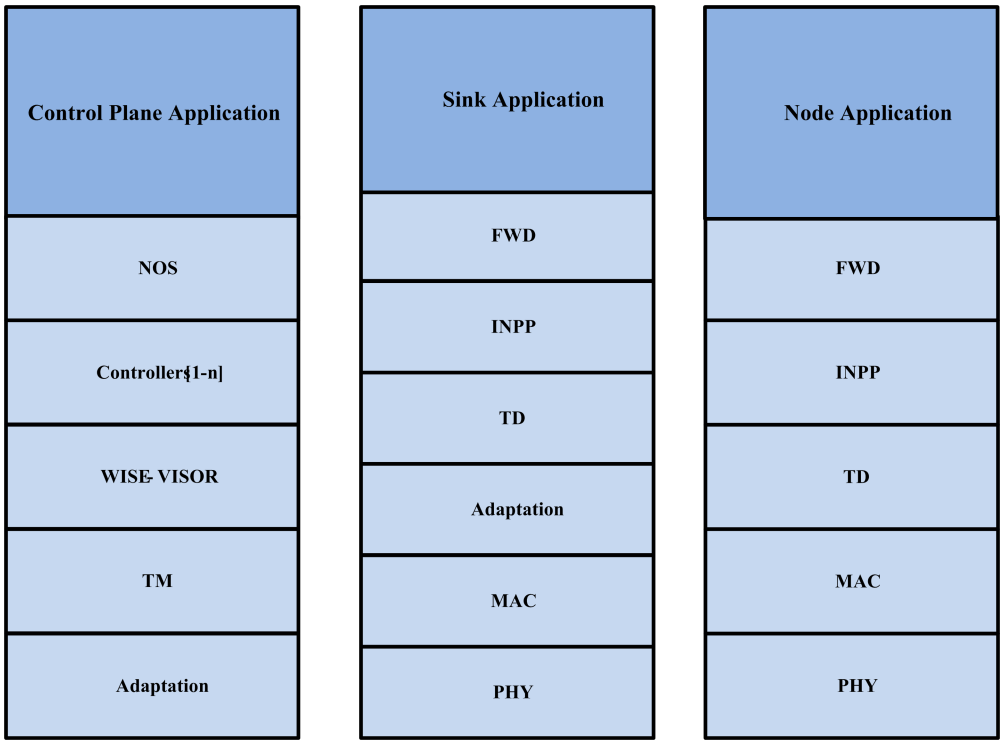

Fig. 2.3 SDN-WISE Protocol Stack.

(a) Topology Discovery (TD).
It describes as a protocol layer, which is based on processing and exchanging of packets named TD packets , which are

(i) Beacon packet.
Contains information about SN remaining energy level, the Received Signal Strength Indication (RSSI) and the number of hops that the SN has developed to the nearest SNK node (gateway).

(ii) Report packet.

(iii) Configuration packet.

The main responsibility of this protocol is generating information about the topology from the SN view point and sending it to the WISE-VISOR, these information are

transmitted by Report packet to the WISE-VISOR [29]. This information is collected by broadcasting the Beacon periodically according to the TTI. The reason behind the broadcasting is to keep a clear view and update map of the network elements by sending Report packet to the controller. At the same time, the Beacon is received by the SN to clear its list of neighbours; due to the fact the SN will receive a fully updated list later from the controller by the Configuration packet based TTI. Whenever the SN receives a packet, it will make a comparison with the previous information that has acquired then updates the old information, particularly with regards to the number of hops to the SNK. Furthermore, this shows how the SNs populate their neighbours' list, which contains the neighbouring nodes in the network.

The operation of each SN undergoes as follows [32] [59]:

- The SN will send the Beacon to its neighbours that are included in its list in order to ask about their battery level and RSSI. The list of neighbours in the SN is built by inserting the SN that sent the Beacon signalling. If the neighbour already exists then it will only update the information about the battery level and RSSI.
- The SN will check the distance as a number of hops between the SN and the SNK that recently received a Beacon from it. If it has a number of hops different than the current, then directly it will update to the new value and consider it.
- The Beacon packet is retransmitted in order to update the SN state. The TD layer is the only layer that has the capability to access all the other layers. This provides the TD layer with the possibility of collecting the information and assessing the SN at each layer and how it behaves.
- Transmitting the information by using a Report packet and update the network map by sending a Configuration packet for reconfiguring the network map.
- The WISE-VISOR will receive the Report packets and update the network map by sending a Configuration packet for reconfiguring the network map.

(b) Topology Management (TM).
The TM is a protocol layer as an essential part of the WISE-VISOR controller. It supports the ability of different controllers with different policies using the same physical network elements, presented here as SN, in the same system [58]. It produces an up to date map of all network's elements after receiving the Report packets then sending the updated information to the network elements by the Configuration packets.

This TM protocol is paired with TD protocol to collect, and update the information of the network elements then configure network status for building the flow table.

(c) Forwarding layer (FWD).
This has the responsibility of executing all of the arrival packets that are specified by the WISE-VISOR. It is located on the top of the SN's MAC layer. This layer is responsible for treating the arriving packets from MAC layer and updates the flow table for meeting the aim of dealing with all of the arrived packets. In keeping with the SDN scheme, the flow table entries are defined by three parts, which are

(i) Rule, it figures out the features of the packet that belong to the flow, which must be treated by the node simultaneously.

(ii) Action, which is executed to all packets satisfying the above rule.

(iii) Statistic information, it states the number of packets received in the table flow entry that have satisfied the rule.

Moreover, the PDU arriving at the forwarding layer are provided by the MAC layer. Depending on this, the packet type will be identified. However, if it is a control packet then it will be sent to the In-Network Packet Processing (INPP) layer. Otherwise, if it is a data packet then it will be sent to the forwarding layer to be checked with the rules in the flow table, to see whether it is a match or not. If the packet is a match then it will be dealt with the action that is included in the flow table and is related to this packet. Otherwise it will be forwarded to the INPP layer [32] [29]. This layer has the ability to process all of the packets arriving at the SN based on the information provided by the WISE Flow Table. This table is updated periodically by this FWD layer according to the comments received by the WISE-VISOR [29].

(d) In-Network Packet Processing (INPP) layer.
This layer is applied over the forwarding layer. The responsibility of this layer is implementing the important action needed for aggregating the information by connect the small packets that must be sent through same paths, that will reduce the overhead on the whole network [32]. In addition, it is considered as a local Operating System (OS) analogous to NOS, resides in the SN and responsible of processing data, which will provide the node the capability of making decision.

(e) Adaptation layer.
This layer is included in the WISE-VISOR controller and the SNK nodes; it has the

ability to provide interfacing process between WSN platform or terminal network, which is based on 802.15.4 as shown in Fig. 2.4 and the WISE-VISOR controller, which is based on TCP/IP and Ethernet 802.3 as shown in Fig. 2.5. Consequently, it modifies the TCP/IP address to the network ID and vice versa, to make an adaptation, which is considered in SDN for WSN [32] [60]. As the main responsibility is formatting the received and transmitted PDUs streams in the SNK by such a way, which can be treated by the WISE- VISOR and vice versa.

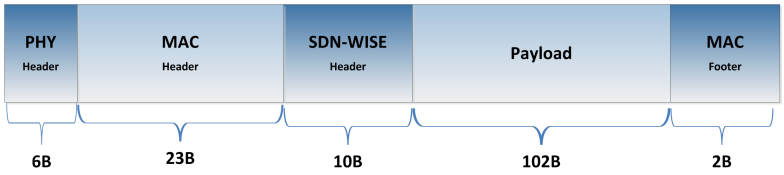

Fig. 2.4 The format of 802.15.4 PHY layer PDU

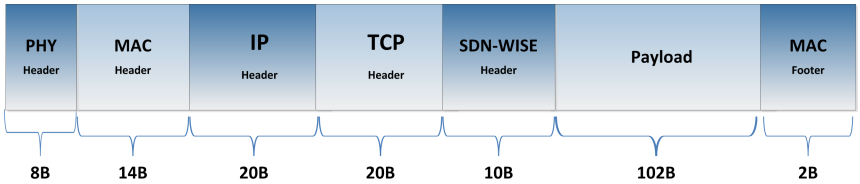

Fig. 2.5 The format of IEEE 802.3 PHY layer PDU

(f) Network Operating System (NOS) layer.
This layer is placed on the top of the whole SDN network and managing the SDN configuration policies [31]. SDN differs from the conventional IP networking in that packet forwarding is based on flows rather than packets. The flow abstraction is independent of, and can accommodate, various network hardware technologies. The NOS is logically a centralized controller, performing network management and control given a global network view.

Network applications may be written on top of the NOS, making it possible to support network programmability and to achieve flexible network management, reconfiguration, and protocol evolution. For instance, adding a new network functionality requires a new application on top of the NOS avoiding the need to install new and expensive hardware to support the new functionality as required in conventional networks [31].

(g) SDN-WISE packet Description.
The PDU of SDN-WISE are divided into two types of packets:

(i) Data packet represents the basic block of data plane traffic .

(ii) Control packet (SDN-WISE packet) represents the basic block of control plane signalling.

Both of the PDUs have 10 Bytes header, its content described in table 2.3. The size of the data packet depends on the payload generated by IoT application and service used by SN. While the size of control packet depends on the control plane signalling that is associated with it, as listed in subsection 5.2.2.

Table 2.3 SDN-WISE PDU header content

Byte(s) ID	**Description**
0	Network Identifier
1	Packet length
2-3	Destination address
4-5	Source address
6	Packet type
7	No. of hops remaining
8-9	Next hop address

2.3 State of the art

2.3.1 IoT application's traffic and MTC QoS

Several studies have been proposed to integrate newly emerged applications and services within 4G network infrastructure. Costantino et al. [61] evaluated the performance of an LTE gateway using the Constrained Application Protocol (CoAP), with the M2M traffic patterns and the network configurations being presented through simulations. The authors argued that the traffic patterns highly depending on the application used in the terminal devices , however, they did not describe or justify their choices. Their work focused on the effect of signals interference, in radio access node, related to the number of connected MTDs.
Lo et al. [62] studied the impact of data aggregation for M2M on QoS in a LTE-A network. In their work, they utilised a relay node as an aggregation and entry point of MTD traffic to improve LTE-A UL efficiency. Specifically, their work was based on tunnelling and aggregation of the MTDs, which were related to a specific destination server or node, via the relay node tunnel entry point and by considering the priority of the class of service. Whilst a significant reduction in signalling overhead was achieved, there was an increase in the delay of the received packet at the destination point and an increase in the number of aggregated MTDs at the entry point.
There have been another several attempts at delivering M2M communication integration with LTE-A. The current state of standardisation efforts in M2M communication and the potential M2M problems, including PHY layer transmissions were discussed in [63], who proposed a solution to provide QoS guarantees by facilitating M2M applications with hard timing constraints. Moreover, the features of M2M communication in 3GPP, an overview of the network architecture, random access procedure and radio resources allocations were provided. The authors in [64] considered one service and proposed a cooperative strategy for energy efficient MTD video transmission with a good NQoS. They achieved promising results, however, in the future, networks with different service and network components will be used in a heterogeneous environment. A relay node was proposed by the authors in [65] to facilitate the integration of M2M, with the proposed work being focused on a relaying feature in LTE-A. In [66], the authors examined the network convergence between Mobile Cellular Networks (MCN) and WSNs, proposing that the mobile terminals in MCN should act as both SNs and gateways for WSN in the converged networks. Their work neither guaranteed the E2E connectivity nor specified RAN's technology involved. There has been no work, as yet, to the best of my knowledge, proposing an entirely heterogeneous model that serves different networks with different services.

Another strand of research considered the radio access interface, including the new Low Power Wide Area Networks (LPWANs), such as Narrow Band IoT (NB-IoT) in the licensed spectrum as well as its competitors $LoRa^{TM}$, $SigFox^{TM}$ and $Ingenu^{TM}$ in the unlicensed spectrum [67]. The unlicensed networks have been deployed around the world since the first quarter of 2016, which motivated 3GPP to introduce NB-IoT in the second quarter of 2016. NB-IoT uses the guard bands in the 3G and 4G licensed frequency spectrum bands to provide a dedicated radio access for IoT devices within the radio spectrum of the currently deployed 3G and 4G RANs [68]. In the same context, the authors in [69] [70] [37] presented a connection-less integration of low rate IoT traffic within the PRACH frequency-time slot of LTE access technology. The previously listed technologies and research attempts did not address the effect of the heterogeneity of MTC application traffic and related QoS performance of HTC application when the network ecosystem resources have to be shared in such a way.

2.3.2 Optimised C-RAN deployment

To date, there has been much research about optimal BBU pool placement for C-RAN. For instance, in [71] the authors introduced the BBU pool placement optimization problem for C-RAN architecture and classified different deployment solutions for this. The problem was addressed based on Integer Linear Programming (ILP) and evolving the proposed model with optimization of the BBU pool and electronic switches placement. In [72] the authors investigated technological options for C-RAN deployment. They derived engineering guidelines for minimizing the CAPital EXpenditure (CAPEX) of C-RAN deployment by using analytical methods. Their work illustrated the population density related to the span of the BBU pool coverage with the usage of fronthaul MicroWave Radio (MWR) and they recommended dividing the area into multiple BBU pools for large scale deployment. The authors in [73] provided a model, which considered the cell site positions in an urban area as input to the proposed algorithm and computed the possible location of the BBU pool for different constraints, as well as, estimating the number of required BBUs in the pool. The scholars in [74] introduced a proposal for the BBU placement, where they are moved to the edges of the network. Moreover, they proposed the use of reconfigurable wireless mmWave links fronthaul instead of optical fibre in order to provide the RRHs with connectivity. In [75], the authors proposed a model by an ILP formulation to determine the BBU pool placement on a converged Multi-Stage Wavelength Division Multiplexing-Passive Optical Network (WDM-PON). The purpose was to choose in which cell to place BBU pool, as well as to take

in account the routing and wavelength assignment of traffic demands in order to minimize the number of BBU pools. Moreover, they studied the maximum latency of Digitized Radio-over-Fibre (D-RoF) between each BBU and RRH, which becomes a constraint on the maximum propagation delay of corresponding nodes.
In [76], the researchers investigated the BBU pool placement issue in C-RAN architecture, trying to minimize the distribution cost of the BBUs with respect to their processing capacities, the signal synchronization between the RRHs and BBUs and the data traffic demands of the RRHs. They proposed an algorithm to solve the problem formulation of the BBU pool planning and placement. In [77], the authors introduced and formalized a BBU placement problem for C-RAN deployment, which considered the fronthaul transport links. Their work was based on realistic data describing suburban, urban and rural scenarios, with different multiplexing/routing choices for the fronthaul and placement of the BBU pools. In [78], the scholars introduced an algorithm for BBU pools placement with their allocated RRHs as subsets of radio access nodes. In [79], the authors defined a cluster set of RRHs and considered the geographical constraints to determine the placement of the BBU pools. In addition, they minimized the installation cost of the C-RAN architecture by minimizing the total optical fibre length. The authors in [21] stressed the importance of optimized clustering of RRHs in single network to prevent the BBU pool from overloading, due to resource limitation, but they did not proposed any solution for this issue. To date, studies have not considered the required number of BBU pools in any specific network. The work in chapter 4 will provide a detailed study and propose a solution about converting a single network to a multiple sub network (i.e. multiple BBU pools) to simplify network management and enhance NQoS.

2.3.3 SDN QoS and energy efficiency

SDN design philosophies in wireless networks at sensors application and services can be logically divided into three categories.

- First group, Sensor OpenFlow is the architecture that virtually enables multi-application environments within a single physical network infrastructure. This design aims to provide compatibility between multiple provided services and simplifies protocol evolution. This philosophy is focused on adaptation of OpenFlow architecture to WSN needs [33]. However, SDN-WISE is the extended version of Sensor OpenFlow, developed to save energy by using software-implemented data aggregation and duty-cycling. Optimised PC with multi-tasking support in the Sensor OpenFlow architecture

can be achieved by decoupling the centralised control plane. Task distribution between control and data planes is employed in the second group of architectures to achieve minimal PC without significant performance degradation in order to keep NQoS at the desired levels [32].

- The next group of architectures includes Software-Defined Wireless Networking (SDWN) and its extension of smart sensors based on SDN , whose main goal is to optimise energy usage through task distribution between the control and data planes [80].

- In the third group, data management and interaction between data and control planes are realised using hierarchical designs.

There are several schemes are also proposed in the context of SDN in WSNs, which address different challenges were involved in the programmable SNs.
A novel SDN over WSN architecture, with sensor nodes based on programmable transceivers has recently been proposed by [80]. Depending on the wireless link propagation conditions, the transceiver switches between adequate radio communication channels and standards in order to optimise the NQoS performance. Therefore, this approach is capable to address different WSN communication issues in the presence of diverse transmission media effects.
In [81], the proposed a framework focused on the network element, which is the SN, acts as a simple forwarders without routing decision-making process. Within SNs, the decision to forward or drop packets is taken as per the rules implemented in their flow tables. The selected routes are elected by the controller, using application specific criteria. To select the routes, the controller uses location information from all SNs. So that flow table entries for network elements can be created, the controller monitors the network by receiving messages with information about the number of hops and link quality in order to improve NQoS.
A flow-table implementation mechanism in sensor networks (Sensor OpenFlow) was proposed in [33], in which the forwarding rule is defined by a centralised controller. Thus, the SDN concepts are applied to WSN to improve NQoS. The implementation of forwarding rules is based on aspects of compact network-unique address and concatenated attribute value pairs. Depending on the used application, which are either the SN address or IoT service and application data, which are compared with the flow table in order to make the decision (forward/drop) the packet. Thus, based on the AQoS specific requirements, the forwarding rules can be deployed in the network to enhance NQoS.
The authors in [82] proposed a software-defined sensor network platform, where each SN is embedded with multiple sensing applications. Different issues are raised in it, which

are SN activation, work mapping, and scheduling. The authors demonstrated that the SNs' energy consumption can be significantly minimised if network elements are controlled in a centralised manner. In the same context, another interesting SDN architecture for sensor networks is proposed in [83]. The SDN aspect in WSN is being restricted to specific network elements to establish network management.
In [84], the authors compared the PC of SDN OpenFlow and Open vSwitch that is running on server grade hardware by using numerical modelling and experimental results. The effect of traffic and configuration management on PC was evaluated. They presented a model that can be used to estimate the PC of various network configurations and for different traffic loads of data plane traffic in wired SDN.
With the objective to reduce information exchange between controller and the SNs, [29] proposed a solution concept for Soft-WSN. In this architecture, a stateful operation is executed at the SNs, which are able to adopt specific policies, which are previously defined by the controller, without consulting the controller every time when needed. Consequently, the proposed scheme minimises the message overhead and energy consumption in the network. Another SDN-based solution for WSNs proposes that a SNK node acts as a gateway between SNs and the controller. This supports data aggregation and radio duty cycling, allowing a periodic radio turn-off to improve energy efficiency. It implements a stateful approach by encoding different features within the data structure, such as WISE state array, accepted IDs, and WISE flow table. The main limitation of SDN-WISE is the necessity to collect data and interact with the controller through the same SNK node. This results in an increase of collisions of data collecting routes, as control plane channels are sharing the same communication channel with data plane. This is related to the work described in this chapter 5 where the key factors when considering data plane traffic payload size and TTI of control signalling in constructing the proposed PC model.

The critical analysis of the existing literature reveals that there is a research gap in the area of SDNs in WSN, specifically toward meeting AQoS requirements of the IoT. The existing literature trend is focused on issues related either to SNs or to flow table implementation. They are either a device-specific and/or a network-specific issue, which should be handled in effective orientations in order to enhance NQoS to match IoT AQoS requirements and exploit network ecosystem in efficient ways.

The PC of network elements represents a significant fraction of CapEx that is handled by services providers and networks operators. The SDN is a fresh network philosophy which aims to enhance NQoS in an optimise manner in different levels of PS communication network, it's a robust platform that can be applied to various networks [82]. Despite this,

there is an issue with extra power that will consumed by network elements, which are used to construct SDN framework such as control signalling. This issue has not been investigated in detail and its relation with the offered NQoS level for IoT AQoS needs. The proposed model in chapter 5 provides a clear perspective about additional cost of control signalling that supports the use of SDN in WSN such as the SDN-WISE scheme. Further more, it is focused on SDN-WISE architecture and introduces a PC mathematical model that considers IoT AQoS provisioning.

Chapter 3

IoT Traffic Management and Integration in the QoS Supported Network

Overview

IoT presents a massive ecosystem of a new element, applications, functions, and services. In spite of the fact that existing MTC traffic flows of IoT devices run over wireless WAN, 3G and 4G networks, the 5G is foreseen to be the main platform for the current and future requirements of IoT traffic demands. EPS protocols and architectures were aimed and enhanced to handle HTC traffic flows. However, with the expected deployment of massive of MTDs, there are concerns in the network operator side, service provider side and application consumer side that the network ecosystem may be exhausted, and the available network resources are not able to meet AQoS traffic flows requirement for HTC and MTC traffic flows simultaneously. MTC traffic characteristics of IoT devices are different from those of HTC and can augment the risk for network performance deteriorations. This chapter proposes a traffic flow management policy, which allocates and organises MTC traffic flow's network resources sharing within EPS, with an access element as a WSN gateway for providing an overlaying access channel between the MTDs and EPS. Furthermore, it addresses the effect and interaction in the heterogeneity of applications, services and terminal devices and the related QoS issues among them. The introduced work in this chapter overcomes the problems of network resource starvation by preventing deterioration of network performance. The scheme is validated through simulation, which indicates the proposed traffic flow management policy outperforms the current traffic management policy. Specifically, simulation results show that the proposed model achieves an enhancement in QoS performance for the MTC traffic flows, including a decrease of 99.45% in PLR, a decrease of 99.89% in packet E2E

delay, a decrease of 99.21% in PDV. Furthermore, it retains the perceived QoE of the real time application users within high satisfaction levels, such as the VoLTE service possessing a MOS of 4.349 and enhancing the QoS of a video conference service within the standardised values of a 3GPP body, with a decrease of 85.28% in PLR, a decrease of 85% in packet E2E delay and a decrease of 88.5% in PDV.

3.1 Proposed model

3.1.1 Integration of MTC traffic into EPS and traffic flow management policy

In order to integrate the IoT traffic in the LTE-A standard, EPS resources need to be used. Consequently, to avoid the substantial impact on the performance of HTC traffic, such as voice, video, HTTP service and FTP service, a specific NQoS for MTCs applications traffic flows needs to be provided to keep the QoE of real time application users within a satisfaction level.

3.1.1.1 Traffic flow management policy and problem formulation

A policy for traffic flow management is proposed in this chapter for defining MTC traffic flows over the EPS network, that differentiates the treatment of EPS nodes and links from the NQoS point of view for the different MTC traffic flows and separates the standard HTC traffic flows from MTC ones. The need for a new policy emerged from the drawbacks of the current traffic flow management policy, one which does not differentiate between MTC and HTC traffic flows from a network resources sharing point of view. The MTC traffic flows and HTC traffic flows compete to take shares of the available network resources. Let us consider the total available network resources related to the network capacity is R, which should be assigned to traffic flows that are transported through the network in each TTI. If the allocated network resources per traffic flow j are r_j and the total number of traffic flows is k, then the total allocation can be expressed as:

$$\Sigma_{j=1}^{k}(r_j) \leq R \tag{3.1}$$

where, $R = (0, C]$ and C is the maximum capacity of the network from a network resources point of view.
The network resource r_j can be assigned to the MTC or HTC traffic flow. If an MTC traffic

flow of a single MTD i has a share of network resources in each TTI of IoT_i, then the number of the network resources assigned to all MTC traffic flows that come from MTDs can be expressed as:

$$\Sigma_{i=1}^{m}(IoT_i) \leq S \tag{3.2}$$

where, m is the maximum number of the handled MTC traffic flows and $S = (0,R]$.
Under the same consideration, the HTC traffic flow of a single Human Type Device (HTD) n has a share of network resources in each TTI of H_n, therefore the number of network resources assigned to HTC traffic flows come from HTDs can be expressed as:

$$\Sigma_{n=1}^{l}(H_n) \leq T \tag{3.3}$$

where, l is the maximum number of the handled HTC traffic flows and $T = (0,R]$. From Equations 3.1, 3.2 and 3.3 we can deduce that:

$$k = m + l \tag{3.4}$$

and

$$R = S + T \tag{3.5}$$

and

$$\Sigma_{j=1}^{k}(r_j) = \Sigma_{i=1}^{m}(IoT_i) + \Sigma_{n=1}^{l}(H_n) \leq R \tag{3.6}$$

where, the lower and upper boundaries of IoT_i and H_n in Equ. 3.6 are $(0,R]$, and the network resources allocation in the Evolved-Terrestrial RAN (E-UTRAN) network part and Evolved Packet Core (EPC) is mainly based on the bearer's ARP and QCI values as well as the associated NQoS values, which are mapped from the AQoS's DSCP value. As expected in the NGN, the MTC/IoT traffic flows will potentially have a share with HTC traffic flows , therefore the network resources could be assigned to the HTC traffic flows if their bearers are higher (and/or) they have network supported ARPs and QCIs comparative to MTC traffic flows bearers, and vice versa. If the MTCs' traffic flow bearers get a resource allocation higher than those of HTC, without determining the management of network resources sharing among them, this will produce some serious issues regarding the offered NQoS and users' QoE. This deterioration in network performance will be clear in NGBR HTC applications, such as FTP and HTTP services.

3.1.1.2 Proposed solution

A proposed solution for the issue of NQoS deterioration is presented here by isolating the available network resources (R), which takes the form of adaptive shared ($\mathscr{R}$) network resources between the MTC network resources share ($\mathscr{S}$) and HTC network resources share ($\mathscr{T}$), by means of two disjoint sets. The size of the two shares ($\mathscr{S}$ and $\mathscr{T}$) is a percentage of available ($\mathscr{R}$), which can be adaptively adjusted based on a dynamic change in the network resources loading share, according to traffic flows conditions. Furthermore, the percentage can be customarily set on a static basis for supporting HTC traffic flows over MTC traffic flows and to reduce the impact of increased network signalling overhead between the E-UTRAN network part and EPC. Therefore, Eq.3.5 can be rewritten as:

$$\mathscr{R} = \mathscr{S} + \mathscr{T} \tag{3.7}$$

$$\mathscr{S} = \beta\mathscr{R} \tag{3.8}$$

$$\mathscr{T} = \alpha\mathscr{R} \tag{3.9}$$

$$\beta + \alpha = 1 \tag{3.10}$$

where, α is the percentage of network resources share allocated/assigned to the HTC traffic flows and the remaining network resources percentage is β. For adaptive and dynamic operation, α and β are set as a function of AQoS demands to ensure the provision of NQoS in terms of network resources for all traffic flows in the network nodes and transmission links. The EPS system primarily depends on the bearers' settings to provide the required NQoS metrics and to cover the needs of ***AQoS*** represented by the ***Terminal Type and DSCP***. From Eq.3.10, α's and/or β's can be used as tuning parameters to provide the required percentage value of network resources share, which are the bearer's setting, binding and modification parameters. In the CN and precisely in the Policy and Charging Rule Function (PCRF), PCEF and Mobility Management Entity (MME) functions units, these parameters as ***NQoS*** are ***Resource Type, ARP, QCI, PDB and PLR***. Then, it is possible for the PCRF and MME to identify α and β by combining the aforementioned AQoS needs and NQoS provided (from network side) . This can be done using a specific lookup rule table that updated data base on TTI basis in order to cover/meet the required performance and to optimise network resources utilisation.

The dynamic variations of α and β in every TTI can be deployed in EPC individually to set traffic policy management into a flavour of terminal device type user (Human or Machine) and the required network resources for the needs of the users' traffic flows, according to Equ. 3.8 and Equ. 3.9. Traffic management policy is realised via an active Policy Charging and Control (PCC) rule setting or can be applied according to the local policy configuration in the network gateways or from the PCRF network core elements and MME.
The aforementioned PCC rule setting is presented as an adaptive algorithm conferring to the network traffic flows. Another methodology can be interpreted from the previous analysis, for the setting of control mechanism of traffic flow management policy. It consists of two components represented by α and β. Each one can work with a distinct approach regarding the network resources allocation, separately within its allowable limit, such as optimisation and scheduling of network resources usage over different parts of the network. This approach sets a traffic flow management policy by defining a fixed network resource share between HTC and MTC traffic flows.
Fig.3.1 shows the flowchart for setting up the traffic flow management policy in each TTI, or it can be built on a specific duty cycle time basis, whereby the procedure is matched with the TTI of EPS to be mixed with the EPS resource allocation policy. The flowchart starts by checking the available network resources and then checks for traffic flow requests of the HTC and MTC terminals. In Fig.3.1a the dynamic adaptive network resource share policy has been applied, whereas in Fig.3.1b a fixed network resource share policy has been applied on a specific HTC terminals network resource share of $\alpha\%$. A specific sort of function is used to match AQoS needs with the NQoS available and to serve the GBR bearers as well as the NGBR bearers for HTC terminal and MTC terminal traffic flows, simultaneously, based on the $\mathscr{T}$ and $\mathscr{S}$ shares.

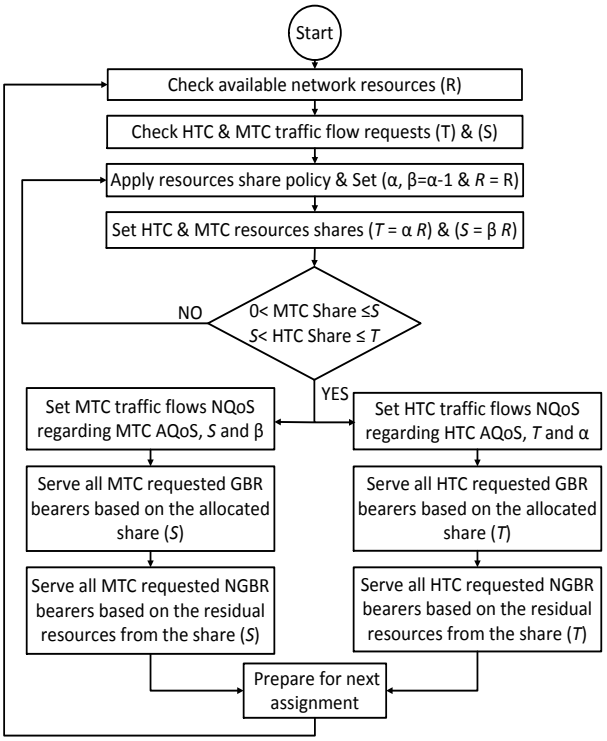

(a) Dynamic network resources share policy.

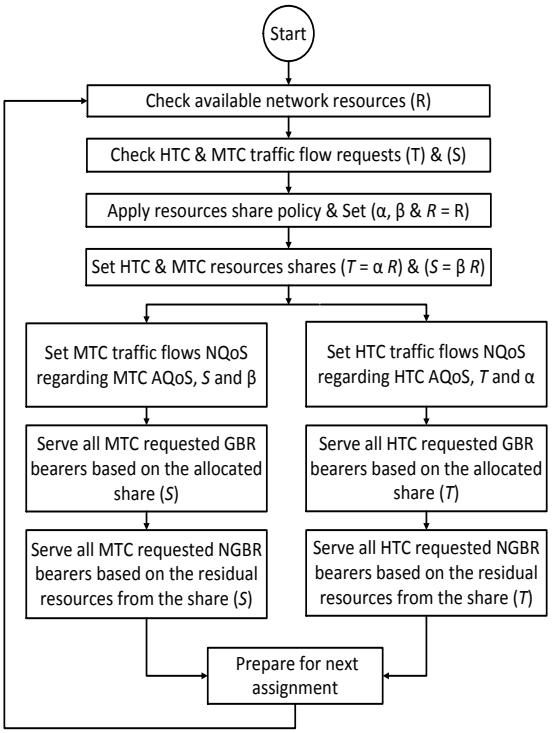

(b) Fixed network resources share policy.

Fig. 3.1 Traffic flow management policy setting.

An estimate and synthetic values set is listed in Table 3.1, for α and β, according to the traffic density pattern from the productive realistic network scenarios proposed in [85, 36].

Table 3.1 Proposed estimated values of α, β and associated network resources share

Function	**Percentage Share of over whole Network Resources**	**Resource Type Percentage (sub share) from each main Share**
α	80%	67% GBR 33% NGBR
β	20%	60% GBR 40% NGBR

There are three main types of MTC traffic, real time, delay sensitive and delay tolerant. The proposed QCIs aimed at these three types, as a base line in this work, could be extended to provide precise differentiation if needed. The index values of the new QCIs are 71, 72 and 73, which are shown in Table 3.2 and chosen from the spare QCI values. The MTC model used in this work is going to join LTE-A mobile broadband wireless network.

Table 3.2 Proposed MTC QCIs

QCI	Resource Type	Priority*	PDB msec	PLR %	Example services
71	GBR	1	100	10^{-3}	Real time, alarm monitoring
72	GBR	2	200	10^{-3}	Real time, live monitoring
73	NGBR	3	300	10^{-6}	Delay tolerant, metering
* The priority is related to MTC traffic type					

In Table 3.2, the GBR resource type has been specified to the real time and delay sensitive MTC traffic, the NGBR resource type has been specified to the delay tolerant MTC traffic, the priority setting is related to the MTC traffic, in order to provide seamlessly integration manner with the standard QCIs assigned priority values. PDB and PLR are specified to fulfil the minimum NQoS required to provide acceptable levels to AQoS needs for MTC traffic.

3.1.2 Proposed network architecture

Fig.3.2 shows the proposed network architecture for bridging the WSN devices with the EPS network. The integration is achieved via a WSN gateway, which is in turn connected to the WSN base stations or coordinators. The infrastructure of the proposed network is a combination of different WSNs that can use different routing protocols, including IEEE 802.15.4 (ZigBee), IPv6 over Low power Wireless Personal Area Networks (6LowPan) and the Low-Energy Adaptive Clustering Hierarchy protocol (LEACH). Each WSN has a coordinator or base station that provides the harvested information to a WSN gateway. The gateway's design, implementation and its related used protocols are explained in detail in the following subsection.

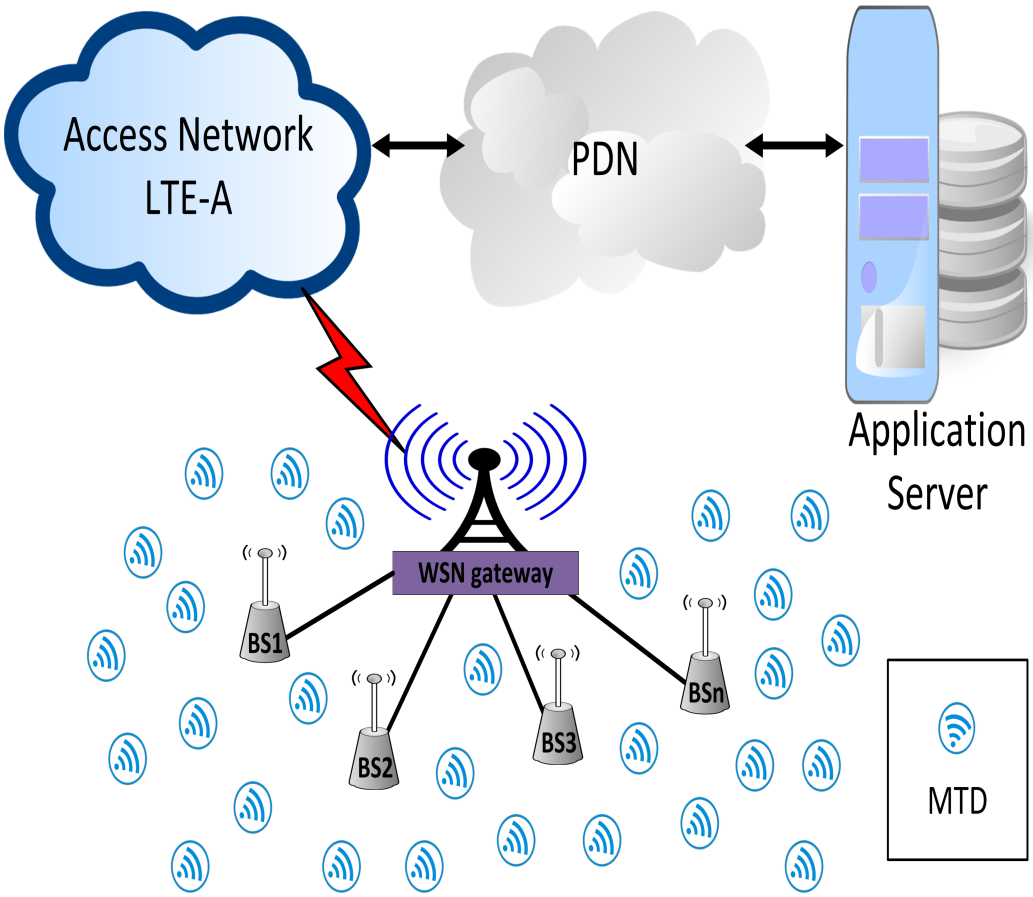

Fig. 3.2 The proposed network architecture.

3.1.3 Access network (WSN gateway design)

WSNs are fundamental aspect for enabling MTC moving towards IoT technology in smart cities; they collect the data from the targeted areas and pass them through wireless communication. These networks can be connected to a higher level system (such as LTE operator networks) via a gateway, the main function of which is to provide connectivity and interaction between the WSN base station and the external PDN, transparently. In the proposed scheme the WSN gateway connects a mobile broadband network access node with WSN IoT infrastructure (as converged networks). In this work, the methodology used to connect a massive WSN to a PDN via mobile broad network infrastructure is focused on the connectivity of the WSN traffic and QoS issues, as well as in consideration of QoE of real time applications users. The WSN gateway serves as a dual mode node and as a protocol converter between WSN base station and an E-UTRAN access node. An LTE-A Pro eNB access node is presented that introduces LTE-A as a mobile broadband network involved as a base line in this study

and for future NGN. The integration of multiple networks has two main types, tight and loose coupling techniques or topologies [86], with each type having its advantages and drawbacks from a QoS point of view. Regarding the loose coupling technique, the integration is offered by the WSN gateway, which provides dual mode connectivity between E-UTRAN and the WSNs. The protocol stack of a WSN gateway is shown in Fig.3.3, where a protocol conversion is applied between the WSN coordinator and LTE-A traffic flows.

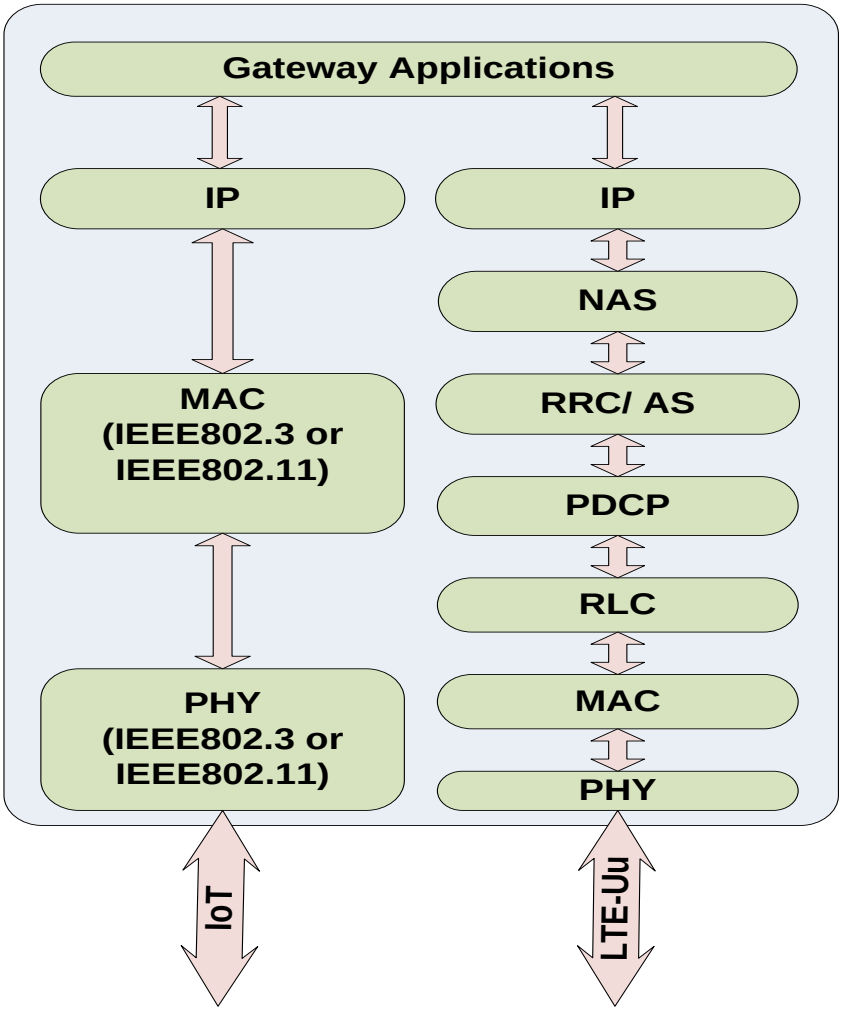

Fig. 3.3 The WSN Gateway protocol stack.

The control plane is assumed to be set up already among the CN, eNB and end devices. This includes the RAP, the Non Access Stratum signalling (NAS), and the Radio Resource Control (RRC). After completing the set up phase, the Packet Data Convergence Protocol (PDCP) applies the Traffic Flow Template (TFT) packet filtering process and assigns bearers

to its logical channel prioritisation levels [87]. This process controls and divides the available network resources in the UL and DL directions among different bearers/SDFs over the entire EPS network [88]. These key features of controlling the QoS level of the initiated bearer between WSN gateway and PDN-GW are performed in PDCP layer in the WSN gateway for the UL direction and the GPRS Tunnelling Protocol User Plane (GTP-U) layer in PDN-GW for the DL direction. The setting of the TFT filtering process, bearer's IDentifier (ID), Tunnel Endpoint IDentifier (TEID) and bearer's IP address are instructed between PCRF and PDN-GW in the CN.

3.1.4 Multiplexing process

An efficient multiplexing algorithm for MTC traffic has been implemented between the WSN gateway and PDN-GW. MTC traffic is aggregated in the WSN gateway and then multiplexed together, which is carried out in the PDCP layer in the UL direction on the bearer level. The aggregation and multiplexing of different MTC traffic is based on newly defined QCI values to match the required QoS levels for MTC traffic flows during their transmission via the mobile broadband network. This WSN gateway is a low cost device; it multiplexes different MTC traffic flows on the bearer level without use of any extra resources at the radio interface and in the backhaul. Instead of requesting a new resource allocation in the UL direction from the eNB for an individual WSN node or base station, the requesting process is performed by the WSN gateway for a group of multiplexed service data flows originating from MTDs, based on the QoS level. This multiplexing is undertaken intelligently in the PDCP layer using TFT and packet filtering on PDCP Service Data Unit (SDU). This comes from the IP layer, representing different MTD traffic flows and then produces a multiplexed PDCP PDU to be mapped to the earlier initiated Data Radio Bearers (DRBs) between the WSN gateway and PDN-GW. An overview of the proposed mechanism is shown in Fig.3.4.

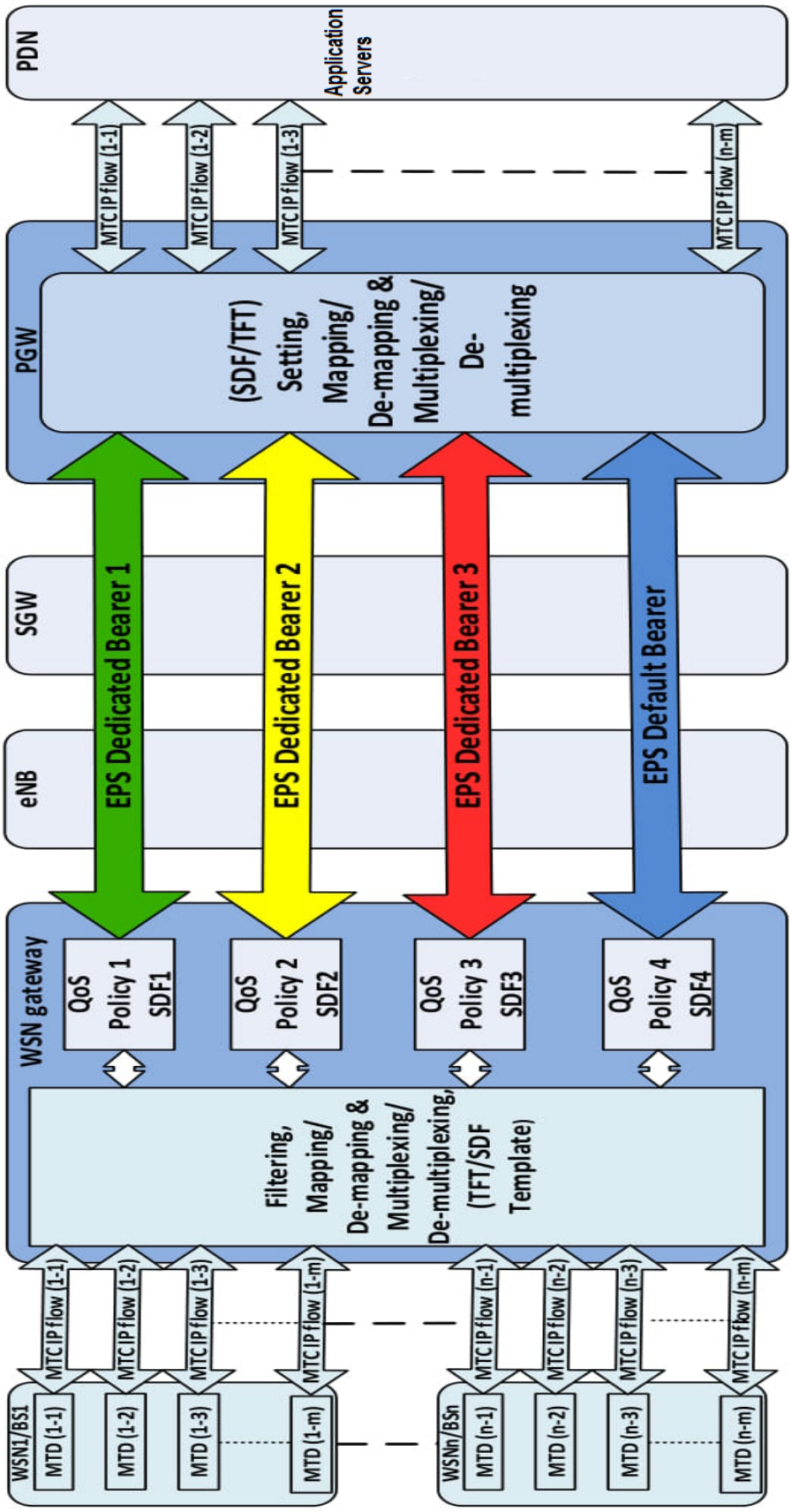

Fig. 3.4 Multiplexing process.

3.2 Simulation setup

The performance of the proposed network model is studied using the Riverbed Modeler version 18.5.1 [9] simulator from Riverbed Technologies Ltd. as a licenced software offered by Brunel University London. This version supports 3GPP standard and the modeler library offers a variety of protocol types and device models for supporting accurate simulation scenarios [89]. The modifications of the standard modeler models are carried out in order to implement the proposed simulation setup [9].

3.2.1 Simulation configuration parameters

The designed E-UTRAN consists of one macro eNB, which is connected to EPC and PDN via an optical transport network comprising 7 WSN gateways and 30 active UEs randomly distributed within the coverage area of the eNB . The WSN gateways and UEs are positioned randomly in the coverage area of the eNB. Each WSN gateway is connected to one WSN base-station (coordinator) via an Ethernet connection using the IEEE 802.3 protocol, which is used to convey the harvested information towards the application server. The application servers are connected to the EPS network through the internet backbone network. End device application's service request and call setup supports the use of Session Initiation Protocol (SIP), which is configured among the UEs, WSN gateways, applications servers and IP and Multimedia Subsystem (IMS) server. The simulated network contains Profile Definition, Application Definition, LTE configuration and Mobility Management entities. Furthermore, the path-loss, fading and shadow models used in the wireless links are the Urban Macro-cell ITU-R M2135 model [90]. 20 MHz has been set in the EPS RAN part with maximum radius of coverage of 2 km, in order to provide a realistic scenario for the wireless part of the simulated network. The typical E-UTRAN parameter settings are listed in Table 3.3.

Table 3.3 Simulation setting parameters

Parameter	Setting
No. of eNB	one single sector
eNB coverage radius	2000 m
MAC Layer/ PSCH Scheduling Mode	Link adaptation & channel dependant scheduling (Max. I_{MCS}=28, I_{TBS}=26)
IP Layer QoS (Scheduling Algorithm)/ Outside EPS rules and functions	Default (Best Effort)
Path loss model, Fading Model and Shadow Fading Loss Model	UMa (ITU-R M2135) [90]
UL Multipath model	LTE SCFDMA ITU Pedestrian A
DL Multipath model	LTE OFDMA ITU Pedestrian A
UE velocity	0 km/sec
eNB, UE and WSN gateway receivers sensitivity	-200 dBm
MIMO transmission technique	Spatial Multiplexing 2 Codewords 4 Layers
UE and WSN gateway No. of receive antenna	4
UE and WSN gateway No. of transmit antenna	1
eNB No. of receive antenna	4
eNB No. of transmit antenna	4
Cyclic Prefix	Normal (7 symbols/slot)
Duplexing Mode	FDD
System BW	20 MHz
PUCCH, PDCCH & PHICH configurations	Modeler default values
UL carrier frequency (operating band 1) [37]	1920 MHz
DL carrier frequency (operating band 1) [37]	2110 MHz
UE and WSN gateway Antennas Gain	-1 dBi
eNB Antenna Gain	15 dBi
eNB, UE and WSN gateway maximum transmission power	27 dBm
Modulation and Coding Scheme (MCS)	Adaptive
No. of TTI	140000
eNB, UE and WSN gateway PDCP Layer Max. SDU	1500 Bytes
PDCP layer Robust Header Compression Ratio (RoHC)	UDP/IP:- uniform (0.5714, 0.7143) TCP/IP:- uniform (0.1, 0.4) RTP/UDP/IP:- uniform (0.1, 0.15)
UL/DL HARQ maximum retransmission	3

3.2.2 Simulation run sequencing management

10 UEs initiate real time voice call by using the VoLTE service, where 5 of them are the voice callers and the other 5 are voice called. This service is set to use high data rate codec (G.711) with voice payload frame size of 10 msec and 80 Bytes per frame [91], this is going to produce one digitized voice payload frame every 10 msec with 64 Kbps rate, which is the voice application layer PDU. The consequential physical layer VoLTE PDU rate will be

96 Kbps, including all the protocols' overhead with RoHC [9]. The VoLTE bearer traffic stream bandwidth in the physical layer matches and occupies the maximum GBR bearer setting, that was designed for the VoLTE service, and this will produce a full utilization to the voice bearer bandwidth and this verifies that G.711 is a resource hungry codec. The size of 10 msec voice frame was chosen to support the QoE estimation process of VoLTE service with the required parameters. Another 10 UEs initiate real time video call by using a video conferencing service, where 5 of them are the callers and the rest are called. Regarding the remaining 10 UEs, 5 uses the FTP application to communicate with remote server 1 and the other 5 utilises the HTTP application to communicate with remote server 2. The H2H Services and application characteristics are listed in Table 3.4.

Table 3.4 H2H service and application characteristics

Service/ Application	**Application Layers Parameter**	**Setting**
Voice	Encoder Scheme	G.711
	Frames per Packet	1
	Frame Size	10 msec
	Compression/ Decompression Delay	20 msec
	ToS/ DSCP	Interactive Voice/ CS6
Video Conferencing	Frame Interarrival Information	10 frames/sec
	Frame Size Information (Bytes)	128x120 pixels
	ToS/ DSCP	Streaming Multimedia/ CS4
FTP	Command Mix (Get/Total)	100%
	Inter Request Time	Uniform, min. 27 sec, max. 33 sec
	File Size	Constant, 500 Bytes
	ToS/ DSCP	Standard/ CS2
HTTP	Specification	HTTP 1.1
	Page Interarrival Time	Exponential, 60 sec
	ToS/ DSCP	Best Effort/ CS0

The 7 WSN gateways receive traffic generated from the MTDs, which is routed via the WSN coordinators. Each MTD is programmed to generate its traffic as a time based event activation. The rate of activation of the MTDs at each WSN platform is 5 MTD per second in an accumulating fashion, starting at 135 seconds and continuing until the end of the simulation. By the end of the simulation, each base station and WSN gateway will have received and routed the traffic of 500 MTDs. The metering MTDs have an 80% share of the generated traffic, while alarm and live monitoring MTDs have 10% for each of them. The MTDs' generated traffic is proposed as being created from one of following WSN protocols: Constant Bit Rate Routing Protocol (CBRP), LEACH or ZigBee and the MTDs' traffic characteristics are listed in Table 3.5, which are related to MTDs' traffic settings in [92]. Moreover, the bearer configuration settings in the Riverbed modeler are listed in Table 3.6.

Table 3.5 MTD's traffic characteristics

Service / Application	**ToS/ DSCP**	**IP Layer Packet Size**	**IP Layer Packet Rate**
Alarm	Excellent Effort / CS3	512 Bytes	4 Packets/sec
Live Monitoring & Remote Monitoring	Streaming Multimedia / CS4		
Metering	Background / CS1		

Table 3.6 Bearer configuration

QCI	ARP	Resource Type	Max. & GBR (kbps)	TFT Packet Filters DSCP value	Service/ Application
1	1	GBR	96	CS6	VoLTE
2	2	GBR	384	CS4	Video Conferencing
6	6	NGBR	384	CS2	FTP
7	7	NGBR	384	CS0	HTTP
71	3	GBR	384	CS3	Alarm
72	4	GBR	384	CS4	Live Monitoring
73	8	NGBR	384	CS1	Metering
5	5	NGBR	384	Modeler default setting	SIP Protocol IMS Signalling
9	10	NGBR	384	BE	Low Priority Application & Undefined DSCP

3.2.3 Statistical validity of simulations

Two identical and separated simulation scenarios were build in a single Riverbed modeler project in order to facilitate the scenarios run sequencing process as well as the comparisons procedures of the measurements. The first one was pertained to considering MTC traffic as a best effort traffic flow, whereas the second was about using the proposed policy for traffic flow management. Each scenario was run for 30 times sequentially with randomly chosen seeds[93] [94], since producing data from a single execution cannot give a correct picture of the performance of the framework [95] . Furthermore, these scenarios' run replications were set with multi-seed value settings of the random number initializer, in order to get an outcome with a confidence interval of 95% as an estimated validity of the results, which is the resultant from above mentioned replications count [9] [93] [95] . Specifically, this approach is designed in Riverbed Modeler software to support confidence estimation for scalar data reporting [9] [96], which is collected in multi-seed parametric runs. The confidence interval marker is not shown in the results' figures, in order to emphasis and highlights the assessment concerning the aforementioned two scenarios. The designed baseline EPS network model is shown in Fig.3.5.

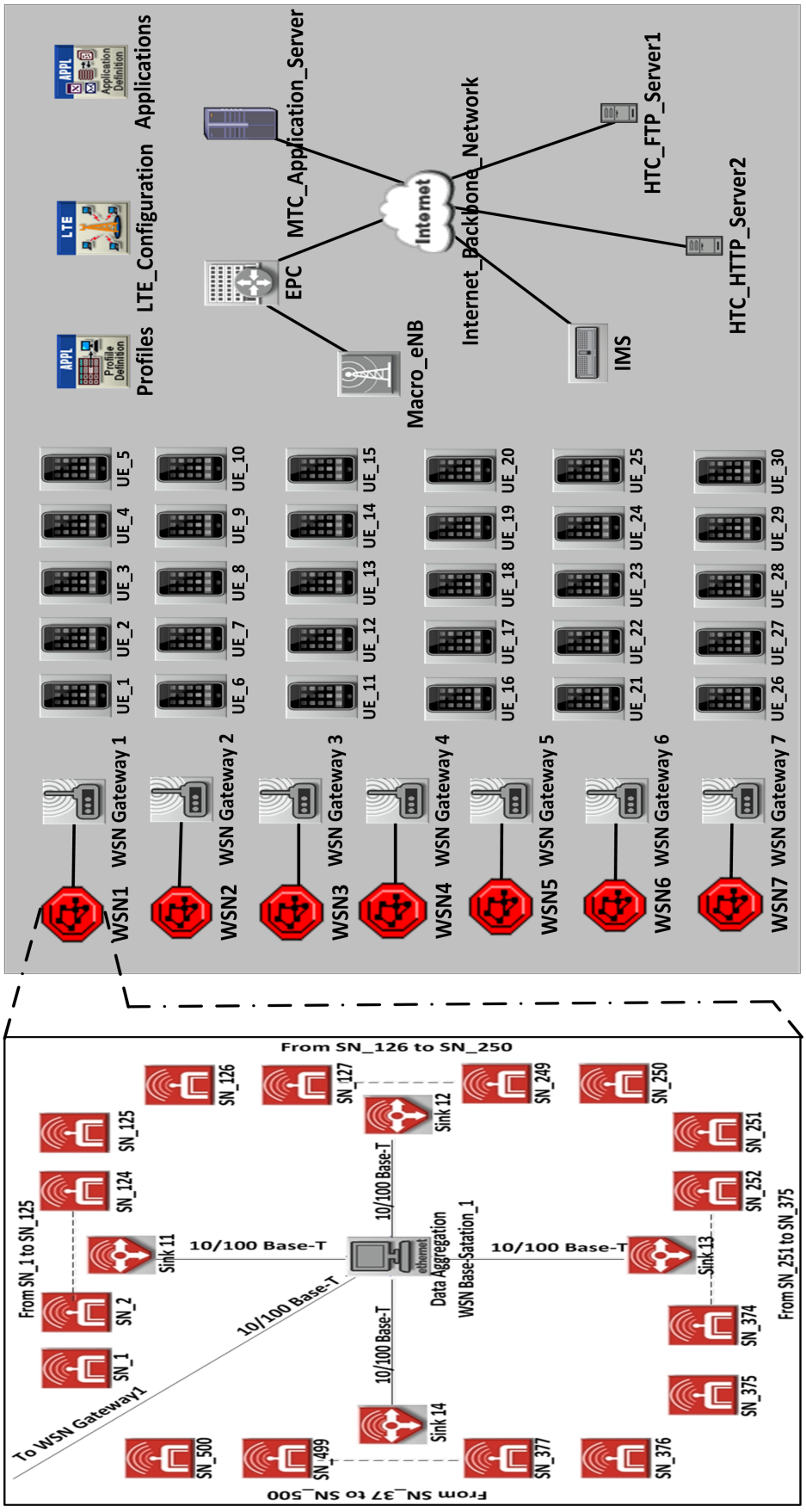

Fig. 3.5 Riverbed Modeler network setup.

3.3 Simulation results

Two Riverbed Modeler simulation scenarios with the proposed WSN gateway have been conducted in order to evaluate and validate the performance of the suggested system. For both scenarios, the simulation run time was set at 240 seconds. This time was specified to match the estimated traffic capacity of the Physical Uplink Shared CHannel (PUSCH), with respect to the number of the attached devices and their aggregated UL traffic loads rates at the eNB. Furthermore, to inspect how the conducted simulation of proposed traffic management policy on the bearer's level provoked at the physical layer level. In this regard PUSCH utilisation and throughput, once the bearers are starting the competition when there is a scarcity in the network resources. UL capacity mainly depends on the proposed physical layer structure parameters, PUCCH and Random access configurations as shown in Table 3.3 of eNB, UEs and WSN gateways.

When the UL traffic loads reach the estimated UL capacity, it will be shared among the number of attached devices to the eNB and their UL traffic loads. The PUSCH capacity represents the bottleneck in the LTE-A networks [97]. According to [9], [98] and [47], the estimated data plane PUSCH traffic capacity is 73.05 Mbps per TTI. Whereas, the planned maximum aggregated data plane PUSCH traffic loads, of the services and applications in the simulation scenarios, they will achieve 70.7 Mbps per TTI at 235 seconds. The reminder 2.35 Mbps per TTI are left for IMS, SIP, SDP, RTP, RTCP and other application layers control signalling traffics, such as Transport, Session, Presentation and Application layers. Since the latter protocols, services, applications and layers traffic loads are measures of data plane traffic loads apart from LTE network control plane signalling overheads such as NAS and RRC [69].

To provide an acceptable estimation of the long term performance measure for the proposed framework. The generated traffic, from applications used by any node in the simulation models, is only created when the application is active. The default setting of Riverded Modeler requires a network warm-up time at the beginning of the simulation experiment [9], which is typically set to be 100 seconds [99]. This time is important in any network simulation model run for the first time from an empty scenario to allow queues and other simulated network parameters reach a steady-state running conditions. In addition, it allows other devices such as routers and servers in the simulated scenario to initialize. Therefore, 100 seconds warm-up time provides a sufficient amount of time for all the network protocols to initialize and converge to their stable states [99] [93]. The RAPs and attaching processes of the HTDs and WSN gateways to the EPS were done between 100 to 105 seconds of the

simulation run time, on the random basis with different time instances for each device. The HTC services request and the applications starting times were set within 105 to 110 seconds of the simulation run time. The MTC services and applications traffic flows starting and initialization times were set at 135 seconds as mentioned in section 3.2.

3.3.1 Radio access node performance

Fig. 3.6 shows the total records of the PUSCH utilization percentage, aggregated PUSCH throughput and Physical Downlink Control CHannel (PDCCH) utilization percentage of the eNB respectively during the simulation runs.
In Fig. 3.6a and Fig. 3.6b, the proposed model gave a better utilization percentage and a good throughput, respectively. The default model utilized 100% of PUSCH at 174 seconds, with maximum aggregated PUSCH throughput of 37 Mbps per TTI. While the proposed model achieved 100% PUSCH utilization at 228 seconds, with maximum aggregated PUSCH throughput of 64 Mbps per TTI. At 174 seconds there were 1400 active MTDs, while at 228 seconds were 3290 active MTDs. The PDCCH reaches full capacity utilization in the default model at 228 seconds of simulation run time, while in the proposed model performs 95% utilization at congestion condition, as shown in Fig. 3.6c. It is clear from these physical layer KPIs the eNB has got an improvement in PUSCH utilization, PUSCH throughput and PDCCH utilization during congestion, fully or over utilization links, besides normal traffic conditions. The E2E NQoS performance measurements will show us the impact of the proposed traffic flow management policy on the HTC's and MTC's traffic flows, as demonstrated in the next paragraphs.

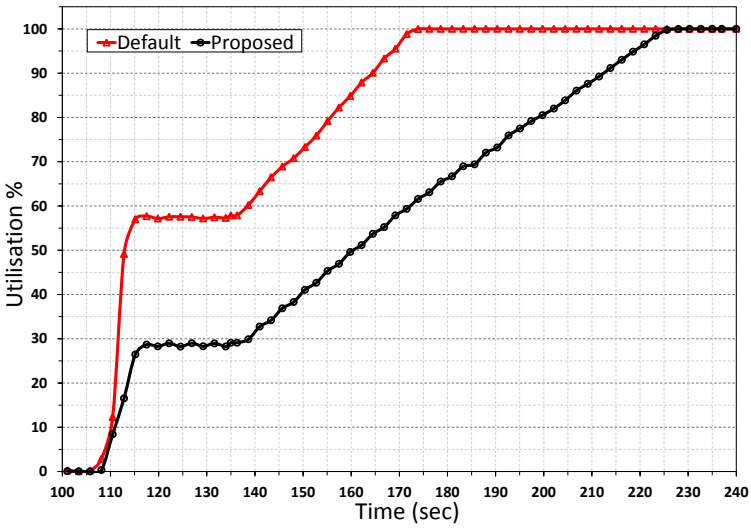

(a) PUSCH utilization.

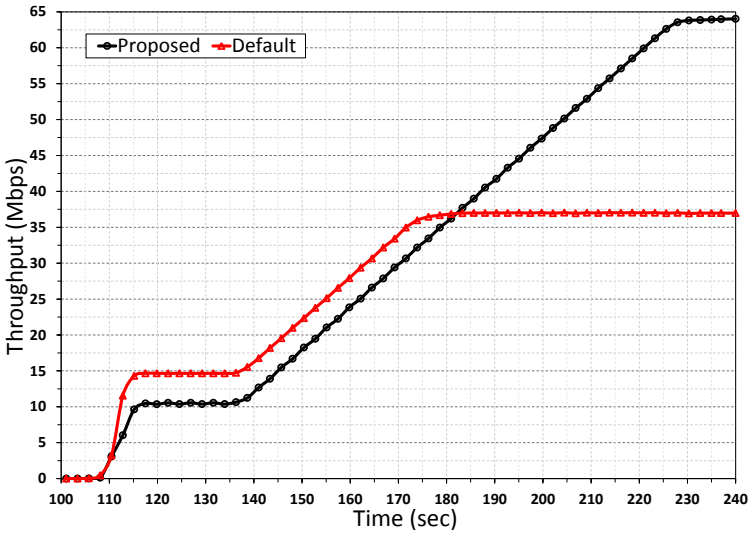

(b) PUSCH throughput.

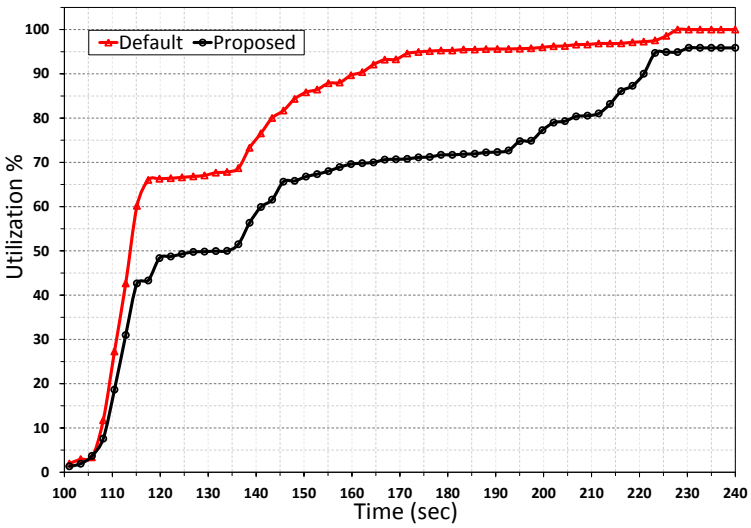

(c) PDCCH utilization.

Fig. 3.6 eNB Performance.

3.3.2 MTC traffic performance

Fig. 3.7 demonstrates the results for the MTC traffic. Fig. 3.7a represent the percentage of the PLR of the received traffic from all active MTDs with respect to their number in the whole network for the default and proposed models. This figure shows a comparison of PLR for these two models and it clearly shows a significant reduction in the packet loss levels for that proposed.

Fig. 3.7b demonstrates one way E2E packet delay between one of the WSN coordinators and the MTC application server at the IP layer, with respect to the simulation run time. The default network model E2E packet delay increased as the traffic generated from newly activated MTDs, they were joined the network cumulatively, the delay was 100 msec at 175 secs of simulation run time, then it was increased dramatically after that time and reached 2016 msec. While the proposed network model gave a significant reduction in the received E2E packet delay levels, where the E2E packet delay range between 11.5 and 15 msec.

Fig. 3.7c shows the average IP packet E2E delay variation in the default and proposed models. This metric was measured in the IP layers of one of the WSN base station (labelled: WSN2) and the MTC application server. The default model gave a maximum average IP E2E delay variation of 615 msec, while for the proposed model, this metric was between 1.87 msec and 4.856 msec. The delay variation is very important, since it affects the monetisation and in sequence delivery of data streams to the transport layer on the receiver side.

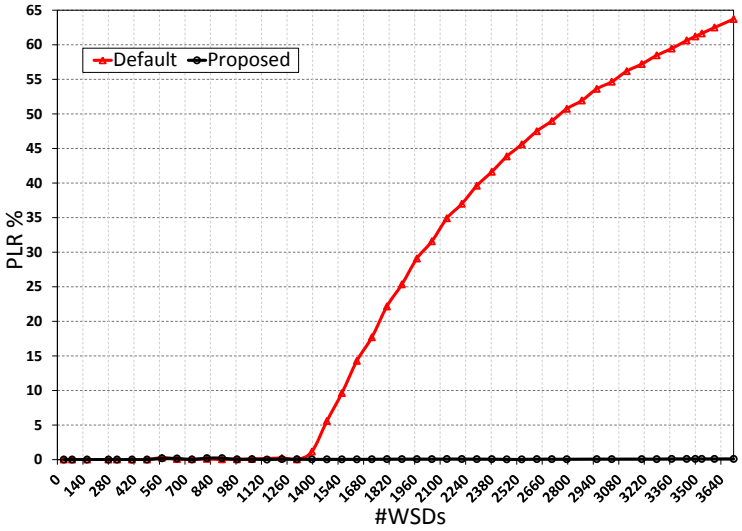

(a) PLR of MTC's traffic.

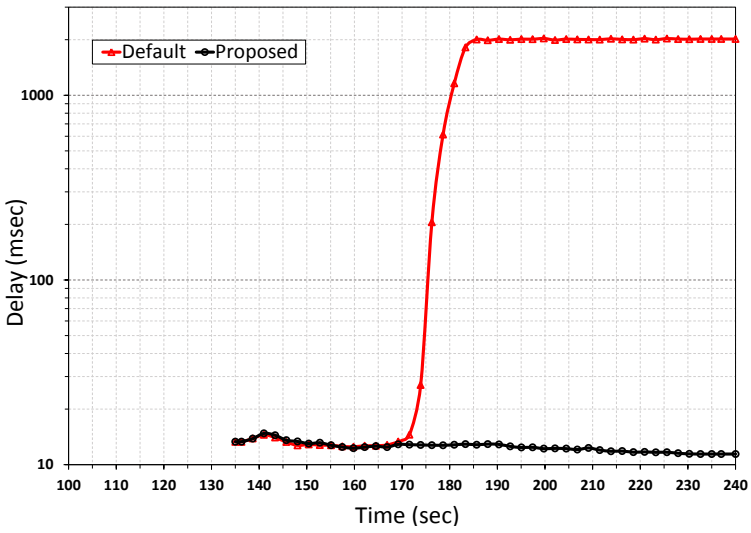

(b) E2E packet delay of MTC's traffic.

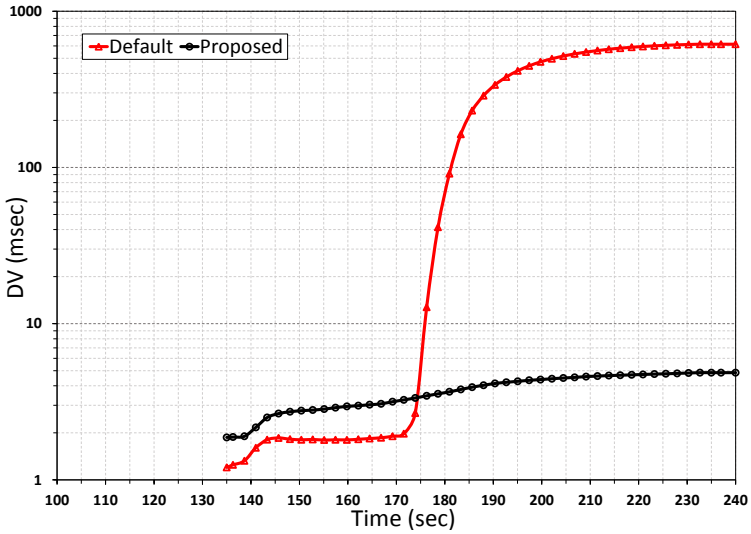

(c) PDV of MTC's traffic.

Fig. 3.7 Simulation results for MTC traffic.

3.3.3 VoLTE service performance

3.3.3.1 Voice call QoS

The simulation results of the VoLTE service are shown in Fig. 3.8, which includes PLR as one of the important metrics of NQoS of VoLTE. It measures the error rate in the packet flow stream, which is forwarded to the voice application by the transport layer.
Fig. 3.8a shows the average E2E PLR in the packets between two calling parties. This figure shows an increase in the PLR value with respect to simulation run time in the default and proposed models. The proposed model's PLR was more than the default one, with the maximum values being 1.81% and 1.61%, respectively.
The PLR per voice bearer in both scenarios remained lower than the maximum allowable limit, which is 1% for the voice application bearer as presented in Table 2.1 [38]. The measured value represents the total accumulated E2E PLR in the UL and DL directions, while the maximum defined voice bearer PLR limit represents a one direction PLR. Therefore, the average of the maximum achieved E2E PLR per voice bearer (UL and DL voice bearers) of the proposed model is 0.905%, whereas for the default model is 0.805%, which is a good level, since most of the up-to-date voice codecs perform well up to 1% PLR [100]. The irregular variation of the PLR during the simulation run time was due to the radio interface environment variation (path loss and fading effects in the UMa model) between eNB and the calling parties as well as the increased traffic loads, during the simulation runs. The consequence of increased traffic loads was throttling the UL, which created congestion in the PUSCH.
VoLTE service packet delay is called mouth to ear delay, which is one of the most important factors to be considered when dealing with the QoS of real time voice service in PS, such as the VoLTE service in the presented network model. Fig. 3.8b shows the average E2E packet delay of the VoLTE in the default and proposed network models.

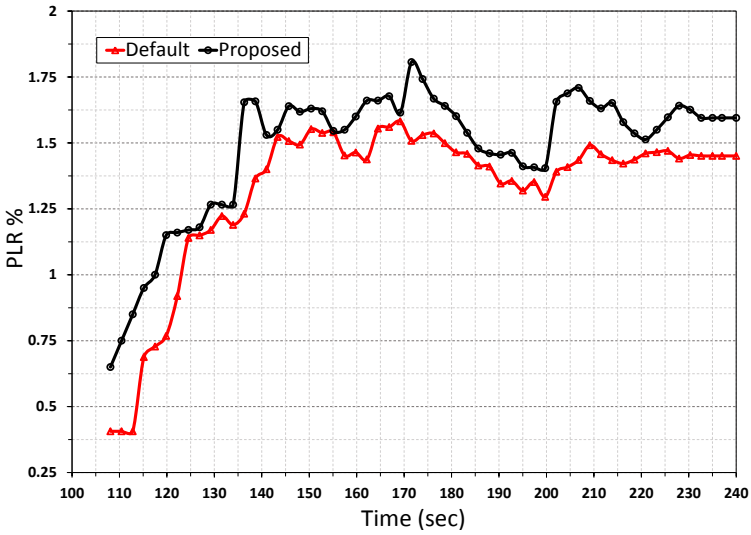

(a) PLR of the VoLTE service.

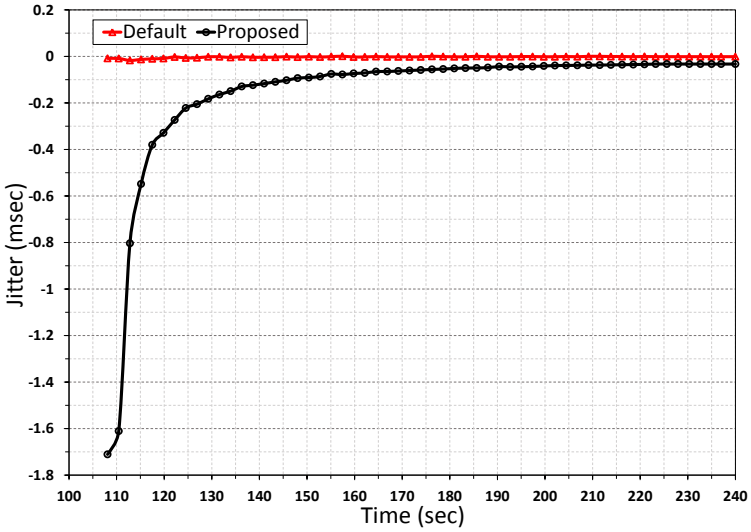

(c) Packet jitter for the VoLTE service.

Fig. 3.8 Simulation results for VoLET service.

The default model average E2E packet delay started at 114.58 msec and reached 116.9 msec at 150 sec of the simulation run time, then remaining at this value until the end of the simulation run. Whereas the proposed network model kept its average E2E packet delay at 122$\pm$0.1 msec from the start of the VoLTE service traffic flow until the end of the simulation run. This measure was taken as E2E, which means it was in the UL/DL directions. Obviously, there was a little degradation in this NQoS, because the proposed model gave higher delay values (about 7 msec) than the default model. These values of average E2E delay in the default and proposed models would still fulfil the 3GPP and the ITU-R standardisations as

well as the requirements for VoLTE service E2E packet delay, where the maximum allowable one way packet delay is 150 msec in order to accomplish high QoE [46, 101] and [102] . Packet jitter is one of the most important QoS metrics of real time services. Fig.3.8c shows the average jitter of the VoLTE service in the proposed and default models. In this figure, the default network model gave a better packet jitter performance than the proposed network model. The average packet jitter values of the default model were between -0.00844 msec and -0.000974 msec for the received packets of the VoLTE service traffic up until the end of simulation run time. Whilst the proposed model's average packet jitter value for the VoLTE service traffic flow started at -1.7 msec and by the end of the simulation it had decreased to -0.0326 msec. Clearly, there is degradation in this NQoS metric, for a consequence of the increased average packet jitter will be an increase in the time delay of the received packets in the de-jitter buffer [103]. The value of the average packet jitter in the proposed model was reduced. The ITU-R has recommended 25 msec jitter as an acceptable value for the delay variation [104].

3.3.3.2 Voice call QoE

The users' QoE levels of real time voice call are a measure of users' satisfaction levels when engaging with the VoLTE service. The MOS is a well-known metric to measure QoE by using its E-Model, according to ITU-T G107 [105]. This QoE metric can be reported as sampled, interval or cumulative metrics, using a modified instantaneous E-Model[106] [107]. MOS statistics are collected using instantaneous E-Model, it was set in the simulation models to report MOS value as a sample mean of 100 MOS instantaneous sampled statistics every 2 seconds, which is called bucket mode [9]. Each one of the 100 MOS instantaneous sample statistic is collected within 20 msec time interval. Whereas, the voice codec frame size is set to treat 1 digitized voice frame every 10 msec, meaning that the voice traffic has an inter-arrival time of 10 msec. Therefore, the MOS instantaneous sampled statistics analysis relies on 2 current and 2 previous digitized voice frames QoS metrics, such as received voice application, frame delay and error rate [107] [108]. Fig. 3.9 shows the MOS of the default and the proposed network models. The default model started with MOS of 4.3532 then dropped to 4.3518, whereas the proposed network model started at MOS of 4.347 then increased to 4.349. Moreover, the levels of QoE represented by the MOS value, maintained within good acceptable levels during the whole voice call time for both models.

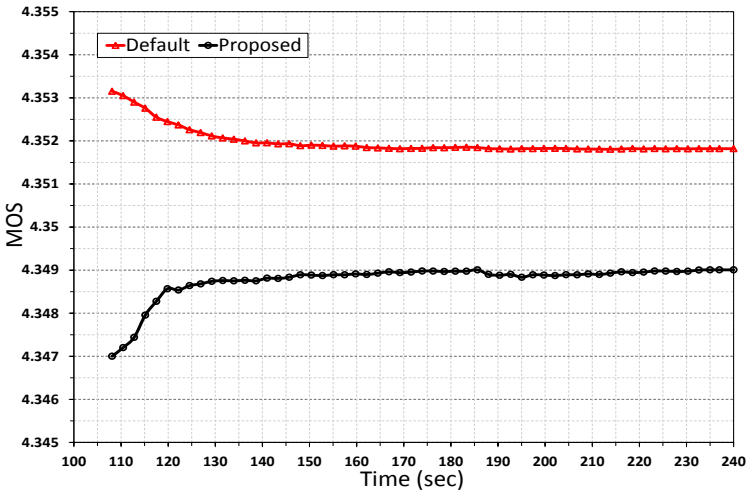

Fig. 3.9 MOS of the VoLTE service.

3.3.4 Video conferencing service performance

A Video conferencing service over LTE QoS parameters represented by PLR, packet delay and packet jitter should be assured at certain levels in order to maintain a good QoE. Fig. 3.10a demonstrates the PLR for the default baseline and proposed network models with respect to the simulation run time. This QoS metric was measured in the received packet stream forwarded by the transport layer to the video conferencing application. The default model average PLR at the start of traffic flow at 108 sec was 4.231% and this increased to 92.8% at the end of the simulation. Whilst the proposed network model was started with a PLR of 0.846%, which then increased to 8.3% at the end of the simulation.

Fig. 3.10b shows the average E2E packet delay of the video conferencing service packet stream forwarded to the application layer from the transport layer at the destination point. In this figure, the QoS metric is represented by the average E2E packet delay for the default and proposed network models. The measurement starts from 108 sec of simulation run time, when the video conferencing service starts its traffic flow, until its end. The proposed network model gave a better average packet delay performance than the default one during the whole period of the simulation run, especially at the end of simulation, which represents the heavy load traffic period. In this part, the proposed network model gave a better packet delay performance than the default one, since the maximum average packet delay in the proposed network model started with 24.9 msec and ended with 36.5 msec. Whereas, for the default network model maintains on 35 msec, then at 228 seconds it was increased dramatically and reached 256.5 msec at the end of simulation runs.

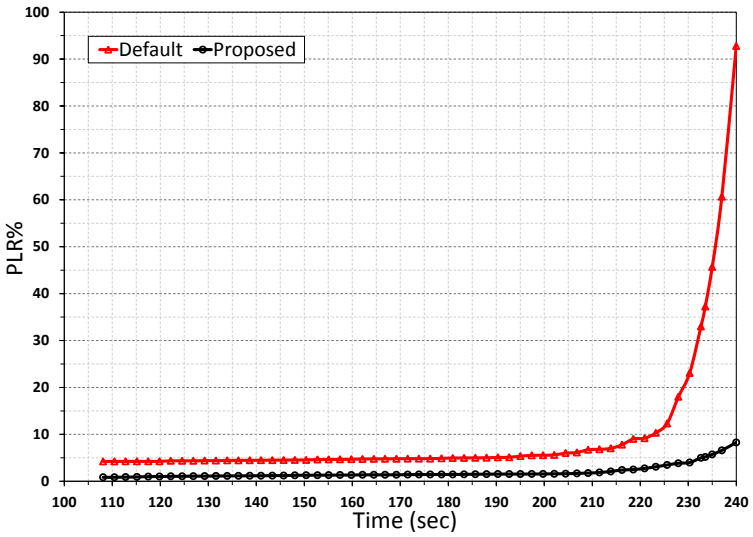

(a) PLR of the Video conferencing service

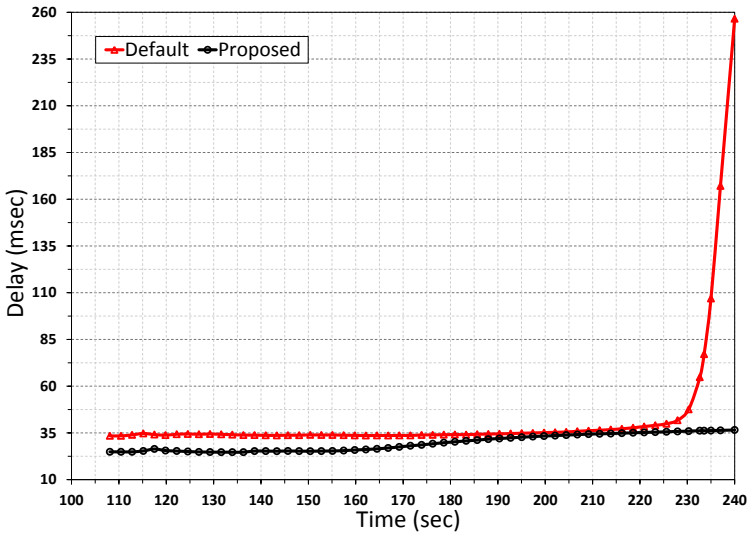

(b) E2E packet delay of the video conferencing service

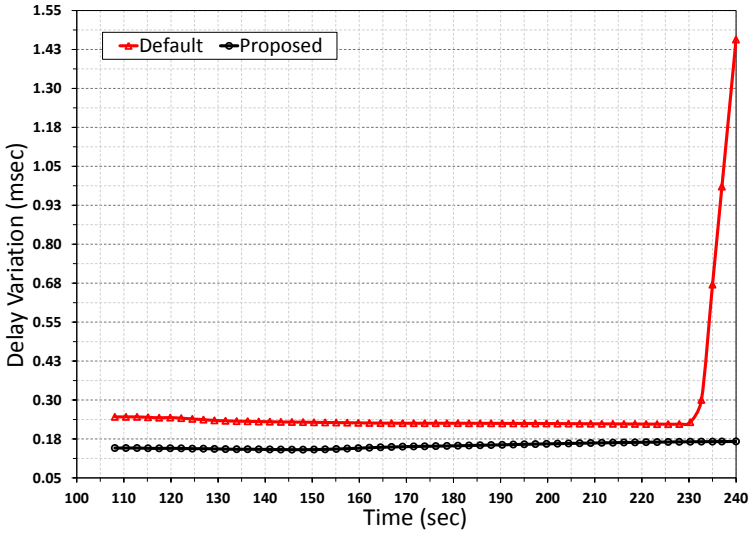

(c) PDV of the video conferencing service

Fig. 3.10 Simulation results for video conferencing service.

Another important QoS factor that has an impact on the interactive real time video conferencing service's QoE, is the PDV. Fig. 3.10c shows the Average PDV (APDV) with respect to the simulation run time of the video conferencing service for the received packets stream, which was forwarded from the transport layer towards the application layer at the called end device. This APDV was measured between the two video calling parties. In the Fig. 3.10c, it can be seen that the proposed network gave a higher APDV between 0.144 msec and 0.167 msec up to the end of the simulation run time. However, the default network model was started with 0.2458 msec and then, it gave a lower APDV of 0.2228 msec. Furthermore, at point 227 sec of simulation run time, the APDV increased rapidly and reached 1.457 msec by the end of the simulation. It is clear that the default model's APDV increased rapidly, when the network was under a heavy traffic load, which could be a serious issue on the receiver side for real time playback video application [103]. The improvement of the video NQoS metrics in the proposed model over the default model is related to the GBR video bearer setting and allocation, such as QCI and ARP. It is also related to the use of the proposed traffic management policy, which is set as fixed share represented by α function (as listed in Table 3.1). Its impact was clear when the eNB's UL has been fully utilized by HTC and MTC traffics. In the default model the video bearer's NQoS metrics such as PLR, packet delay and PDV was kept within a specific range. However, at 228 seconds the capacity of PDCCH utilization in the default model reaches 100% as shown in Fig. 3.6c. All traffics now compete for the PDCCH space. Therefore, the aforementioned NQoS metrics in default model it were shot up rapidly at the end of simulation, while in the proposed model it were kept within acceptable levels, as shown in Fig. 3.7, Fig. 3.8, Fig. 3.9 and Fig. 3.10.

3.3.5 FTP and HTTP services performance

Figuers 3.11 and 3.12 show the results obtained of the FTP and HTTP applications in terms of E2E packet delay, PDV and TCP retransmission metrics.

3.3.5.1 FTP application QoS:

FTP NQoS metrics has been inspected in the FTP application server as a destination point at the transport layer. The FTP as a non-real time service and it uses the TCP retransmission mechanism between the source and destination points.
Fig. 3.11a shows the average E2E packet delay for all packets with respect to the simulation run time, which was sent from the UEs that using FTP application, for the default and proposed network models. The proposed network model gave a higher packet delay in comparison to the default network model. Specifically, the proposed network model's average packet delay was between 13.74 msec and 14.04 msec, whereas that for the default model was between 12.76 msec and 13.47 msec.
E2E delay variation represents another important QoS factor for the FTP application and Fig. 3.11b shows the average for packets at the IP layer between one of the UEs and the FTP application server. It is clear that the proposed network model's delay variation was higher than the default network model. The maximum average for the former was 9 msec, while that for the latter was 7.5 msec. As was mentioned before, the FTP application will use the TCP retransmission request mechanism, which could be reflected as lost or outdated packets at the transport layer.
Fig. 3.11c demonstrates the average TCP retransmission count per TTI with respect to simulation run time for the default and proposed network models. It shows that, with the default model, no retransmission occurred during the FTP application traffic flow period. While for the proposed network model it did happen, which means that either there was a network congestion or a loss of packets received in the transport layer.

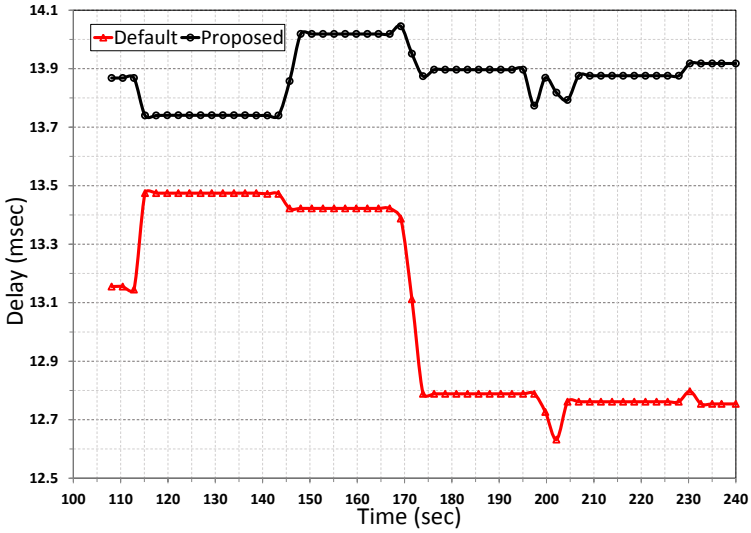

(a) E2E packet delay for the FTP application.

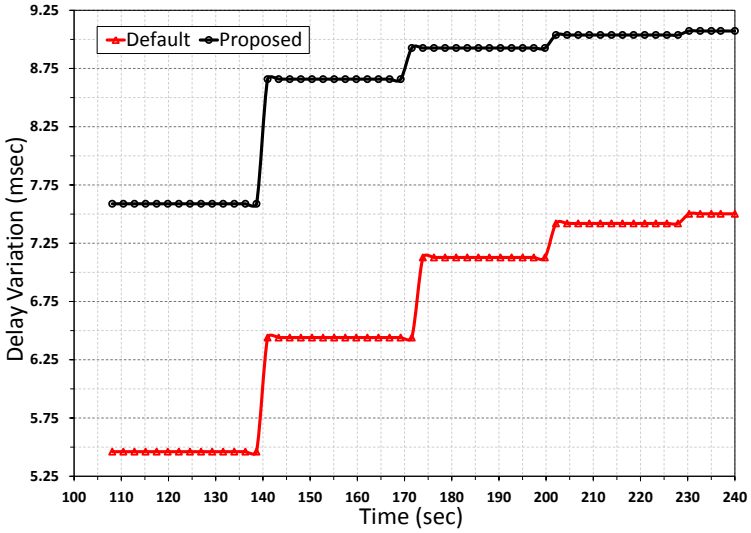

(b) Packet delay variation of the FTP application.

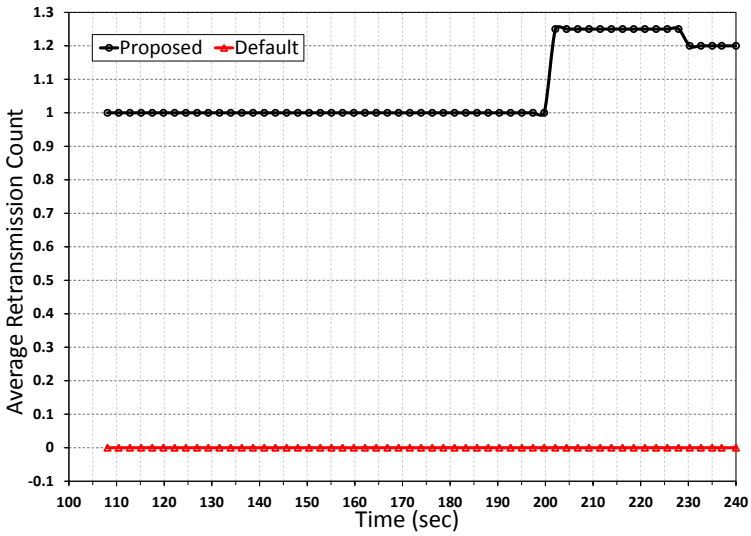

(c) TCP retransmission count per TTI of the FTP application.

Fig. 3.11 Simulation results for the FTP application.

3.3.5.2 HTTP application QoS:

HTTP service QoS factors were checked at the HTTP Application server in the transport and IP layers. This is a non-real time service, which uses the TCP retransmission mechanism between the user and the application server.

Fig. 3.12a shows the average E2E packet delay for all received packets at the transport layer with respect to the simulation run time, which has been sent from the UEs that use the HTTP service application, for the default and proposed network models. The proposed network model gave almost a constant average delay, whilst the default network model did not.

The proposed network model's average packet delay was between 19.6 msec and 18.6 msec, whereas that for default network model was between 16.8 msec and 22 msec. E2E delay variation is another important QoS factor for the HTTP service and is shown in Fig. 3.12b. This figure shows the average E2E delay variation of received packets at the IP layer between one of the UEs and the HTTP service application server. The proposed network model's delay variation was higher than for the default network model. The maximum average E2E delay variation of the former was 16.8 msec, while that for the latter was 13.5 msec.

Fig. 3.12c demonstrates the average TCP retransmission count per TTI with respect to simulation run time for the default and proposed network models. It shows that, in the default model, no retransmission happened during the HTTP application traffic flow. While in the proposed network model this did occur, which reflects that either there was a network congestion or a loss of packets received in the transport layer.

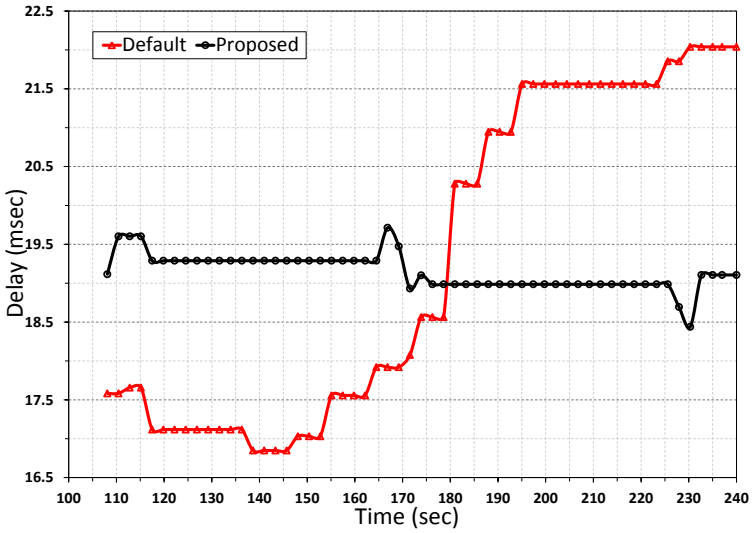

(a) E2E packet delay for the HTTP application.

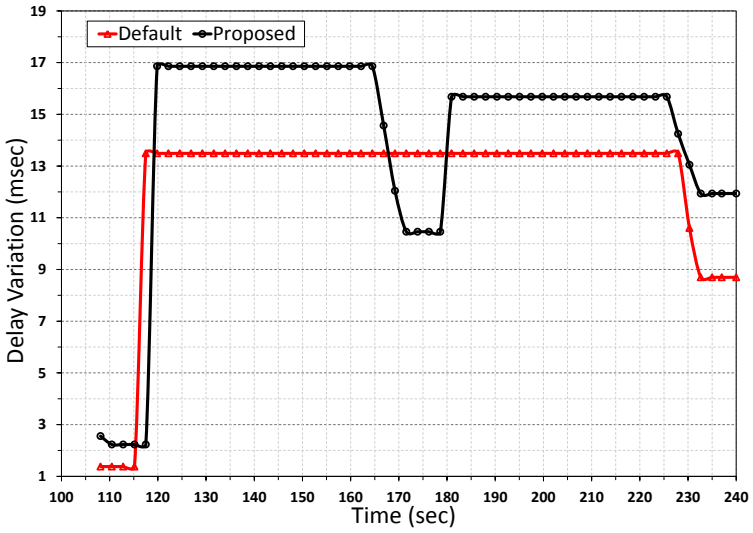

(b) Packet delay variation of the HTTP application.

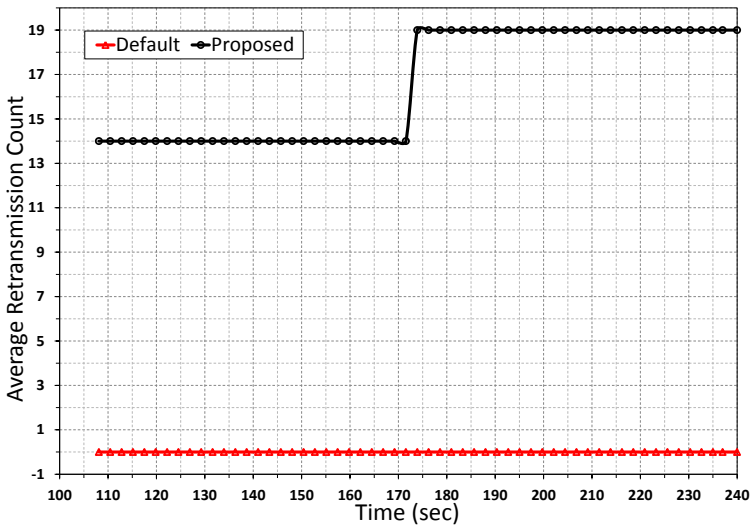

(c) TCP retransmission count per TTI of the HTTP application.

Fig. 3.12 Simulation results for the HTTP application.

3.4 Discussion

NQoS is a measure of the reliability and performance of the network nodes and links. It is a composite metric, being based on various factors that specify the characteristics of the network situation and consequently, deteriorations or improvements in the NQoS level can be brought about through some combined factors so as to fulfil AQoS requirements.
The proposed traffic management policy, with the assistance of WSN gateway, achieved high QoS, as presented by all the NQoS measurements of the MTC and HTC traffic flows in this work at the IP and transport layers. The eNB performance achievement in terms of the UL and DL capacity enhancement was in PUSCH utilization, PUSCH throughput and PDCCH utilization. In the proposed model the PUSCH utilization was reduced on average by 33.6% over the default model. The PUSCH throughput of the proposed model was achieved 73.2% increase over the default model, specifically when congestion was arisen. Another impact of the proposed flow management policy, it was on the PDCCH utilization achieve 5% decrease at congestion condition over the default model. Furthermore, an increase of 179% in the radio access node connectivity, from the number of active connected MTDs point of view. The achieved NQoS enhancement was in terms of the radio access node physical layer performance parameters as well as of the MTC traffic flows exhibiting a decrease of 99.45% in the PLR, a decrease of 99.89% in the packet E2E delay, a decrease of 99.21% in the PDV. Despite there being an increase of 12.42% with respect to the default baseline model occurred in terms of the VoLTE service as represented by its PLR, several offsetting achievements were delivered by the proposed traffic management policy, including a decrease of 9.5% in the PLR with respect to the 3GPP maximum PLR allowable limit for the VoLTE service, an increase of 4.5% from the baseline model for the packet E2E delay, a decrease of 18.79% from standard 3GPP maximum standard packet E2E delay, a reduction of 99.87% from the standard 3GPP maximum jitter value for the packet jitter and a decrease of 0.074% in terms of QoE from the default model values, with an increase of 8.73% from the standard values. The E2E VoLTE NQoS are the PLR, packet delay and packet jitter, as a composite metrics. The degraded level of them can be improved by using a lower rate voice codec or adaptive multi-rate voice codec at the VoLTE application layer level [109]. It can be also improved by employing a scheduling algorithm at the physical layer level, specifically for VoLTE service bearer, such as TTI bundling and Semi-Persistent Scheduling (SPS) [110]. These scheduling techniques are exploiting processing delay difference between application layer voice frame generation process and physical layer transmission procedure [111].

Another NQoS improvement was for video conferencing, specificaly at congestion condition, where a reduction of 85.75% regarding PLR, 85% of packet delay and 88.5% of PDV were achieved, when compared with the default model values.
The HTTP service NQoS achievement regarding packet E2E delay was a decrease of 13.31% and the PDV provided an increase of 37.26% to those of the baseline model. In spite of the obtained increment in the PDV, it represents a decrease of 52.26% from the standard maximum specified value.
FTP service NQoS delivered packet delay and delay variation increases of 9.12% and 20.9%, respectively, when compared to the default model. Compared with the standard specified maximum allowable limits, the proposed policy achieved a rapid decrease of 95.36% in the packet delay and a reduction of 63.71% in delay variation.

Finally, the proposed model achieved the specified bearer settings for the HTDs and MTDs. Moreover, the QoE of the real time application users of the VoLTE service was maintained within the satisfaction level, as measured by the E-Model's MOS scale. The QoE of the video conferencing service has been attained according to the perspective of obtainable NQoS metrics compared to the standard AQoS requirement of this service.

3.5 Summary

This chapter has addressed the challenges of heterogeneity by integrating HTC and IoT traffic through their mutual interaction within network elements (nodes and links), in terms of the resultant and distinct E2E NQoS metrics. The motivation for the chapter was based on the fact that the existing LTE-APro PCC rules and procedures do not differentiate between the user type of the terminal devices, which produces a lack of NQoS levels being offered and hence, potentially not meeting the AQoS demands made by the used service.

An access WSN gateway has been proposed to provide E2E connectivity for MTC's traffic flow within the licence spectrum of LTE-APro media. An approach of protocol conversion and facilitation of the control of the EPS network resources' QoS level assigned for MTC traffic flows, in the context of PCC functions and rules, has been provided. A policy for traffic flow management that defines MTC traffic flows over the EPS network has been put forward, in order to use a fraction of the available network resources in a seamless manner, accompanied by a new specific group of QCIs, assigned to define the QoS levels of the MTC bearers' connectivity. The allocation of network resources for MTC traffic flows are tuned based on terminal type needs, i.e. on the level of importance of the traffic type sent by MTD. In addition, The QoE of real time application human users is assured within the perceived quality levels.

The simulation results have shown that the proposed policy of traffic flow management within the LTE-APro network infrastructure outperforms the current one in terms of NQoS levels, not only for HTCs traffic flows but also, for those of MTCs. However, in terms of the VoLTE service, it some degradation was encountered with the offered NQoS, due to the use of high rate codec in the application layer and the absence of a specific scheduling procedure to the VoLTE bearer at the radio interface. Nevertheless, the VoLTE service QoE level was retained within the recommended standardisation level.

Chapter 4

Heterogeneous Dynamic C-RAN Deployment Based on a Multiple BBU Pools Approach for NGN

Overview

With the innovation of C-RAN, the allocation of BBU pools, such as best locations and an optimized number of BBU pools with connected numbers of RRHs, have become a crucial issue due to network resource limitations. In this chapter, an approach for allocating existing 4G installed network radio access nodes to multiple BBU pools, which is proposed to deploy 5G C-RAN and improve the offered NQoS. The proposed approach involves performing four sequent algorithms starting with i) radio access node clustering based on the PSO algorithm then, ii) model selection BIC through iii) a measure of spread technique then ends by, iv) Voronoi tessellation, which is used to consider a DC-RAN operation, that adaptively adjusts the main RRH coverage range according to the traffic load required as well as providing energy saving. The numerical results of the approach show that the optimized partition of the proposed network model is 41 BBU pools, with an average density of RRHs per pool area, which matches the primary average density of the radio access nodes per network area. A real heterogeneous LTE data network has been provided by an operator to evaluate such approach.

4.1 System Model and Problem Formulation

A geographical area $\mathscr{S}$, has N number of radio access nodes, as shown in Fig. 4.1, that represents actual sites of radio access node locations.

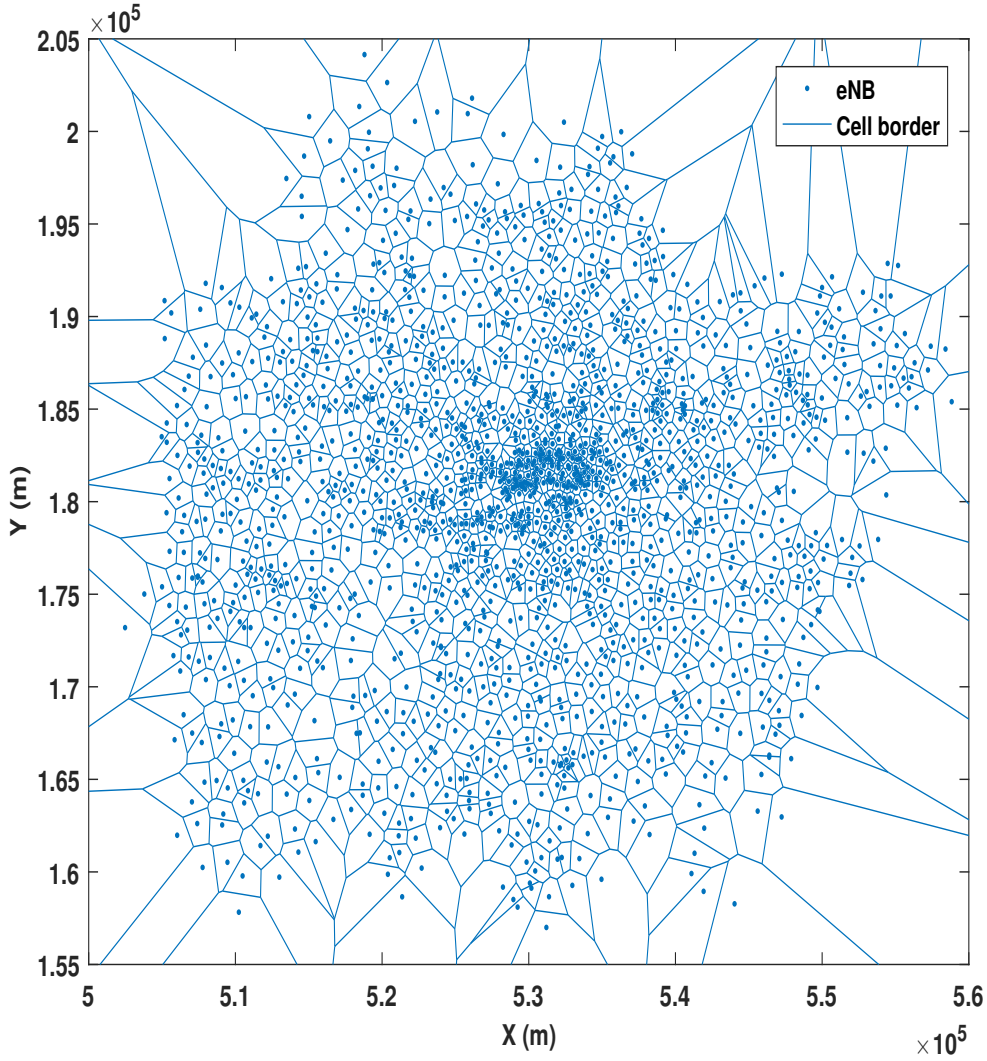

Fig. 4.1 LTE BSs deployment

The main objective of the proposed approach is finding the optimal C-RAN multiple BBU pools configuration that achieves high NQoS through:

- Optimal number of pools.
- Optimal pools sites configuration.

- Optimal location of CO.
- Optimal number of connected RRHs with each CO.

for the introduced real network deployment model that proposed for deploying the C-RAN.

The multi pooling deployment in d-dimensional Euclidean space is the process of partitioning N given nodes into a group of M pools as shown in Fig. 4.2. This figure shows M pools partitioning process, that will be done on the network model which was shown in Fig. 4.1, this figure is presented for describing the related formulas that will be used to run the proposed optimisation algorithms.

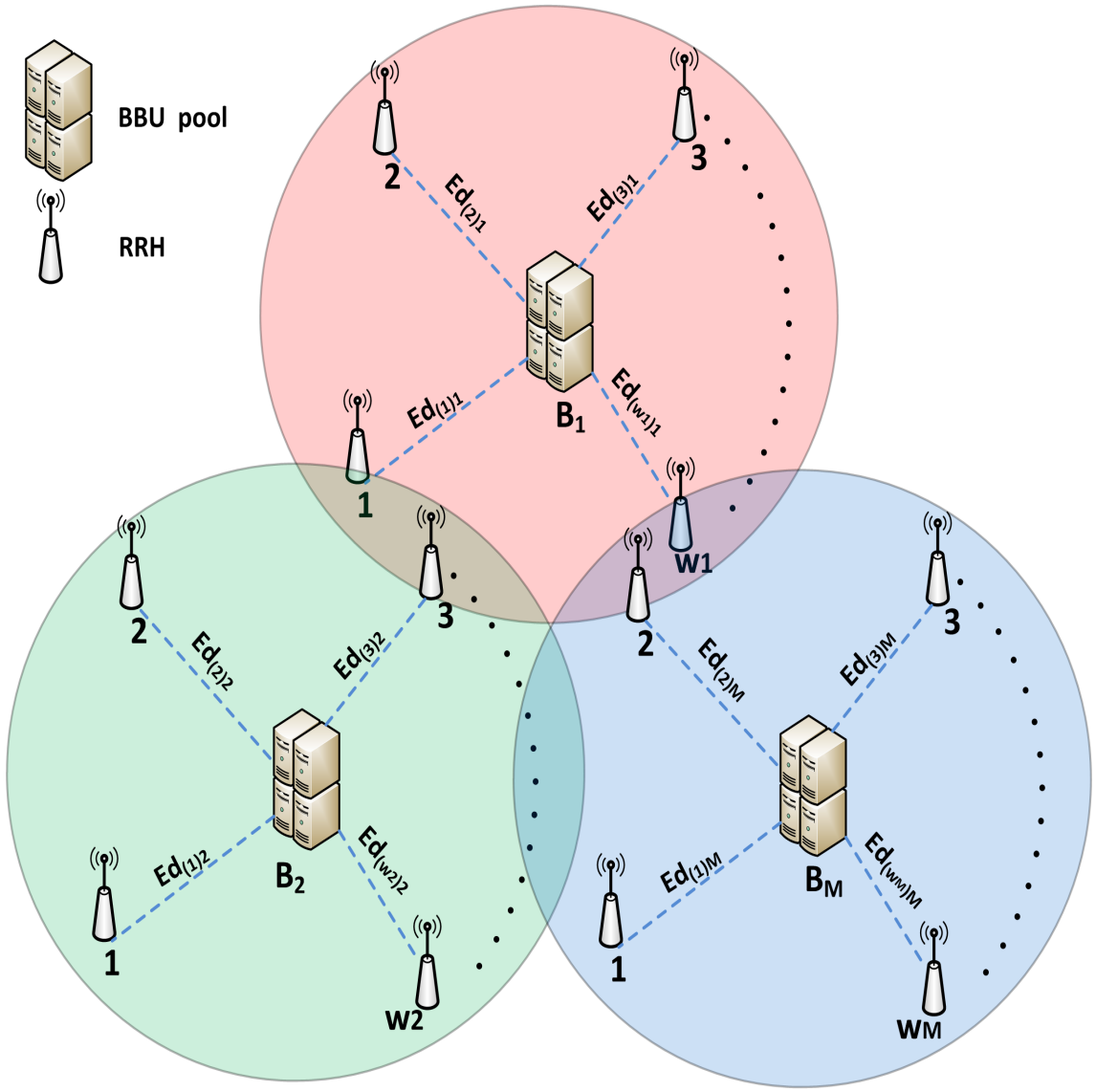

Fig. 4.2 Multiple BBU pooling and RRH clustering scheme

Let's take a two dimensional space of x and y, where, (x_r,y_r) are coordinates of the r^{th} BBU pool position B_r, [$r = 1$, ..., M], M is the maximum number of pools in the network, and (x_{v_r}, y_{v_r}) are the coordinates of the vth RRH position R_{v_r} within the r^{th} pool, where, $[v_r = 1, ..., w_r]$ and w_r is the maximum number of RRHs in the r^{th} pool. Each RRH's site R_{v_r} has its Euclidean distance with respect to its B_r pool position as in Eq. 4.1.

$$Ed_{(B_r,R_{v_r})} = \sqrt{(x_r - x_{v_r})^2 + (y_r - y_{v_r})^2} \tag{4.1}$$

The sum of all the distances of the pool r from the B_r pool site location to all its RRHs positions is d_{Br} , which is represented by Eq. 4.2.

$$d_{B_r} = \sum_{v_r=1}^{w_r} \sqrt{Ed_{(B_r,R_{v_r})}} \tag{4.2}$$

In the single BBU pool network configuration, this function can be used as a fitness/cost subject to a minimum, which helps the search process on the optimal solution as Br with respect to its associated R_{v_r}. In this case $r = 1$, $v_r = [1, ...,$N] and $w_r =$N.
In terms of the multiple pooling situation, when the proposed network number of BBU pools to be formed is M. The Global Sum (GS) of d_{B_r} as shown in Eq. 4.3.

$$GS = \sum_{r=1}^{M} d_{B_r} \tag{4.3}$$

Hence, to achieve a candidate M pool network configuration that is subjected to conform for the minimization of the global optimization function among all other pools' solutions. That achieves a minimum possible front-haul distance, then the cost function can be expressed as a minimisation of GS as in Eq. 4.4,

$$cost\,function = min\ GS \tag{4.4}$$

which is considered as a global fitness/cost function in the search for the optimized solution.

4.2 Multiple-Pools Partitioning Based PSO Algorithm

Methods and approaches for solving Non Polynomial (NP) hard problem have become a very important topic in recent years. Genetic Algorithm (GA) and Particle Swarm Optimization (PSO) are considered very popular and they are similar evolutionary algorithms for solving

the NP-hard problem. The GA is more proper for discrete optimization, while the PSO is more suitable for continuous optimization [112]. The GA has an expensive computational cost in comparison with the PSO. The authors in [113] attempted to proof that the PSO algorithm has the same effectiveness in finding the optimal solution as the GA but with less function evaluations. Thus, the work in this chapter are based on PSO algorithm to find optimal solution. PSO algorithm is built based on the location of the centres (BBUs' pool position) that achieves minimum distances with all cluster members (RRHs' positions), this is called centre of minimum. The network partitioning process based on the proposed PSO algorithm has been used to search the solution space to find the solutions which are:

(a) Optimal partitioning allocation configuration for M pools in the whole network.

(b) Optimal RRH number w_r in each BBU_r pool area.

(c) Optimal position allocation (x_r, y_r), which is B_r of each BBU pool within the r^{th} pool area.

With the PSO algorithm, as particles have random speeds through the solution space [114], where each particle i is assessed at instance t by the minimized cost function, with adjusted position toward

- Particle's best solution (position) found as $pbest_i(t)$.
- Best overall solution as $gbest_i(t)$.

Then, based on the particle parameters at instance t, which are $B_i(t)$ at (x_i, y_i) as a current solution, its speed $s_i(t)$ as well as its best position $pbest_i(t)$ and its best global position with respect to other particles $gbest_i(t)$, then the speed update formula, in the pool r, of the particle i at instance $(t+1)$ will be represented as in Eq. 4.5.

$$\begin{aligned} s_{ri}(t+1) = a * s_{ri}(t) + C_1 * b_1 * [pbest_{ri}(t) - B_{ri}(t)] \\ + C_2 * b_2 * [gbest_{ri}(t) - B_{ri}(t)] \end{aligned} \tag{4.5}$$

where, $s_{ri}(t)$ is the current velocity, $s_{ri}(t+1)$ shows the updated future velocity, $B_{ri}(t)$ represents the current position of the BBU pool , C_1 and C_2 are the acceleration coefficients, b_1 and b_2 are vectors of uniformly distributed random numbers in the range [0 1], and a represents the initial value. Each new iteration will produces a new $B_{ri}(t+1)$ as the updated position of the r^{th} pool, as in the following Eq. 4.6

$$B_{ri}(t+1) = B_{ri}(t) + s_{ri}(t+1) \tag{4.6}$$

until the iteration process reaches the projected cost function. Each individual particle represents a possible optimal solution; they will be updated interactively with other particles for all pools simultaneously.

The proposed PSO algorithm undergoes the process that is described in Algorithm 1. Where for each single B_r the Euclidean distance of its possible related RRH as R_{v_r} is calculated amongst each possible particle position (x_r, y_r) as a possible solution for the B_r as pool position, as in Eq. 4.1, which settles inside the r^{th} possible BBU pool area. Thus, each particle i needs to achieve minimum distance from its (current or future) position to all its anticipated RRH sites that can provide minimum cost, according to d_{B_r}, as in Eq. 4.2. Additionally, regarding the interaction with the others pools' particles with their sets of possible associated RRHs, the anticipated B_r's RHH sites' Euclidean distances maximum limits constraint is according to Eq. 4.7.

$$d_{B_r} \leq d_{B_l} \quad (where,\ l \neq r) \tag{4.7}$$

specifically, for the r^{th} pool as well as for all the other BBU_l $\{l = [1,...,\mathrm{M}],\ where,\ l \neq r\}$ pools during the search procedure simultaneously. This constraint limit represents the interactive relationship among all the other particles in all M pools simultaneously.
This constraint criterion effects the proposed cost function Eq. 4.4, which produces an updated $gbest_r(t)$ $\{r = [1,...,\mathrm{M}]\}$. These processes are performed in each iteration, for as many as the number of the populations until the iteration reaches the required solution for all M pools in the network area $\mathscr{S}$.

Algorithm 1 Multiple-Pools Partitioning-PSO

Input

(i) Specified network, $\mathscr{S}$.

(ii) RRH number and their (x,y) coordinates.

(iii) Number of BBU pools, M.

(iv) Set MAX ITERATION.

(v) Set PopSize

(vi) Set $\{a, C1, C2\}$

Output

(i) Optimal multiple BBU pools number.

(ii) Optimal RRH number in each BBU pool.

(iii) Optimal BBU pool site position (COs).

Initialisation Choose the number of M random initial COs' coordinates

1: **for** $r = 1 \rightarrow$M **do**
2: $B_{ri} = gbest_{r_i}$
3: **end for**
4: **for** $it = 1 \rightarrow$ MAX ITERATION **do**
5: **for** $t = 1 \rightarrow$ PopSize **do**
6: **for** for each r^{th} pool particle i **do**
7: Select the connected group RRHs w_{ri}
8: **if** $d_{B_{ri}} <= d_{B_{li}}$ $(where,\ l \neq r)$ **then**
9: $Ed_{(B_r, R_{v_r})}$ as in $Eq.4.1$
10: **end if**
11: **end for**
12: **end for**
13: **if** $cost function(t) == cost function(t+1)$ Eq. 4.4 **then**
14: go to **21**
15: **end if**

Create the next generation particles

16: For each particle i in $\mathscr{S}$
17: Update velocity, s_{ri} as in $Eq.4.5$
18: Update new position, B_{ri} as in $Eq.4.6$
19: next it
20: **end for**
21: **END**

4.3 Bayesian Information Criterion

For a predetermined number of BBU pools M, the PSO multiple pools algorithm gives optimal pools locations and optimal number of connected RRHs, which are subject to the introduced cost function and constraint limits.
The required number of pools for a particular network can be determined in order to fit a specific requirements of the network operators or services and applications needs. For example, it can serve to establish the:

- Fronthaul latency requirements [115].
- Limitation of the BBU pool processing capacity [71].
- Backhaul capacity limits [116].

Therefore, this optimal number of BBU pools in the specified network is needed. Additionally, the optimization process aims in this chapter for the equilibrium in the RRH densities (RRH number/pool Area) with minimum delay and minimum latency fronthaul considerations among all COs. Accordingly, the PSO algorithm based center of minimum has to be complemented with another technique to find the optimal number of BBU pools that conforms to the required network planning goals.
The most popular technique is the BIC, which aims at selecting the number of BBU pools that maximizes the posterior probability among the RRH sites' geographical coordinates information.
BIC focuses on an information approach that takes into account the specific statistical analysis, by estimating the likelihood function of all set of models of interest for each candidate model; the model here referring to the multiple pools network configuration as an output of the PSO algorithm [117]. In general, BIC can be defined as a means of selection among a finite set of models, where the system with the lowest BIC value is chosen as the optimal solution [26]. The BIC formula is shown in Eq. 4.8 [72].

$$BIC = [N * ln(\frac{GS}{N})] + [M * (d+1) * ln(N)] \tag{4.8}$$

where, d is number of the dimensions of coordinate system, which is two as counts of x and y. The BIC has been successfully applied to integrate the PSO multiple BBU pool algorithm by determining the candidate set of the multiple BBU pools network configurations as shown in Algorithm 2, which runs the BIC evaluation K times as the number of the achieved network partition configuration.

Algorithm 2 Bayesian Information Criterion (BIC)

Input: PSO result [1 C]
Output: BIC=[]
1: **for** K=1 to C **do**
2: Clear old GS value
3: Calculate GS as in Equ. 4.3
4: Calculate BIC as in Equ. 4.8
5: Next K
6: **end for**
7: **END**

4.4 Measure of RRH Spread Technique

BIC algorithm has been adopted in order to choose the optimal number of partitioned pool configurations of the proposed network. However, it gives a group of optimized solutions for the multiple BBU pool configurations, which are approaching to the required optimal solution. Hence, it is still necessary to find the optimum number within this filtered group of partitioned network configurations. Another criterion can be used to narrow the search toward the optimized number of partitions, which is based on the fair distribution of the number of connected RRHs among all the BBU pools.

The measure of spread technique [118] relies on analysis of the statistical characteristics of each multiple pool network configuration for the number of connected RRHs with each BBU pool, which are the outcome of BIC. These statistics are Range, Stdv and Variance, which serve to measure the spread of RRH connections for each multiple BBU pools network configuration. When the evaluated model achieves minimum values of these statistics among others models that will indicate that this model will provide the essential equality among all other models in the sharing of network loads and fair distribution of the network resources of the observed network.

4.5 Effect of BBU pool area and interaction of the main RRH coordinates

After the optimal network configuration has been identified for each pool area. The main RRH location is chosen as the nearest RRH to the position of the BBU pool. This choice was made because the fronthaul link of the nearest RRH to the BBU pool has the highest NQoS, such as achieving lower latency. Hence, the main RRH can provide high NQoS requirements when set as a central radio access point among the other RRHs within the pool area. The abovementioned process is undertaken in all the BBU pool areas within the network. Then, it is necessary to consider the interactions among all the homotypic main RRHs. These interactions serve to determine the borders and areas of each BBU pool as well as helping to specify the connected number of RRHs belonging to it, such that the main RRH can cover them and thus, work under the umbrella of DC-RAN.

This can be verified by the Voronoi Diagram (VD) local effect, as shown in Fig. 4.3, which represents part of the presented network. The borders and coverage area of each pool are calculated after activation of the main RRHs, whilst the others are put into sleep mode so that coverage through the interaction of the main RRHs can be determined. It is taken that all the main RRHs are homotypic and their antenna radiation patterns are the omni sector antenna type. It is clear that the Voronoi tessellation is governed by the main RRH sites' coordination, such that each tile area's size and shape is tied with its site coordinate [119]. The actual attained maximum coverage range is Rmax, as shown in Fig. 4.4, which comes from the interaction of the main RRH site's coordinates with its neighbouring main RRHs, which is called the local effect in VD construction. Thus, it is possible to calculate the maximum coverage range accomplished by each radio access node, which is represented here as main RRH coordinates. This calculation can be made through an algorithm that has been programmed using Matlab that deploys the Voronoi function.

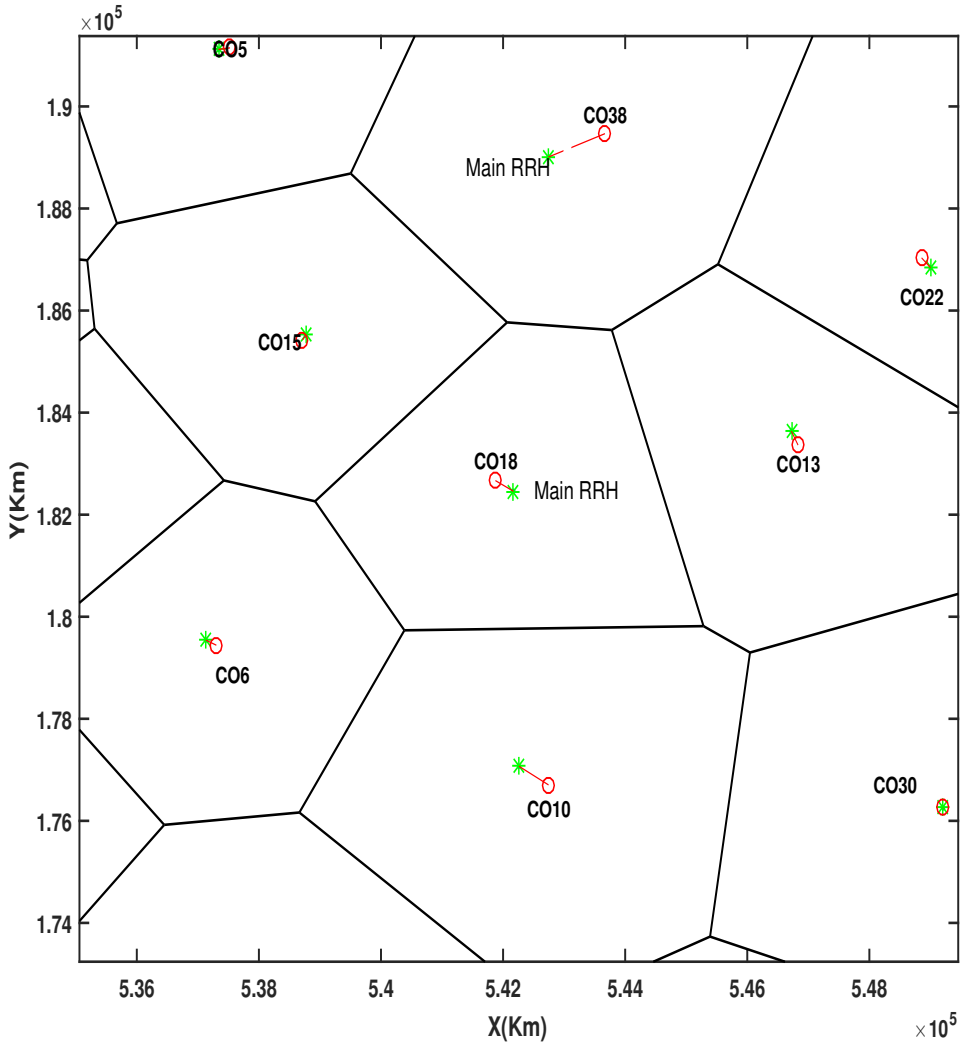

Fig. 4.3 Voronoi Diagram (VD) local effect

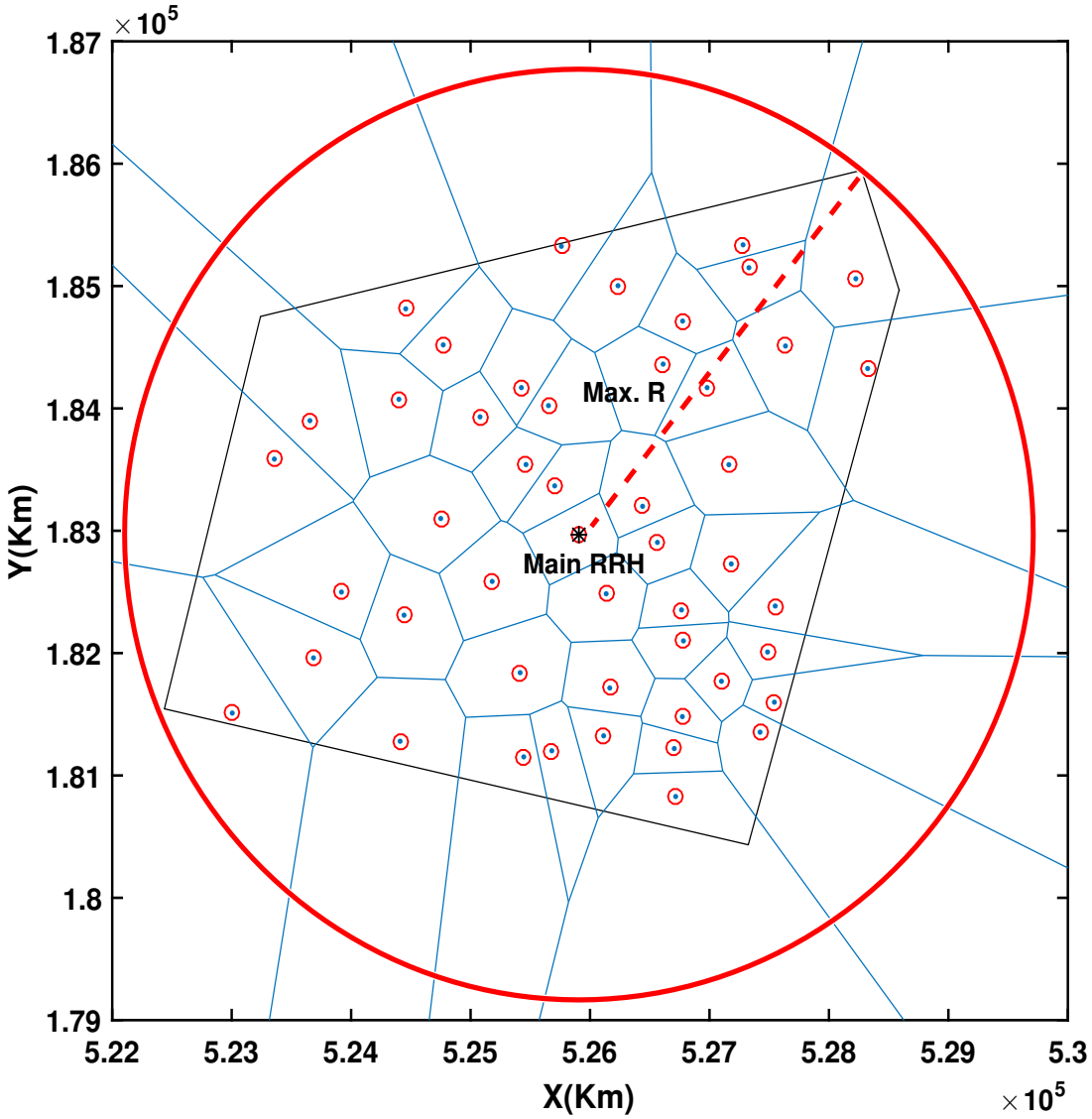

Fig. 4.4 Main RRH maximum coverage range span

4.6 Numerical Results

4.6.1 Multi-pooling

In this section, the following results are determined:

(a) Optimal multiple pools configuration of the predetermined number of BBU pools in the whole network.

(b) Position of each BBU pool inside its pool area.

(c) The number of connected RRHs for each BBU.

(d) The related coverage area of the main RRH for each BBU.

Fig. 4.1 shows the proposed network radio access nodes locations; this being for real 4G network deployment, which has to be anticipated as being the C-RAN architecture deployment for the future 5G network.
The proposed PSO algorithm was used to provide the optimal multiple pools configuration, the BBU positions and the number of connected RRHs to each BBU for a predetermined number of pools. It was run to divide the whole network radio access nodes into clustered groups as BBU pools, starting with 1 pool network configuration, then ending with a 70 pools network configuration as shown in Fig. 4.5. Which represents examples of PSO results of selected solutions, as in Fig. 4.5a represents 2 pools network configuration, Fig. 4.5b represents 11 pools configuration, Fig. 4.5c represents 37 pools configuration and Fig. 4.5d shows 70 pools network configuration. This figure shows the COs coordinates for each pool as well. The decision to stop the network partition process with respect to the number of pools which is 70 was based on the observation of the value of the BIC function, since it was showing an increased pattern. This procedure was done through the calculation of the BIC function, which was the resultant for each network partition process.
The BIC function versus the number of BBU pools is shown in Fig. 4.6, which shows an increase after 44 clustered groups of RRHs, the partitioning process K was taken up to 70 to widen the observation and to increase the accuracy of the proposed algorithm.

The abovementioned two manipulations gave a group of candidate solutions of partitioned network configurations, they can be determined from Fig. 4.6, they are laid between 27 to 44 pools because they have achieved minimum BIC values. That is, within this range of solutions, the optimal number of BBU pool network configurations shall lie. Consequently, the optimal network configuration is within these candidates' solutions. It could be chosen subject to

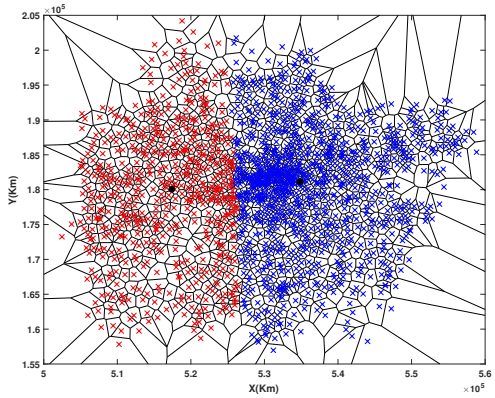

(a) 2 BBU pools network

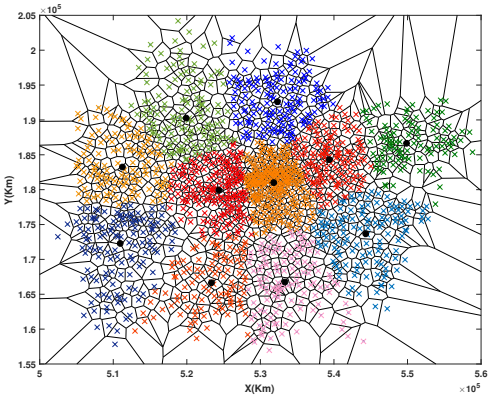

(b) 11 BBU pools network

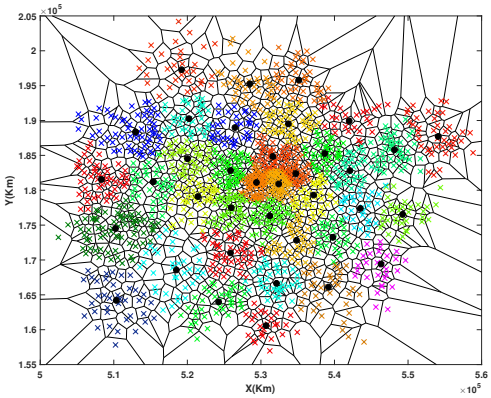

(c) 37 BBU pools network

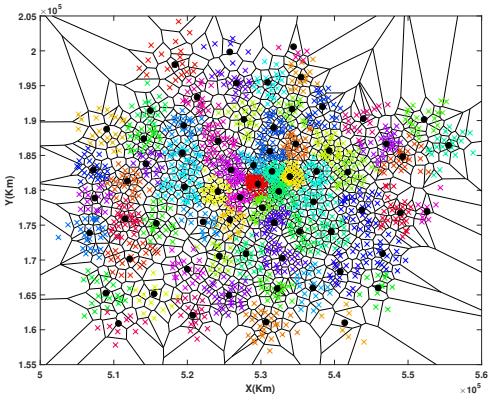

(d) 70 BBU pool network

Fig. 4.5 PSO results for different number BBU pools deployment partition configuration

the measure of spread characteristics of the statistical analysis to the all aforementioned candidates with respect to the number of the connected RHHs among all the BBU pools in each configuration. This has been achieved, as abovementioned, in terms of the values of the Stdv, Range and Variance. Fig. 4.7 shows Stdv and Range values of the data represented by the number of connected RRHs with their pools in all the multi-pool network configurations with respect to the number pools. In this figure and within the elected pool configurations, the selected number of BBU pools is 41, as this attains the minimum Stdv. Furthermore, Fig. 4.8 shows that a 41 BBU pool network configuration achieves minimum variance. According these measures, this network partition configuration can provide fairness in the loading of each BBU pool from the perspective of the number of connected RHHs point of view. Hence, the optimal number of the BBU pools, based on PSO clustering, with respect to the minimum BIC algorithm as well as the statistical analysis based on the number of connected RRHs to each BBU pool is 41.

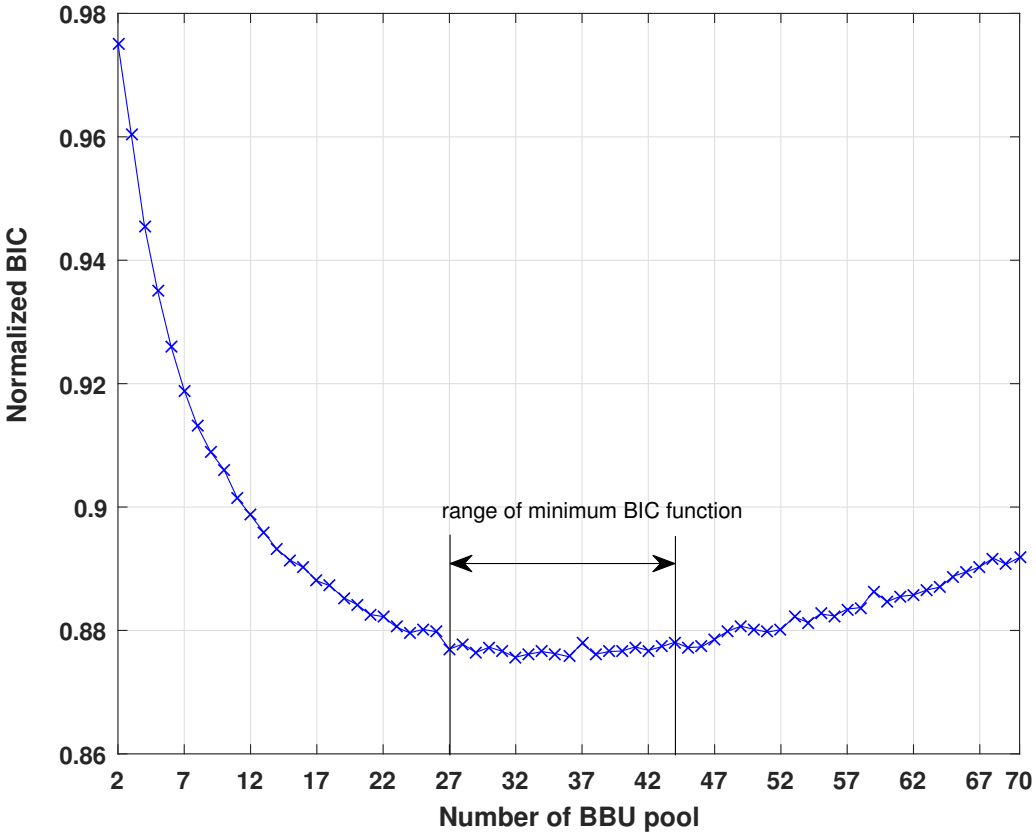

Fig. 4.6 BIC function versus the number of BBU pools

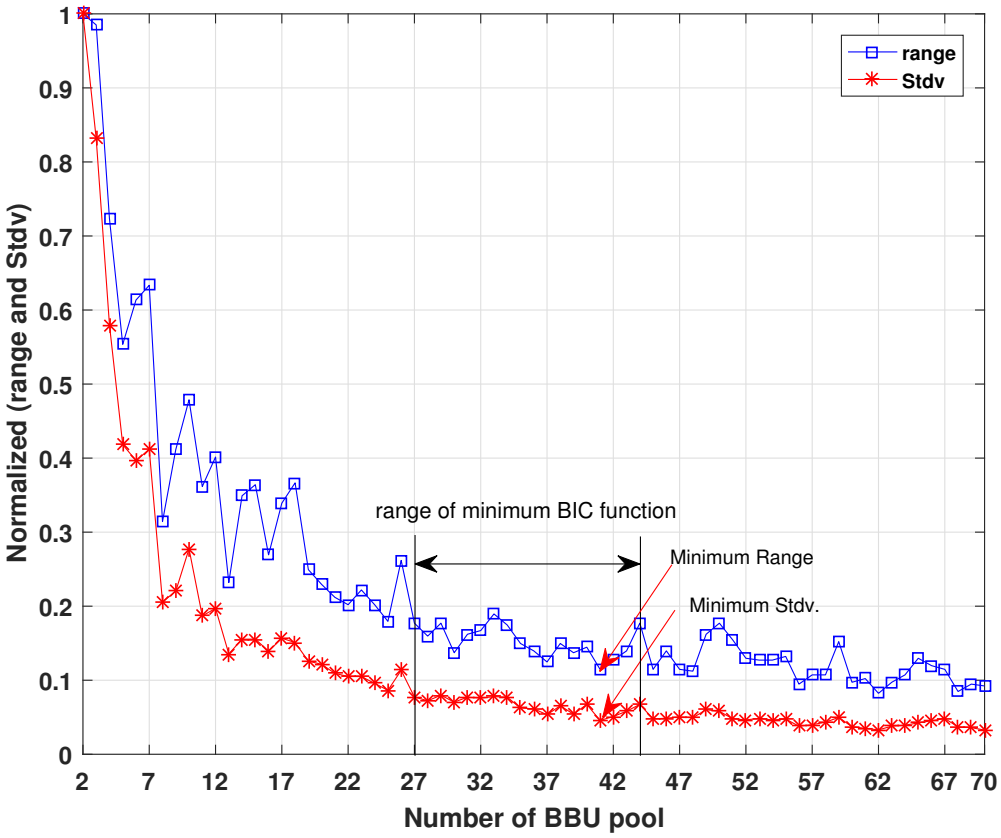

Fig. 4.7 Stdv and statistical Range values versus number of BBU pools

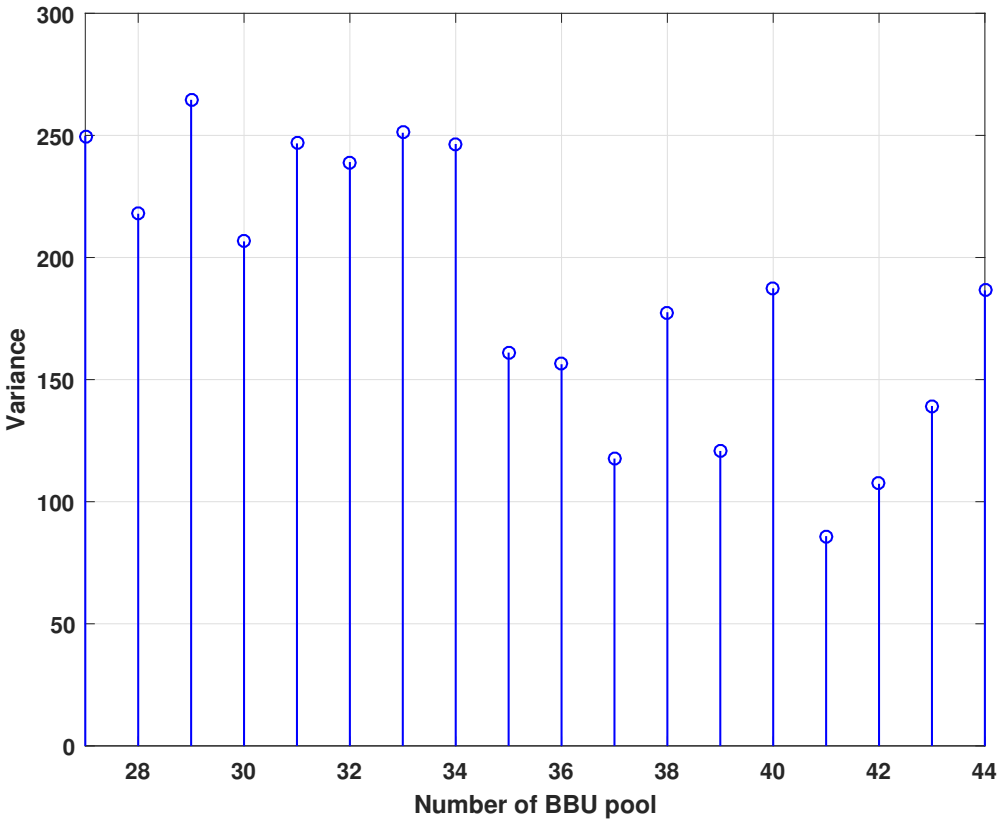

Fig. 4.8 Variance versus number of BBU pools

Fig. 4.9 shows the optimal 41 BBU pools network partition result by using the PSO algorithm for a heterogeneous network deployment of area 2,657.04395 km^2 (56×47 km) that contains 1517 radio access nodes. The algorithm uses the positions of the RRHs and the required number of BBU pools, which is 41, as an input to find optimal COs' positions as well as the optimal number of connected RRHs in each single BBU pool in the network. The PSO algorithm considers in the optimization process the latency constraints in terms of the maximum distance between the pool CO site location and its selected RRHs' positions. The positions of the COs were chosen as a closest location of all its related RRHs, as in the proposed algorithm that was defined in the PSO cost function.

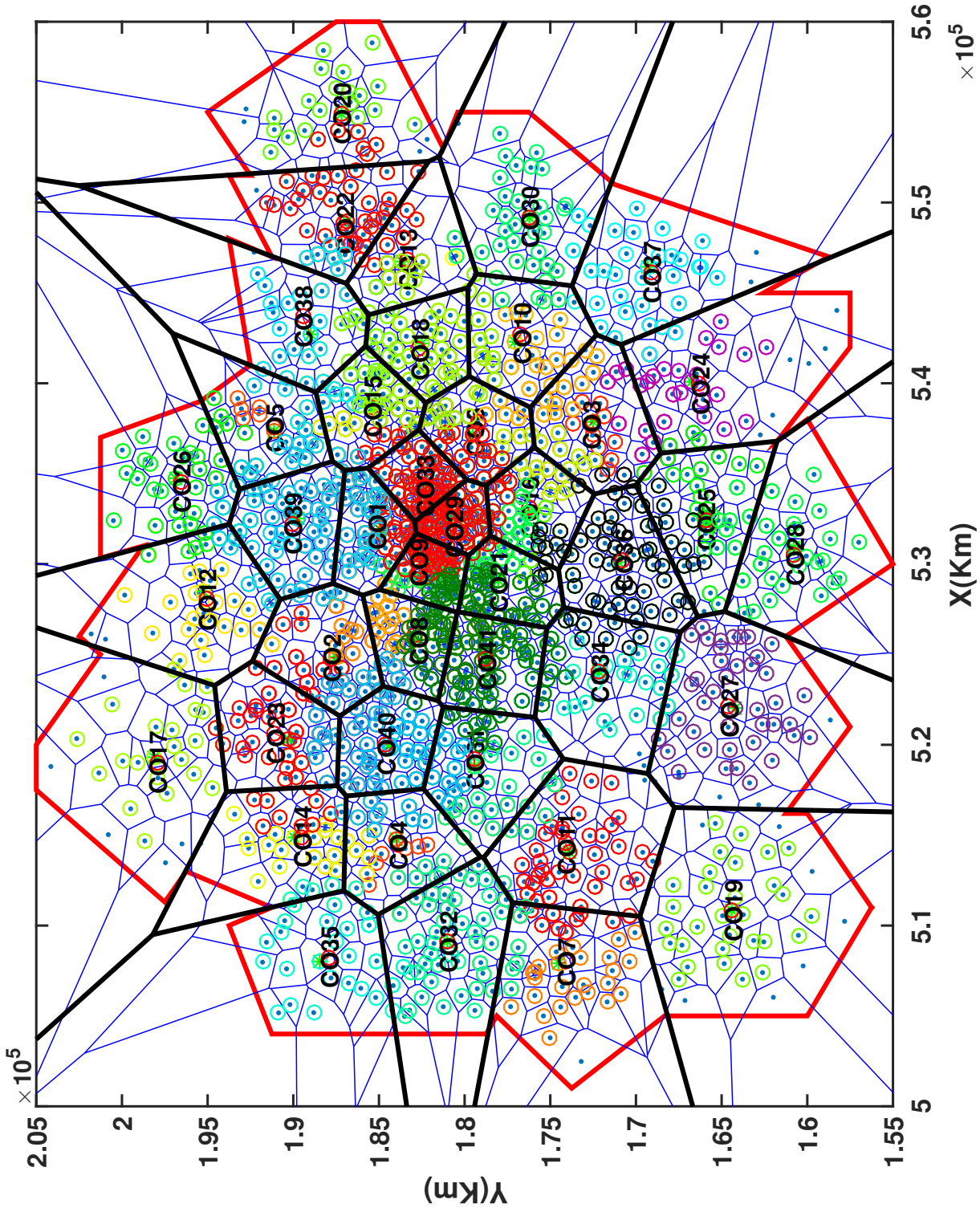

Fig. 4.9 Multi pool partitioning for the network planning

Fig. 4.10 shows best cost versus the number of iterations of the PSO algorithm for 41 pools network configuration. It can be seen that the best cost decreases as the number of iterations increases and the optimum 41 partitioning pooling is achieved after the 350^{th} iteration (i.e. optimal configuration of 41 pools network). Moreover, the RRH density (no. of RRHs/network area) of the actual network is 0.781 (RRHs/unit area,) which was calculated prior the proposed algorithm being deployed. This could be considered as a reference measure for checking the RRH density of the final optimum solution, which is represented by the average RRH density of all the pools in order to verify the accomplished pooling configuration. The average density of the RRHs in the partitioned network (41 BBU pools) was 0.78098 (RRHs/unit area), as shown in Fig. 4.11. In comparative terms, the difference between the original density and achieved average density of the RRHs is just 0.002% , as shown in Fig. 4.11 as doted red line, which is very low.

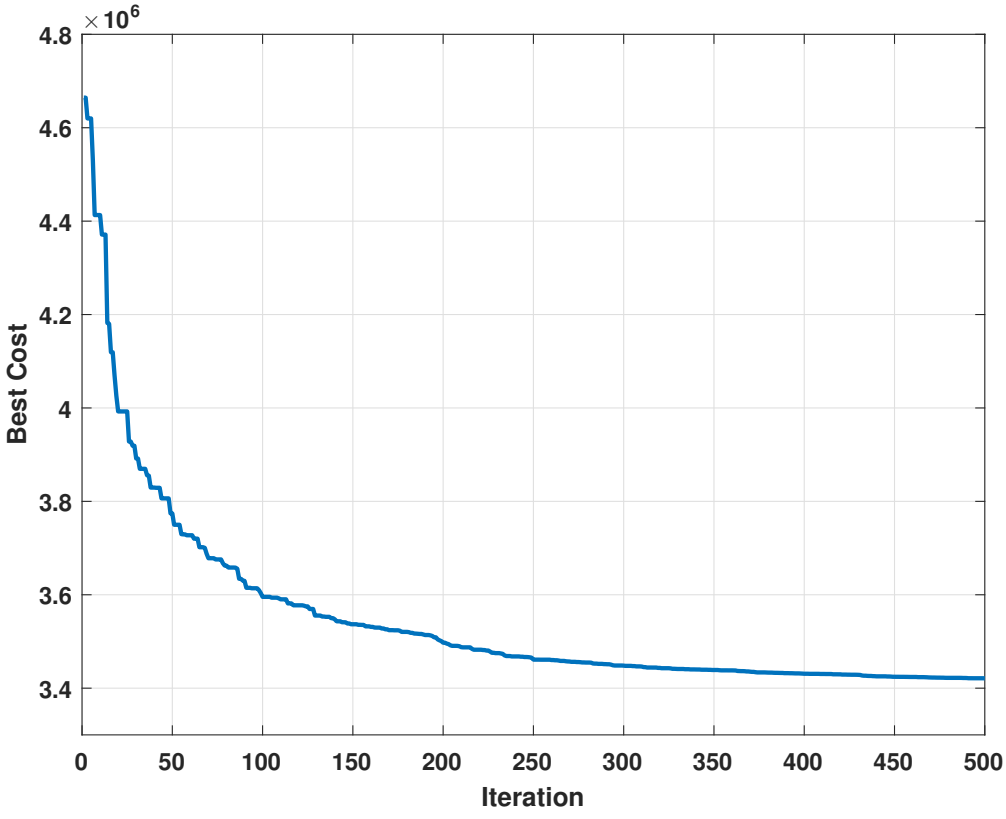

Fig. 4.10 Iterations number of the performance system

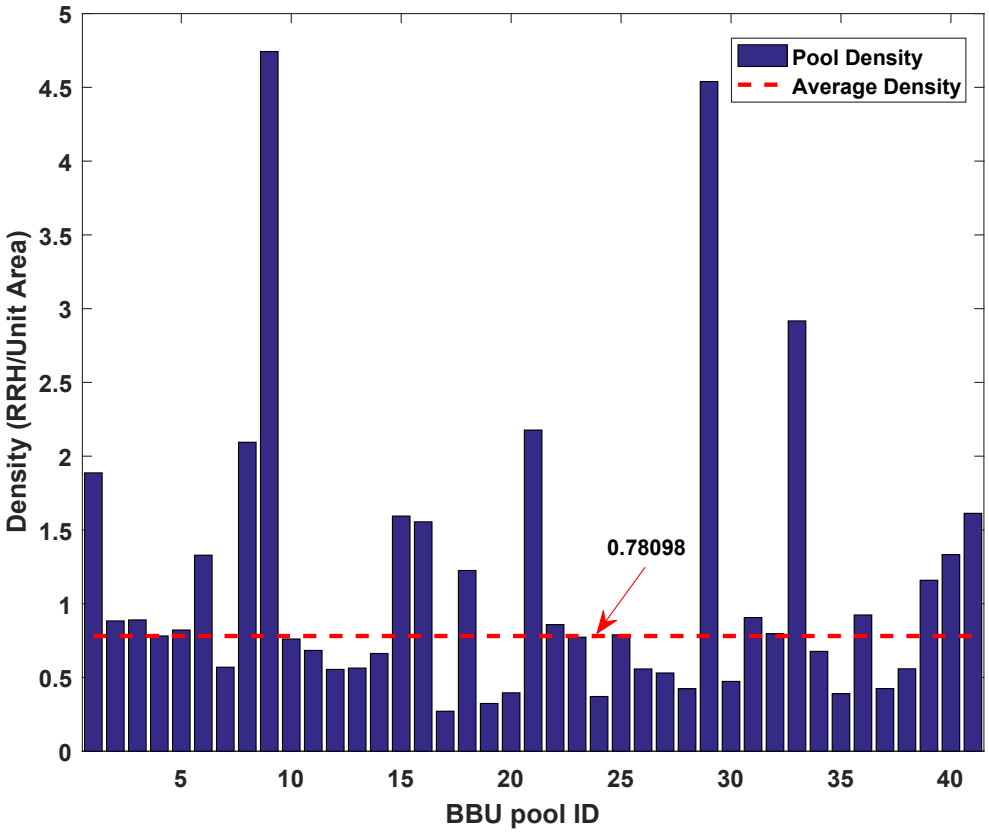

Fig. 4.11 RRH density of the optimal network configuration

4.6.2 DC-RAN action

Fig. 4.12 shows the DC-RAN model example for a single pool, namely number 08, which is one of the 41 pools in multiple pools C-RAN network deplyoment. The main idea of DC-RAN is that of organising the transmission and reception processes by the BBU pool among all the related RRHs with UEs within the pool area. The introduced example is based on switching off a number of RRHs that have a low traffic load demand and to serve their UEs by the main RRH. The main RRH can use CRE in order to change its coverage range with respect to the traffic load demand, as shown in Fig. 4.12.
Another use for DC-RAN, is to get the main RRHs to provide the DL connection to the UEs, whilst the UL connection can be provided by other RRHs that are related to the same BBU. Furthermore, the main RRH for each pool can be used to transmit a Multimedia Broadcast Single Frequency Network (MBSFN) to deploy mobile TV network (Broadcasting/Multicasting) services through the existing network.
The number of active RRHs in the single BBU pool number r by using DC-RAN can be calculated as in Equ. 4.9.

$$active.rrh_r = [w_r - (D_r * C_{mainRRH_r})] + 1 \tag{4.9}$$

Whereas, the total number of active RRHs in multi pool network by using DC-RAN can be calculated as in Equ. 4.10.

$$ACTIVE.RRH_{net} = [N+M] - \sum_{r=1}^{M} D_r * C_{mainRRH_r} \tag{4.10}$$

where, $C_{mainRRH_r}$ denotes the achieved coverage area of the main *RRH* of the r^{th} pool, and D_r is density of the r^{th} pool *(rrh/m^2)*.

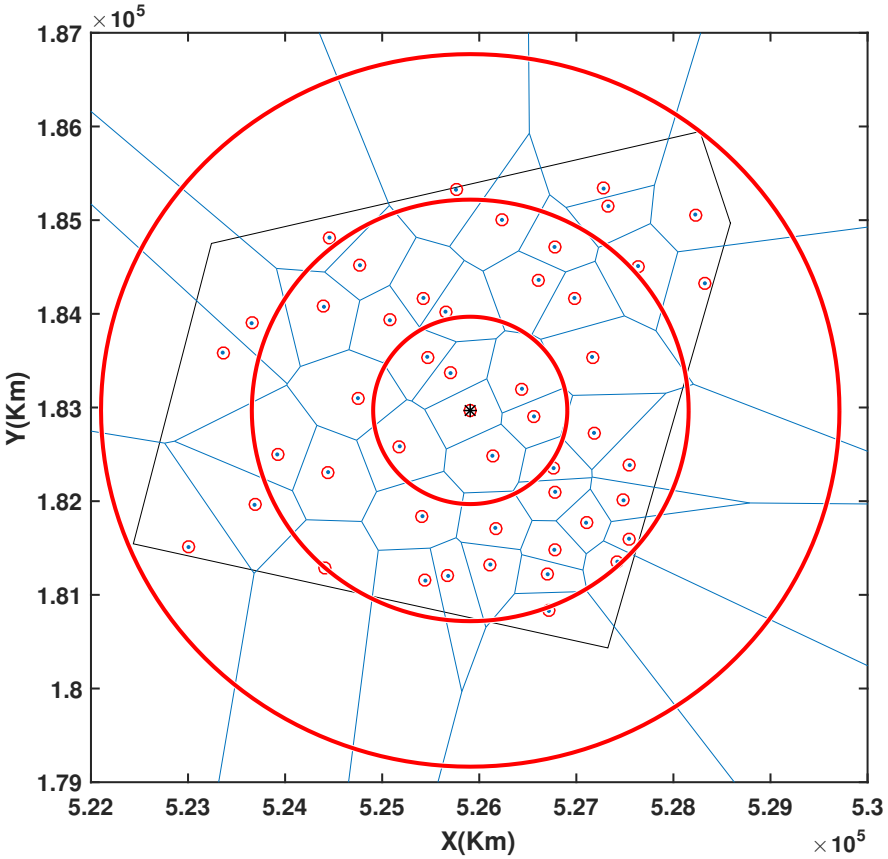

Fig. 4.12 D-CRAN concept for a single BBU pool

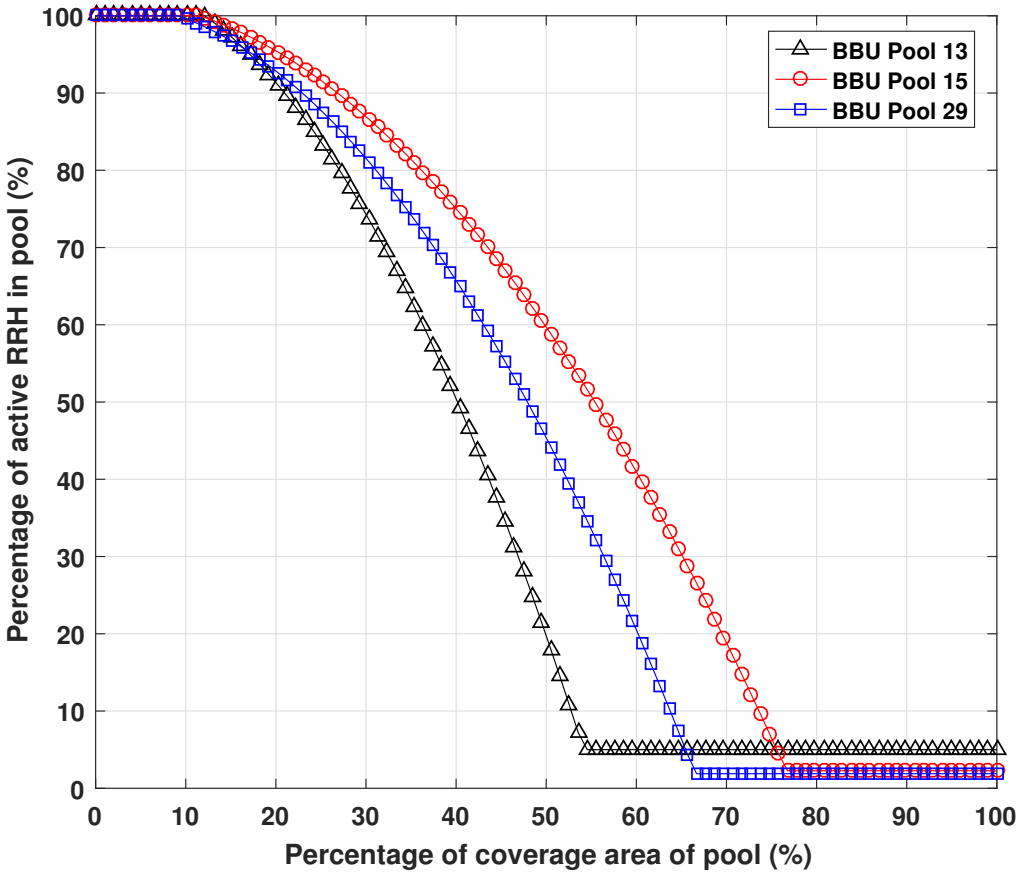

Fig. 4.13 Number of active RRH in single pool using DC-RAN for different pools

Fig. 4.13 shows the consequence of the introduced example of DC-RAN in pools no. 13, 29 and 15 when the main RRHs use CRE. As can be seen, when the main RRH in specific pool work with 50% of the coverage area, then it possible to switch off up to 20% of the active RRHs in pool no. 13, while it possible to switch off about 45% and about 60% of active RRHs pools no. 29 and no. 15, respectively. These differences in percentage of active RRHs are due to the differences in the RRH densities, D_r, among the BBU pools. The DC-RAN has a significant effect in saving energy and increasing throughput in the network.

4.7 Summary

The main challenges in the multiple pools C-RAN architecture are the partition of the network for a required number of BBU pools, their positions and the number of connected RHHs per each pool. In this chapter, an algorithm for partitioning a single network into a required number pools as well as finding the optimal BBU pool positions over the DC-RAN architecture has been proposed.

Under this approach the set of RRH positions is considered in terms of a set of feasible locations and the number of BBU pools in a specific network. The multiple pooling based PSO clustering algorithm has been used to solve the RRH pooling configuration problem, with the optimal BBU pool location allocation, after first, determining their optimal number. That is, the BIC criterion have been used to narrow the search problem of identifying the range of the candidate multiple pools numbers in the search for the optimal multiple pools configuration. Subsequently, the measure of spread technique of the RRH numbers among the candidate multiple BBU pool configurations has been successfully used to choose the unique optimal multiple pool configuration for the proposed network. Finally, Voronoi tessellation interaction of the activated main RRHs of DC-RAN has facilitated allocating the pools areas as well as the number of connected RRHs with each BBU pool. It was shown that there was a significant change in the number of active RRHs within each pool area as a result of using the CRE criterion.

Chapter 5

Interaction of SDN KPI with IoT KQI and Power Consumption

5.1 OVERVIEW

Mathematical framework that investigates the PC profile for the interaction of IoT AQoS with NQoS in wireless SDN as SDN-WISE has been developed in this chapter. This profile model offers flexibility for managing the structure of the M2M system in IoT environment. It enables controlling the provided NQoS, precisely the achieved PHY layer transmission link throughput, combined with the AQoS, represented by IoT data stream payload PDU size. The investigation is composed of two essential SDN traffic parts, they are control plane signalling and data plane traffic PCs and their relevance with QoS. The results show that 98% PC in data plane companion with a control plane PC of 2% in overall of the proposed system PC, these figures were achieved with a high signalling rate for control plane TTI of 5 sec and a maximum data plane payload size of 92 Bytes as a worst case scenario.

5.2 Profiling PC model for SDN-WISE

The PC model is considered in WSN based on SDN architecture of IoT applications and services as an important part for solving the complexity problem in the deployment and management phases of the WSNs. Measuring how efficient of PC in SDN-WISE, which is considered as a crucial factor for fulfilling the requirements of the IoT AQoS regarding energy efficient network resource utilisation with improved NQoS.

5.2.1 System model

This section is described the network elements of the proposed system model regarding SNs, SNKs and WISE-VISOR, with all of the traffic streams that are contributing to the generated data plane traffic and SDN control plane signalling. All of the introduced models in this chapter proposes an observation of PC modelling in the SDN-WISE based on the prototype parameters in [29] as a base line model for the developed model.

5.2.1.1 Network components

A sensing field is logically divided into multiple sections, depending on the number of SNKs nodes, as shown in Fig. 5.1.

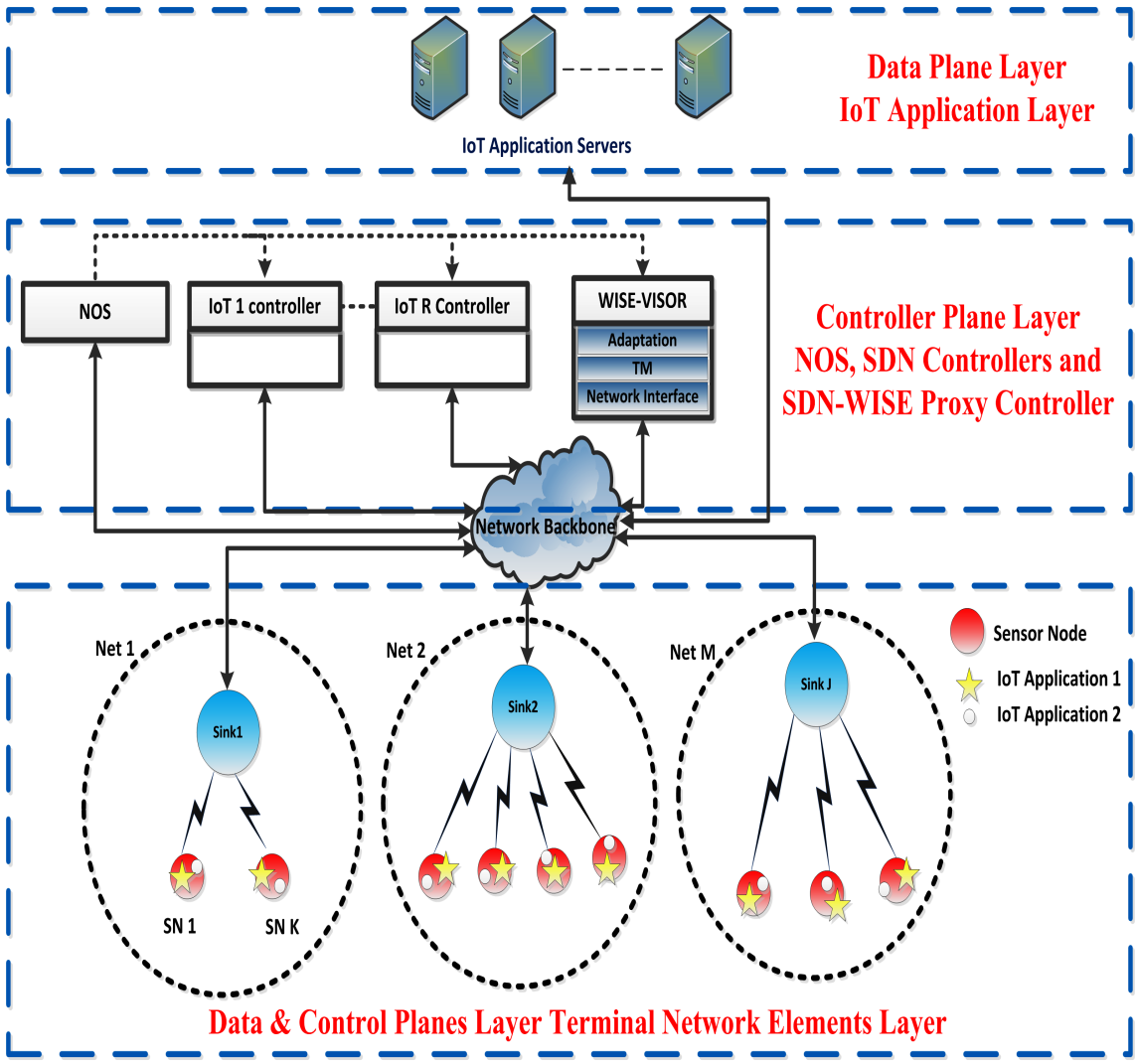

Fig. 5.1 Architecture of SDN-WISE system model.

In addition, the SDN-WISE protocols stack as shown in Fig. 2.3 is based on the SDN-WISE architecture proposed in [29], with complete layers related to the proposed architecture. The introduced network model is based on the power model parameters' definitions and the proposed simulation network model parameters, which are listed in Table 5.1 and Table 5.2 respectively. The terminal netwok represented as a sensing field of size $NxN\ m^2$.

Table 5.1 Parameter definitions

Parameters	**Definition**
SN	Sensor Node
SNK	Sink Node
CTR	ConTRol Plane Signalling
DAT	DATa Plane Traffic
PC_{SN}	Power Consumption in SN
PC_{SNK}	Power Consumption in SNK
PC_{NOS}	Power Consumption in NOS
PC_{TM}	Power Consumption in Topology Management
PC_{Adapt}	Power Consumption in Adaptation Processing

Table 5.2 Simulation Parameters

Parameter Name	**Value**
$PC_{(idle)}$	24 mW [120]
Energy consumption of electronic circuit (Eelect)	50 nJ/bit
Channel Parameter of free space model (E_{fs})	10 $pJ/bit/m^2$
Energy consumption for INPP	5 $(nJ/bit)/packet\,processing$ [57]
Energy consumption for FWD	5 $(nJ/bit)/packet\,processing$ [57]
Energy consumption for TD	5 $(nJ/bit)/packet\,processing$ [57]
PC (SDN controller), $PC_{WISE-VISOR}$	0.3909 W [121]
Energy consumption for Adaptation process	197.208 $nJ/(packet\,processing)$ [122]
Network Size (NxN)	350mx350m
Distance between each SN and its Gateway (SNK)	155 m
Number of SNs	2000 SNs
Number of $SNKs$	16 $SNKs$
Number of Terminal $WSNs$	16 $WSNs$
Number of SNs per Terminal WSN	125 SNs

The proposed network model would contain the following elements:

(a) **Sensor Node (SN)**
It contains the following layers:

(i) *IoT Application layer*.

(ii) *SDN-WISE layers*.

- Forwarding layer (FWD).
- In-Network Packet Processing (INPP) layer.
- Topology Discovery (TD) layer

(iii) *802.15.4 MAC layer*.

(iv) *802.15.4 PHY layer*.

(b) **Sinks Node (SNK)**
It is a traffic aggregation point from SNs with short-range interface through to the external natworks with a specific network ID. It is presenting as the gateway of the proposed terminal SNs network aggregated traffic as a bidirectional protocol convertor. It is the same as a SN but with unlimited energy capability. This SNK roots the same layers in SNs in addition to extra layers, which are the Adaptation layer, as well as TCP/IP protocol with Ethernet 802.3 as an interface to the external network. Therefore, the SNK has two ports one deals with 802.15.4 for communicating with SNs and the other corresponds to the Ethernet 802.3 for connecting with other networks as well as SDN-WISE controller.

(c) **WISE-VISOR**
It is an SDN controller device as a proxy server among the SDN-WISE network components (SNs and SNKs) and other networks. This WISE-VISOR is responsible for creating and managing the SDN-WISE flow tables. It has its Adaptation Layer and the Topology Management (TM) layer.

(d) **NOS layer**
This layer is runs beyond the application layer as described in Chapter 2, subsection 2.2.3.3, item (f).

5.2.2 PC model components

The proposed PC model introduces all SDN-WISE architecture network components such as terminal SDN-WISE terminal networks elements represented by SNs and SNKs, as well as

external SDN-WISE elements such as WISE-VISOR and NOS based on Fig. 5.1 as shown in the Equations 5.1 and 5.2 .

$$PCmodel = PC_{SDN-WISE} \tag{5.1}$$

$$PC_{SDN-WISE} = \sum_{Net=1}^{M} (\sum_{SN=1}^{K_{Net}} PC_{SN(CTR+DAT)} + \sum_{SNK=1}^{J_{Net}} PC_{SNK(CTR+DAT)})_{Net} + PC_{(WISE-VISOR)} + PC_{NOS} \tag{5.2}$$

where, M is the total number of terminal WSNs, $[Net = 1, ..., M]$, K_{Net} and J_{Net} are the numbers of *SNs* & *SNKs* in each *Net* respectively. The SDN-WISE's PC model parts are defined in TABEL 5.1.

The first part of the Equation 5.2 is composed of the power consumed by each single *SN* as PC_{SN} and *SNK* as PC_{SNK} related to DATa (DAT) plane traffic PC combined with ConTRol (CTR) plane signalling PC.

The second part is the power consumed by the WISE-VISOR controller, which is considered as part of the control plane signalling PC. Moreover, the last part is according to SDN architecture, which is representing the NOS layer PC that has included as part of the total SDN-WISE related functions and applications PCs.

5.2.2.1 PC in SN PC_{SN}

$$PC_{SN} = PC_{SN(DAT)} + PC_{SN(CTR)} + PC_{SN(idle)} \tag{5.3}$$

The first two parts of PC in SN in Equation 5.3 are related to the control plane and data plane in SN respectively. Each part in the Equation 5.3 is described in detail in the following (a) and (b) sections as well as of idle in section (c):

(a) **Power Consumption for Data Plane Traffic in SNs** $PC_{SN(DAT)}$.
This PC model is based on single-hop transmission and it is related to the power required to transmit and receive data between source and destination. This PC model based on the PC model that has been used in [57]. Moreover, the contribution of the SDN-WISE layer is related to three processes of the SDN-WISE sub-layers in SN, which are INPP, TD and FWD. The PC of data plane traffic in SN is a composite of transmission and reception processes PC as shown in the following.

$$PC_{SN(DAT)} = PC_{SN(DAT)(Tx)} + PC_{SN(DAT)(Rx)} \tag{5.4}$$

Where $PC_{SN(DAT)(Tx)}$ and $PC_{SN(DAT)(Rx)}$ representing the PC for transmission and reception processes respectively.
The transmission PC of the transmitted data plane traffic for single SN described as

$$PC_{SN(DAT)(Tx)} = E_{Tx} * R_{dataTx} + E_{Tx(SDN-WISELayer)} * R_{Tx(SDN-WISELayer)} \quad (5.5)$$

where R_{dataTx} and E_{Tx} are the bit rate of data traffic stream and consumed energy per bit in 802.15.4 layers respectively. In addition, $R_{TX(SDN-WISELayer)}$ is the bit rate of transmitted data streams in SDN-WISE layers.
The PC for the reception process of data plane traffic in a single SN as

$$PC_{SN(DAT)(Rx)} = E_{Rx} * R_{dataRx} + E_{Rx(SDN-WISELayer)} * R_{Rx(SDN-WISELayer)} \quad (5.6)$$

where R_{dataRx} and $R_{Rx(SDN-WISELayer)}$ are the bit rates of received data streams in 802.15.4 and SDN-WISE layers respectively as well as E_{Rx} and $E_{Rx(SDN-WISELayer)}$ are the energy consumption rates of 802.15.4 reception process and SDN-WISE layers streaming process respectively.
Thus the total PC of transmitted data plane traffic in a single terminal WSN contains K SNs will be the sum of each individual SN that sends data plane traffic as in the Equation 5.7.

$$PC_{SN(Tx)} = \sum_{n=1}^{K} \left(E_{Tx(n)} * R_{dataTx(n)} + E_{Tx(SDN-WISELayer)(n)} * R_{Tx(SDN-WISELayer)(n)} \right) \quad (5.7)$$

where n represents each individual SN and K is the total number of SNs.
Moreover, the total PC of received data plane traffic in a single terminal WSN contains K SNs will be the sum of each individual SN that receives data plane traffic.

$$PC_{SN(Rx)} = \sum_{n=1}^{K} \left(E_{Rx(n)} * R_{dataRx(n)} + E_{Rx(SDN-WISELayer)(n)} * R_{Rx(SDN-WISELayer)(n)} \right) \quad (5.8)$$

where E_{Tx} of energy is consumed by each sensor node to transmit each PDU of Length $(L_{PHY802.15.4})$ $bits$ over a distance d as in Equ. 5.9,

$$E_{Tx}(L_{PHY802.15.4}, d) = L_{PHY802.15.4} * E_{elec} + L_{PHY802.15.4} * \varepsilon_{fs} * d^2, d \leq d_o \quad (5.9)$$

And the energy that is consumed by receiving the packet is $E_{Rx}(L_{PHY802.15.4})$.

$$E_{Rx}(L_{PHY802.15.4}) = L_{PHY802.15.4} * E_{elec} \tag{5.10}$$

where,

$$d_o = \sqrt{\frac{\varepsilon_{fs}}{\varepsilon_{mp}}} \tag{5.11}$$

$$E_{Tx(SDN-WISELayer)} = E_{Rx(SDN-WISELayer)} = E_{INPP} + E_{TD} + E_{FWD} \tag{5.12}$$

In this model, the energy consumed per bit is E_{elec} and it is used to run the transmitter or receiver circuit, while ε_{fs} represents the amplifier efficiency of the transmitter that depends on transmission link conditions [57] [123].
The model is based on free space power loss model. A free space model is calculated based on the distance between a transmitter and receiver.

From all above, $PC_{SN(Tx)}$ is the PC of the transmission process that are related to data plane traffic in SN, $PC_{SN(Rx)}$ is the depleted power when the SN receives data streams that are related to the data plane traffic, while R_{data} is the achieved data rate in 802.15.4 PHY layer presented by the wireless link between Tx node and Rx node as proposed in the introduced model with single hop transmission distance.
Moreover, $R_{Tx(SDN-WISELayer)}$ and $R_{Rx(SDN-WISELayer)}$ are the data rate in SDN-WISE layer for transmitting and receiving data streams respectively. Furthermore, $E_{Tx(SDN-WISELayer)}$ and $E_{Rx(SDN-WISELayer)}$ are the densities of energy consumption per bit for data streams in SDN-WISE layer, which are a composite of E_{INPP}, E_{TD} and E_{FWD} as energy densities of aggregation layers as presented in [29] [57] [32].

(b) **PC control plane signalling in SNs** $PC_{SN(CTR)}$.
The PC of control plane signalling that has been processed in SN as $PC_{SN(CTR)}$ analogous to the PC of processing data plane traffic. It is a composite of transmission and reception processes PCs as presented in Equ. 5.13 below:

$$PC_{SN(CTR)} = PC_{SN(CTR)(Tx)} + PC_{SN(CTR)(Rx)} \tag{5.13}$$

where $PC_{SN(CTR)(Rx)}$ and $PC_{SN(CTR)(Rx)}$ representing the PC of transmission and reception processes in the SN of control plane signalling respectively.

The PC for transmission process of control plane signalling in a single SN can be described in Equ. 5.14, as PC of processing *REP* and *BEC* signalling streams:

$$PC_{SN(CTR)(Tx)} = PC_{(REP)(Tx)} + PC_{(BEC)(Tx)} \tag{5.14}$$

The PC for reception process of control plane signalling in a single SN can be described in Equ. 5.15, as PC of processing $OPEN$, $Config$, BEC and RES signalling streams:

$$PC_{SN(CTR)(Rx)} = PC_{(OPEN)(Rx)} + PC_{(Config)(Rx)} + PC_{(BEC)(Rx)} + PC_{(RES)(Rx)} \tag{5.15}$$

(c) **Idle PC in SN** $PC_{SN(idle)}$
In this section, the $PC_{SN(idle)}$ is related to the power dissipated in idle mode. The measured PC of the idle part is considered according to wireless module device developed by *Embit company* for LR-WPAN applications. The module combines high performance to small dimensions and low cost, providing the system integrator a simple and easy way to add IEEE 802.15.4 (ZigBee) low range wireless connectivity and multi-hop networking into existing products. This device is configured as an embedded micro system or simple data modem for low power applications in the 2.4 GHz ISM band. It is based on a Texas Instruments EMB-Z2530PA [120] based on [29] as shown in TABEL 5.2.

The total PC of Tx and Rx processes of control plane signalling of K SNs are shown in Equs. 5.16 and 5.17 respectively:

$$PC_{(SN(CTR)(Tx))} = \sum_{n=1}^{K} (PC_{(REP)(Tx)} + PC_{(REQ)(Tx)} + PC_{(BEC)(Tx)}) \tag{5.16}$$

$$PC_{(SN(CTR)(Rx))} = \sum_{n=1}^{K} (PC_{(OPEN)(Rx)} + PC_{(Config)(Rx)} + PC_{(BEC)(Rx)} + +PC_{(RES)(Rx)}) \tag{5.17}$$

Furthermore,
$PC_{(REP)(Tx)}, PC_{(REQ)(Tx)}, PC_{(BEC)(Tx)}, PC_{(OPEN)(Rx)}, PC_{(Config)(Rx)}, PC_{(BEC)(Rx)}$ *and* $PC_{(RES)(Rx)}$, are listed in the following Equs.

$$PC_{(REP)(Tx)} = E_{Tx} * R_{REP} + E_{SDN-WISE} * R_{REP-SDN-WISELayer} \tag{5.18}$$

$$PC_{(REQ)(Tx)} = E_{Tx} * R_{REQ} + E_{SDN-WISElayer} * R_{REQ-SDN-WISE\,Layer} \tag{5.19}$$

$$PC_{(RES)(Rx)} = E_{Rx} * R_{RES} + E_{SDN-WISElayer} * R_{RES-SDN-WISE\,Layer} \tag{5.20}$$

$$PC_{(OPEN)(Rx)} = E_{Rx} * R_{OPEN} + E_{SDN-WISElayer} * R_{OPEN-SDN-WISE\,Layer} \tag{5.21}$$

$$PC_{(Config)(Rx)} = E_{Rx} * R_{Config} + E_{SDN-WISElayer} * R_{Config-SDN-WISE\,Layer} \tag{5.22}$$

$$PC_{(BEC)(Rx)} = E_{Rx} * R_{BEC(SN-SNs-SNK)} + E_{SDN-WISE} * R_{BEC-SDN-WISE\,Layer} \tag{5.23}$$

$$PC_{(BEC)(Tx)} = E_{Tx} * R_{(SN-SN)} + E_{SDN-WISElayer} * R_{BEC-SDN-WISE\,Layer} \tag{5.24}$$

where R_{REP}, R_{REQ} and R_{BEC} are the associated PHY layer PDU rates related to the packets' sizes of such control plane signalling, which are processed and manipulated by SNs as transmission streams toward the controller. Therefore the WISE-VISOR builds the flow table according the information carried by them. However, R_{RES}, $R_{Openpath}$ *and* R_{Config} are bit rates received by SNs from control plane. In addition, $R_{(SDN-WISELayer)}$ is the bit rate in SDN-WISE layer. All of the control signalling SDU length (Bytes) excluding the SDN-WISE header are described in TABEL. 5.3 based on [58]. E_{Tx} and E_{Rx} are same as the Equs. 5.9 and 5.10.

The control signalling bit rate can be calculated according Equ. 5.25, which is related to the related PHY layer PDU size and TTI.

$$CTRSignallingRate_{PHYLayer} = PDU_{PHYLayer}(bit)/TTI(sec) \tag{5.25}$$

5.2.2.2 PC for SNK Node (PC_{SNK})

$$PC_{SNK} = PC_{SNK(DAT)} + PC_{SNK(CTR)} + PC_{SNK(idel)} + PC_{SNK(Eth-Port-Config)} + PC_{SNK(Adapt)} \tag{5.26}$$

where $PC_{SNK(DAT)}$, is the power depleted in SNK related to the data traffic as discussed in subsection (a) below, $PC_{SNK(CTR)}$ is the PC in the SNK node related to the control signalling as discussed in subsection (b) below.

These two parts presented in this chapter as SNK's PC of 802.15.4 protocol. Whereas, the TCP/IP data plane traffic and control plane signalling PCs are represented by $PC_{SNK(Eth-Port-Config)}$, as an Ethernet port speed configuration PC of the connection interface of the SNK, which depends on the achieved 802.3 PHY layer link speed as well as transmitted and received PHY layer PDU size. This PC are related to the port speed configuration and based on the Equ. 5.27 and Table 5.2, the presented Equ. 5.27 and table Table 5.2 values are depending on the [124].

$$PC_{SNK(Eth-Port-Config)} = \begin{cases} 0.0183^{*}\ L_{802.3PHY} + 277.913 & 10\ \text{Base-T} \\ 0.0026^{*}\ L_{802.3PHY} + 291.326 & 100\ \text{Base-T} \end{cases} \tag{5.27}$$

where $L_{802.3PHY}$ is the size in Bytes of 802.3 PHY layer PDU of TCP/IP protocol.

$$L_{802.3PHY} = SDN - WISEPacketSize + 66 \tag{5.28}$$

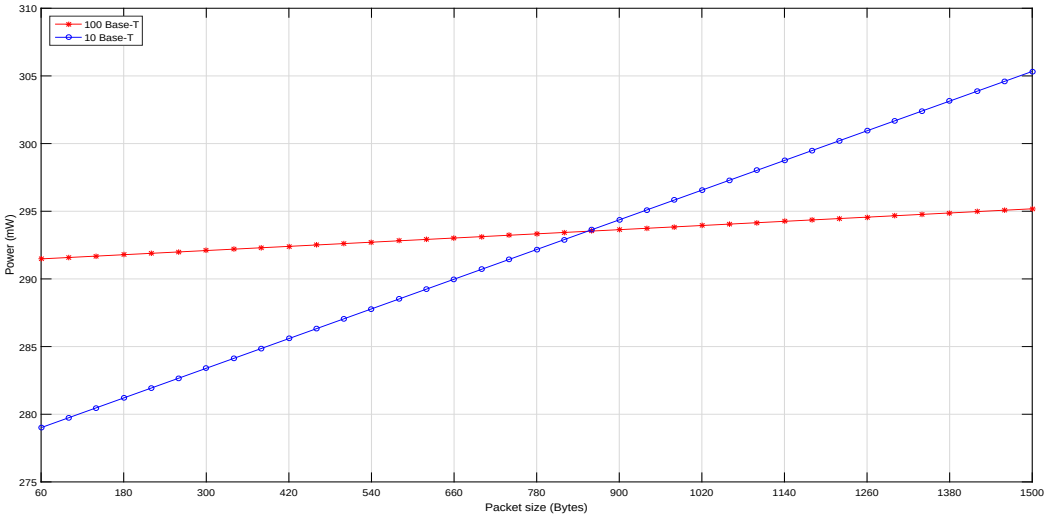

Fig. 5.2 Port Configuration.

Table 5.3 SDN-WISE control signalling packets' sizes

Control Signalling PDU Types	Size (Bytes) without SDN-WISE Header	Source	Destination
Report*	18	SN, SNK	WISE-VISOR
Config	3	WISE-VISOR	SN, SNK
Request**	92	SN, SNK	WISE-VISOR
Open Path***	11	WISE-VISOR	SN, SNK
RegProxy	28	SNK	WISE-VISOR
Beacon	2	SN, SNK	SN, SNK
Response	6	WISE-VISOR	SN, SNK
* This is for 5 neighbour nodes [29], ** Max value, *** This is for window size=2 and nodes=3 [29].			

The proposed connectivity with the WISE-VISOR and data plane destination end devices, such as services servers (and/or) end users, is provided via an Ethernet link, in order to generalise the PC model, which adapts to the IEEE 802.3. This study investigates the demand for PC of this port in two operation modes, 10 Base-T and 100 Base-T, as shown in Fig. 5.2. Fig. 5.2 clearly illustrates the effect of port traffic speed configuration conditions, which are demonstrated by the achieved Ethernet port traffic. This Port-Config shows one of the important parts between PC and QoS, since it contributes to the offered NQoS that defines the maximum PHY layer link throughput, as well as IoT application PDU size which is shaping the size of PHY layer PDU $L_{802.3PHY}$ bits as defined in Equ. 5.28 that contributes to the transmitted or received TCP/IP PDU's size of UL/DL traffic streams as one of AQoS metric, which is considered as an effective contributor to the NQoS. This demonstrates the contribution of QoS in the total PC. Furthermore, the size of PDU for control signalling is considered as well and it is depending the type of the specified control signalling where their packets' sizes as listed in Table 5.3.

Another component of PC in SNK is the adaptation process $PC_{SNK(Adapt)}$, which is dissipated due to the packet formatting process of the up and down data streams of the messages received (and/or) transmitted by the SNK node. This value of adaptation process PC are assumed to be per *(packet processing)* for up and down data streams. $PC_{SNK(Adapt)}$ value is assumed as used in [123] as it was considered in the measurement of PC.

(a) **PC for Data Plane Traffic in SNKs** $(PC_{SNK(DAT)})$**.**

This section related to the SNK PC of data plane traffic, which is based on the upstream traffic from IoT end devices toward its destination points. The SNK node will act as

a gateway and this $PC_{SNK(DAT)}$ will be a reception process PC of 802.15.4 interface as $PC_{SNK(DAT)(Rx)}$ and a transmission process PC of TCP/IP with 802.3 interface or Ethernet interface as $PC_{SNK(Eth-Port-Config)}$. Then, $PC_{SNK(DAT)}$ is written as in Equ. 5.29:

$$PC_{SNK(DAT)} = PC_{SNK(DAT)(Rx)} + PC_{SNK(Eth-Port-Config)} \tag{5.29}$$

where

$$PC_{SNK(DAT)(Rx)} = E_{Rx} * R_{dataRx} + E_{Rx(SDN-WISELayer)} * R_{Rx(SDN-WISELayer)} \tag{5.30}$$

This $PC_{SNK(DAT)}$ is based on the UL direction; therefore the flow of traffic will only deal with the received up-stream data flow, while the transmission PC of TCP/IP with Ethernet port will be processed as $PC_{SNK(Eth-Port-Config)}$ will depend on the transmitted PDU size $L_{802.3PHY}$.

(b) **PC of Control Plane Signalling in SNKs** $(PC_{SNK(CTR)})$**.**
The control plane signalling is directed into two directions UL and DL as it specifies both groups of signalling as shown in Equ. 5.31.

$$PC_{SNK(CTR)} = PC_{SNK(CTR)(Tx)} + PC_{SNK(CTR)(Rx)} + PC_{SNK(Eth-Port-Config)} \tag{5.31}$$

for single SNK node the PC for transmission process of 802.15.4 radio and SDN-WISE processing $PC_{SNK(CTR)(Tx)}$ is written as in Equ. 5.32:

$$\begin{aligned} PC_{SNK(CTR)(Tx)} = {} & (E_{Tx} * R_{Config} + E_{SDN-WISELayer} * R_{Config-SDN-WISELayer}) \\ & + (E_{Tx} * R_{Open} + E_{SDN-WISELayer} * R_{Open-SDN-WISELayer}) \\ & + (E_{Tx} * R_{BEC} + E_{SDN-WISELayer} * R_{BEC-SDN-WISELayer}) \\ & + (E_{Tx} * R_{RES} + E_{SDN-WISELayer} * R_{RES-SDN-WISELayer}) \end{aligned} \tag{5.32}$$

and $PC_{SNK(CTR)(Rx)}$ represent the PC for reception process of 802.15.4 radio and SDN-WISE processing for single SNK node is written as in Equ. 5.33:

$$\begin{aligned} PC_{SNK(CTR)(Rx)} = {} & (E_{Rx} * R_{REP} + E_{SDN-WISELayer} * R_{REP-SDN-WISELayer}) \\ & + (E_{Rx} * R_{REQ} + E_{SDN-WISELayer} * R_{REQ-SDN-WISELayer}) \\ & + (E_{Rx} * R_{BEC} + E_{SDN-WISELayer} * R_{BEC-SDN-WISELayer} \end{aligned} \tag{5.33}$$

The Beacon signalling is excluded from $PC_{SNK(Eth-Port-Config)(CTR)}$ as its signalling traffic streams do not pass out via Ethernet port to the external network.

5.2.2.3 PC in SDN-WISE proxy controller

The power consumption for SDN-WISE controller as shown in Equ. 5.34,

$$PC_{WISE-VISOR} = PC_{CTR} + PC_{TM} + PC_{Adapt} \tag{5.34}$$

which includes:

- SDN-WISE (PC_{CTR}) as Controller Application PC.
- TM PC (PC_{TM}).
- Adaptation process PC as (PC_{Adapt}).

The controller application is assumed to have a constant PC value based on the controller as an application as described in [121] as shown in Table 5.2.

5.3 Results and discussion

This section introduces the numerical results and its analysis for proposed network model in order to identify the PC in terms of the interaction of KQI with KPI regarding network setting as shown in TABEL 5.2, which were chosen based on [29] with a scenario of 2000 SNs and 16 SNK nodes. Thereby each SNK node as a WSN terminal gateway are attached with 125 SNs. The results with their discussion are divided into two parts control plane PC and data plane PC.

5.3.1 Assumptions

There are some specific assumptions were considered, as listed below, in the calculations of total PC of the proposed network model using the introduced PC model. This has been done in order to introduce a fair comparison in the results and data analysis. Additionally, These assumptions are set to focus on the interaction between data plane traffic and control plane signalling streams effects on PC in different network elements, such as SNs and SNKs.

- The TTI of the control signalling assumed to be the same signalling rate for all of them.

- A single hop transmission between SNs and SNK in the 802.15.4 radio is considered.
- The maximum allowed 802.15.4 link rate in Packets Per Seconds (PPS) is achieved according to the Equ. 5.35 below:

$$LinkRate_{802.15.4}(PPS) = [LinkRate_{802.15.4}(bps)]/[[PayloadSize(Byte/Packet)+41]*8] \quad (5.35)$$

- Achieved NQoS represented by maximum available link rate (throughput) in bps as KPI of 802.15.4 radio link.
- Requested AQoS represented by payload size in Byte/Packet as KQI of IoT application or service.

Fig. 5.3 shows the analysis of packet rate as a function of IoT application payload size for different 802.15.4 physical layer link rates between SN and SNK. Maximum of PPS = 235 required for 92 (Bytes) payload packet size when the link rate is 250 (kbps), while 612.7 PPS for 10 (Bytes) payload when the link rate is 250 (kbps). In the proposed model 802.15.4 link throughput has been set to 66.667 PPS, when needed, as in the original model of SDN-WISE presented by [29].

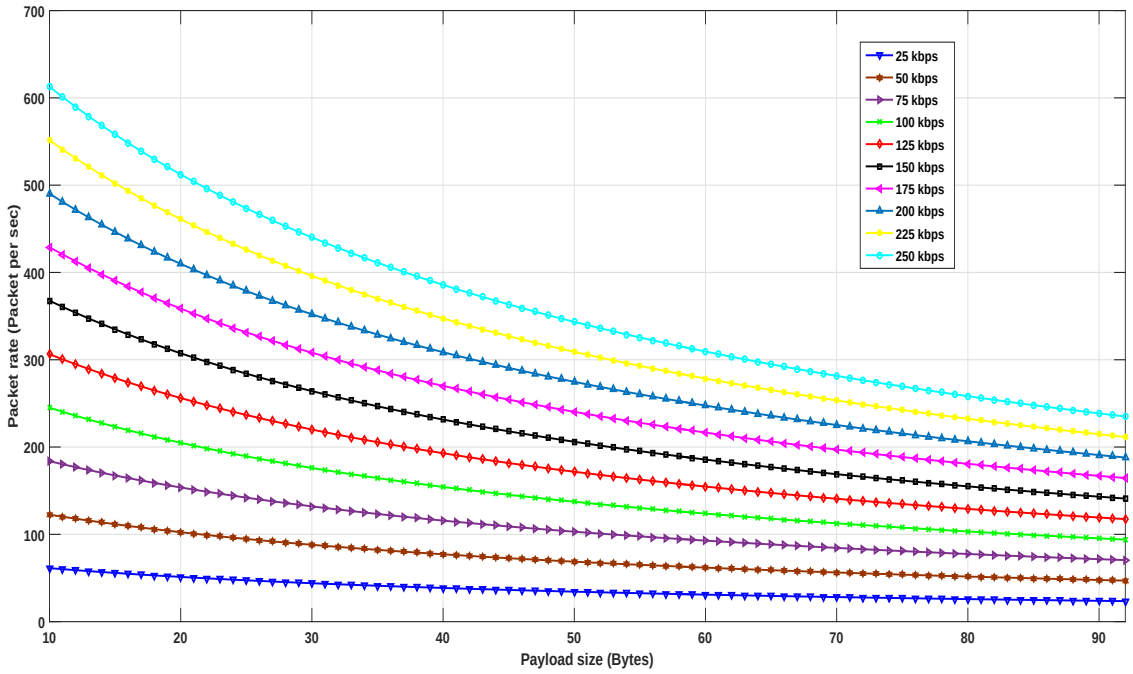

Fig. 5.3 802.15.4 PHY PDU rate with respect to the IoT application PDU size for different wireless link rates.

5.3.2 Control plane PC

In control plane, the controllers and WISE-VISOR are determined the SDN logics. The power consumed in the control plane is related to the aspects below:

(a) **Topology Discovery PC.**

The first set of the PC model elements to consider here is TD signalling PC with regard to the TTI. Because the construction of the network topology initiates at the network elements, which are SNKs and SNs as described in TD [29].

Fig. 5.4 shows an overview of all the elements of the TD signalling PC in the network elements of the proposed network scenario. Fig. 5.4 (a) presents the PC of the Beacon signalling. The most interesting aspect of this graph is the interaction between the PC of the Beacon traffic in the network elements and TTI. Furthermore, Fig. 5.4 (a) provides the percentage decrease in the Beacon process's PC with respect to TTI. It shows a significant reduction of 50% in the consumed power when the TTI is increased to 10 sec, and 75% at 20 sec. Surprisingly, only a 20% extra reduction in power consumption is achieved when the TTI reaches 90 sec in comparison with 20 sec (TTI beacon PC).

Fig. 5.4 (b) and (c) demonstrate the PC and percentage decrease of the Report signalling and Configuration signalling with respect to TTI. The Report and Configuration signalling represent the complementary processes of the network TD framework, since they are accompanying with the Beacon signalling process. Report signalling is used to send the required information from the terminal devices SNs and sink nodes to the WISE-VISOR as well as to the TM application. The Configuration signalling is employed to send the related modification/adjustment information from WISE-VISOR to the terminal devices. As shown in Fig. 5.4 (b) (the PC of Report signalling decreases with an increase in the TTI. The percentage decrease of Report PC gives 33.71% decrease in PC at 10 sec TTI and achieves 50.56% decrease of PC at 20 sec TTI, whereas the percentage decrease gives 63.67 at 90 sec TTI.

Fig. 5.4 (c) shows a decrease in Configuration PC with the increase in TTI, as the percentage decrease of configuration signalling PC achieves 13.15% at 10 sec TTI and 19.73% at 20 sec, while the percentage decrease only reaches 24.85% at 90 sec.

Fig. 5.4 (d) provides the total PC and percentage decrease of all TD signalling PC; the Beacon, Report and Configuration PCs were added together, and the PC of the total TD signalling decreased as the TTI increased. The percentage decrease of TD PC gives 47.73% and 71.6% at 10 and 20 sec TTI respectively, whereas it achieves

90.16% at 90 sec of TTI. Table 5.4 lists the PC percentage share of Beacon, Report and Configuration of total TD signalling PC. Closer inspection of the Table 5.4 shows the Beacon's share decreased as the TTI increased. Furthermore, the Report and Configuration PCs' shares within TD signalling were increased with the increased TTI.

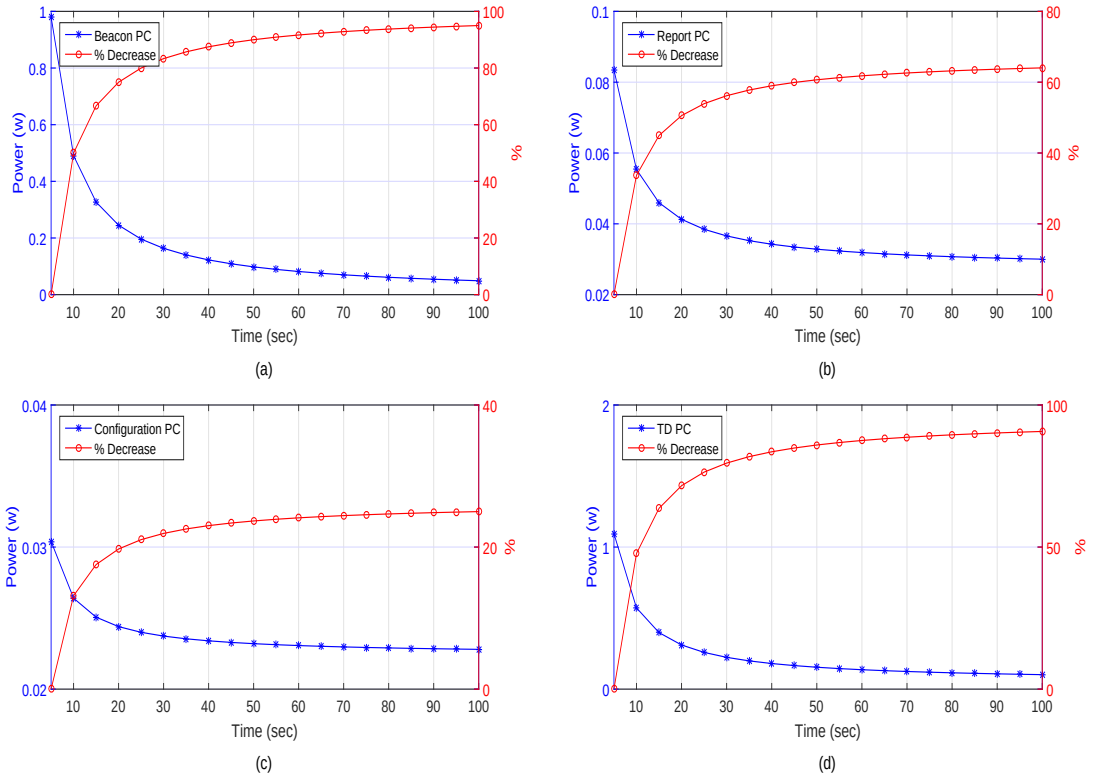

Fig. 5.4 PC of TD control plane signalling (a) BEC, (b) REP, (c) Config and (d) TD Total

Table 5.4 Percentage share of TD signalling PC

TTI (sec)	BEC %	REP %	Config %
5	89.59	7.842	2.778
10	85.71	9.677	4.616
20	78.87	13.28	7.852
40	68.01	19	12.99
80	53.33	26.74	19.93
90	50.6	28.18	21.22

(b) **Request and Response PC**

When the network element receives the arrived packet, and if it passes the accepted ID inspection process. Once there is no matching, no match occurs in the Flow Table or there is a specific amount of delay happening in FWD process and when the INPP cannot state any decision about the processed packet, then Request packet will be sent to the WISE-VISOR. Consequently the Response packet containing updated flow rules will be reacted and activated according to the received Request. Fig. 5.5 (a) and 5.5 (b) provides an overview of the PC for Request and Response control signalling in the network elements respectively, assuming all network elements, excluding the SNK nodes, was sending Request and receiving Response. Essentially, the transmission of the Request packet and its complementary Response one they are not carried out on a periodic basis; their presence as part of the control signalling rules framework, which is set by NOS.

Fig. 5.5 (a) presents the sum of the Request signalling PC and the percentage decrease in PC with respect to TTI. The PC decreases as the TTI increases; the percentage decrease provides an indication that the decrease will be 36.1% at 10 seconds and 68.18% at 90 seconds.

Fig. 5.5 (b) introduces the Response signalling PC and the percentage decrease in PC with respect to TTI. It shows a decrease in the PC as the percentage decreases, giving 13.25% at 10 sec TTI and 25.01% at 90 sec.

Fig. 5.5 (c) gives both the Request and Response processes PC and their percentage decrease with TTI. The PC decreases as the TTI increased, which is clear from the percentage decrease as it gives 32.56% at 10 sec, 48.84% at 20 sec and 61.5% at 90 sec. The most interesting aspect of this graph is that the percentage decrease variation rate of PC reduces as the TTI increases, as the reduction in PC performance is 12.66% over 20 sec.

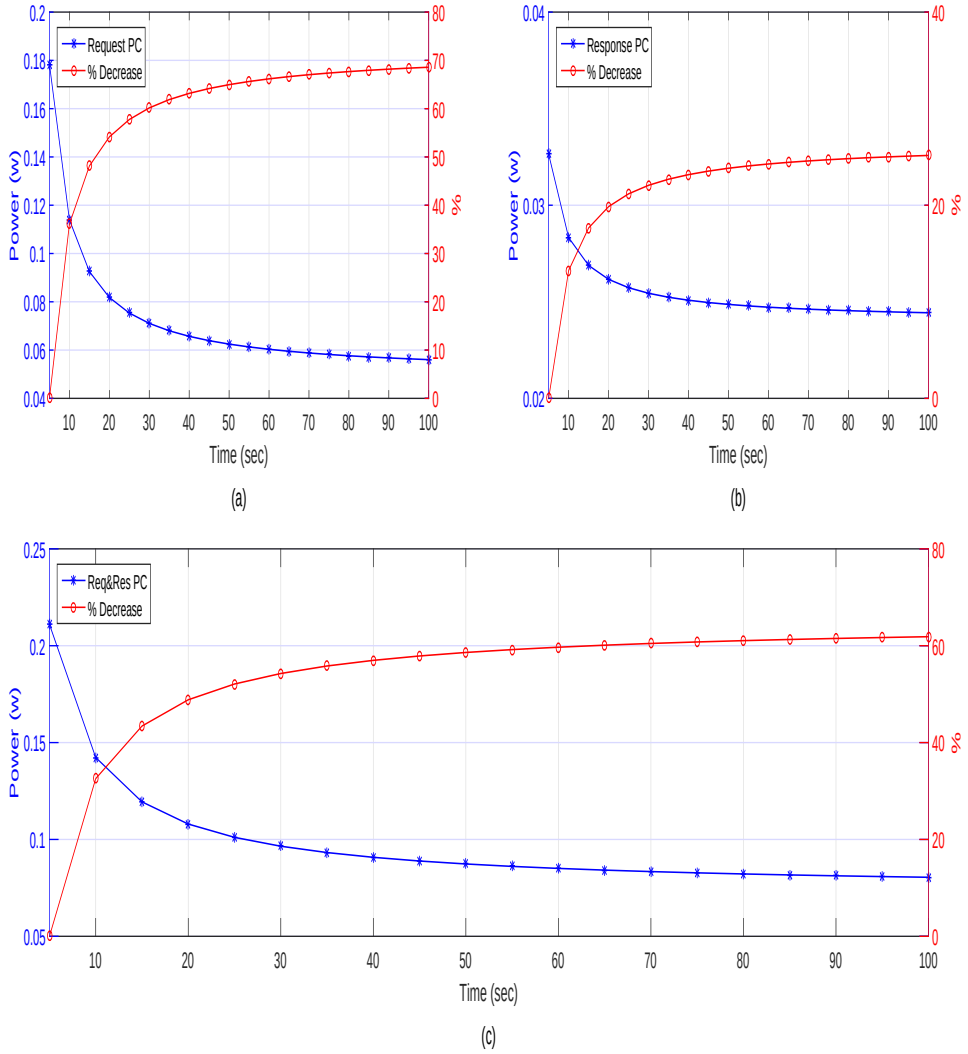

Fig. 5.5 (a) Request, (b) Response and (c) Total Request and Response with respect to the TTI

(c) **Registry Proxy and Open Path PC**

RegProxy signalling could be considered to be a part of the TD signalling of SDN-WISE control plane signalling, as its packet is used to send some information about the existence of the SNK node to the WISE-VISOR in order to prevent the registration of the SNK node as a switch on the other SDN controllers. The openpath signalling is initiated at the SNK nodes towards the WISE-VISOR. It can be classified as an QoS proactive support signalling. What's more, it is considered one of the important features of SDN-WISE, as it is a reactive support signalling to the data plane traffic,

which is used to reduce the control messages transmitted from the control plane toward network elements. Fig. 5.6 (a) shows the PC and the percentage decrease in PC of RegProxy control signalling with respect to the TTI. The PC in the 16 SNKs starts with 30.41 mW at 5 sec TTI and reduces approximately to 30.4 mW at 90 sec TTI. The percentage decrease of RegProxy PC gives 0.0177% at 10 sec and increases to 0.0334% at 90 sec TTI. Fig. 5.6 (b) presents the PC in the network elements of Openpath signalling with respect to TTI. The PC starts with 35.32 mW at 5 sec of TTI and performs 26.14 mW at 90 sec TTI. The percentage decrease in PC with respect to the increase in TTI shows a decrease of 13.76% at 10 sec TTI and it decreases further at 90 sec of TTI to 26%.

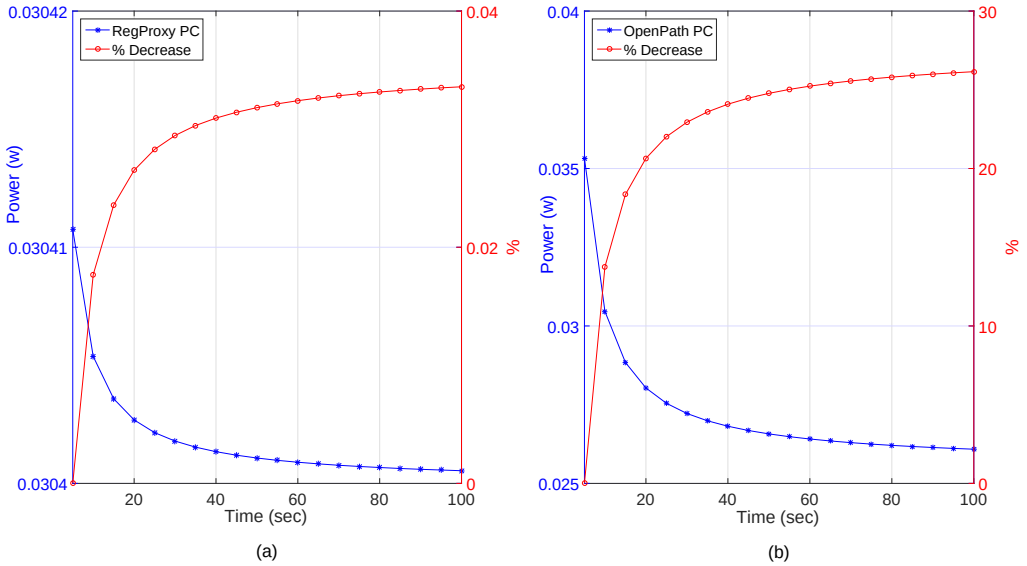

Fig. 5.6 (a) Registry Proxy and (b) Openpath

(d) **Total PC for all control plane signalling**

The aforementioned group of signalling characterises the control plane signalling of the SDN-WISE among the SDN elements. It's shaping the total PC of the control plane in the network elements. Fig. 5.7 represents the total PC of the control plane and the percentage decrease of this PC with respect to TTI in the network elements such as SNs and SNKs in the proposed network scenario and control plane signalling configuration. This figure shows that the PC decreases as the TTI increases.

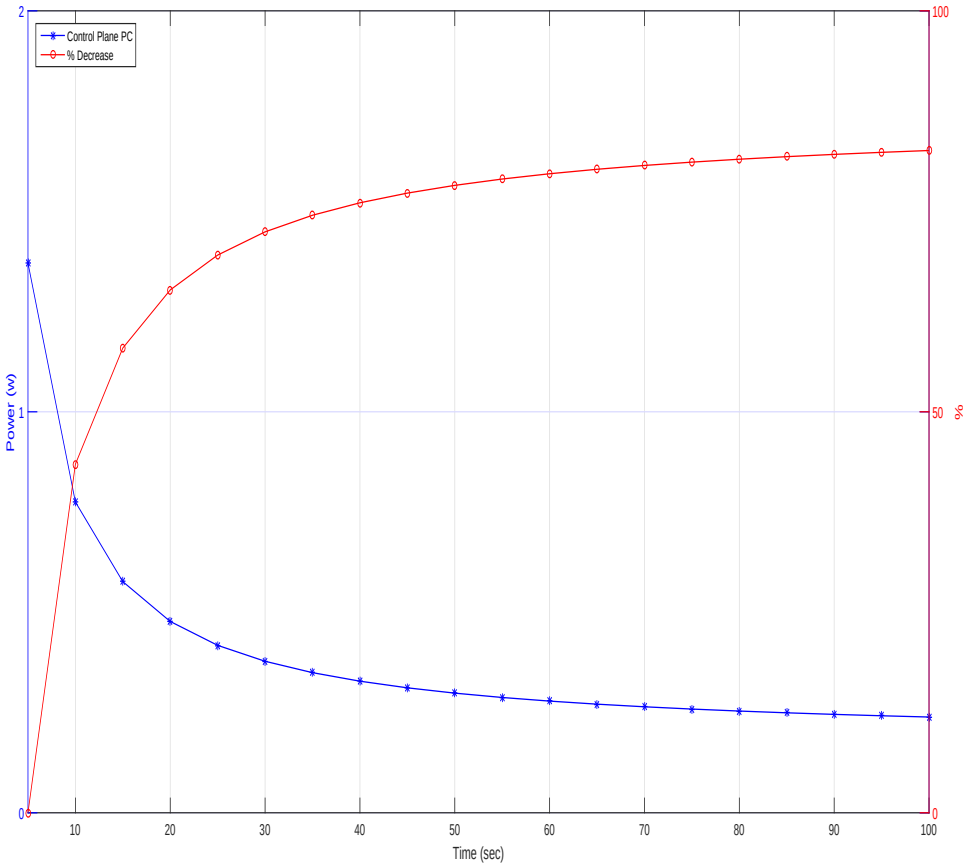

Fig. 5.7 Total Control Plane Signaling PC

The percentage decrease is 43.46% when the TTI is 10 sec, 65.2% at 20 sec and 82.1% at 90 sec TTI. There is a dramatic reduction in the control plane PC in the network elements with respect to TTI, specifically in the range between 0 to 40 sec, where the percentage decrease reached 76.0%. In addition, high NQoS will need higher rate of control signalling, since it aims to update network topology configuration. All these need an additional power to be consumed to achieve the required goals. These percentages can be presented in a pie-chart as shown in Fig. 5.8. Where the data plane traffic data rate as the same as one in the proposed original setting of the introduced scenario of SDN-WISE network by [29], the possibility of having SNs that respond to the incoming messages depending on state variables that reduces the number of control plane messages exchanged between each SN and the WISE-VISOR, thus as a

result this will reduce the number of packets sent over the network and the total energy consumption.

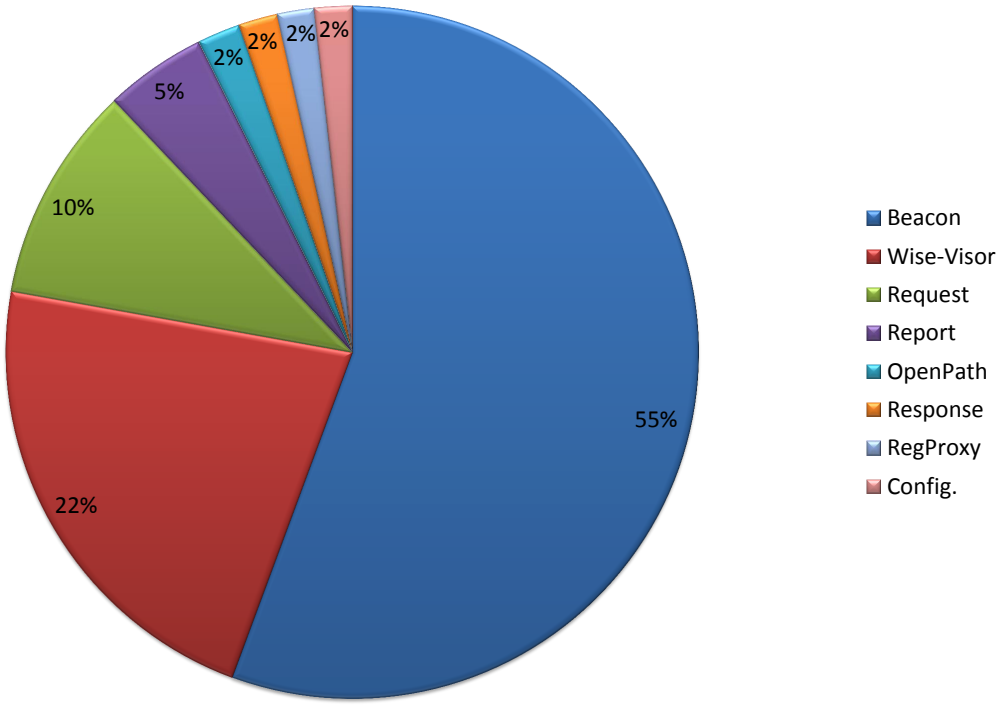

Fig. 5.8 Control Plane Signalling PC

5.3.3 Data plane PC

Fig. 5.9 shows the PC of data plane traffic and the percentage increase with respect to the payload size (Bytes). The payload size starts with 10 Bytes, the same as the prototype testbed of the SDN-WISE in [29], and the maximum payload size is set to 92 Bytes in order to match the maximum allowed packet payload size of 802.15.4 standard [29] [56]. In Fig. 5.9 there is a clear trend of increasing PC with increasing payload size. The percentage increase of PC is not only directly related to the payload size but also includes the power consumed by the packet headers of SDN-WISE and 802.15.4. The PC of Idle in the SNs and SNKs as well as the PC of constant port configuration of the Ethernet port in the SNKs are not included here, because they are just a constant value and to emphasise the dynamic change of PC only with the payload size.

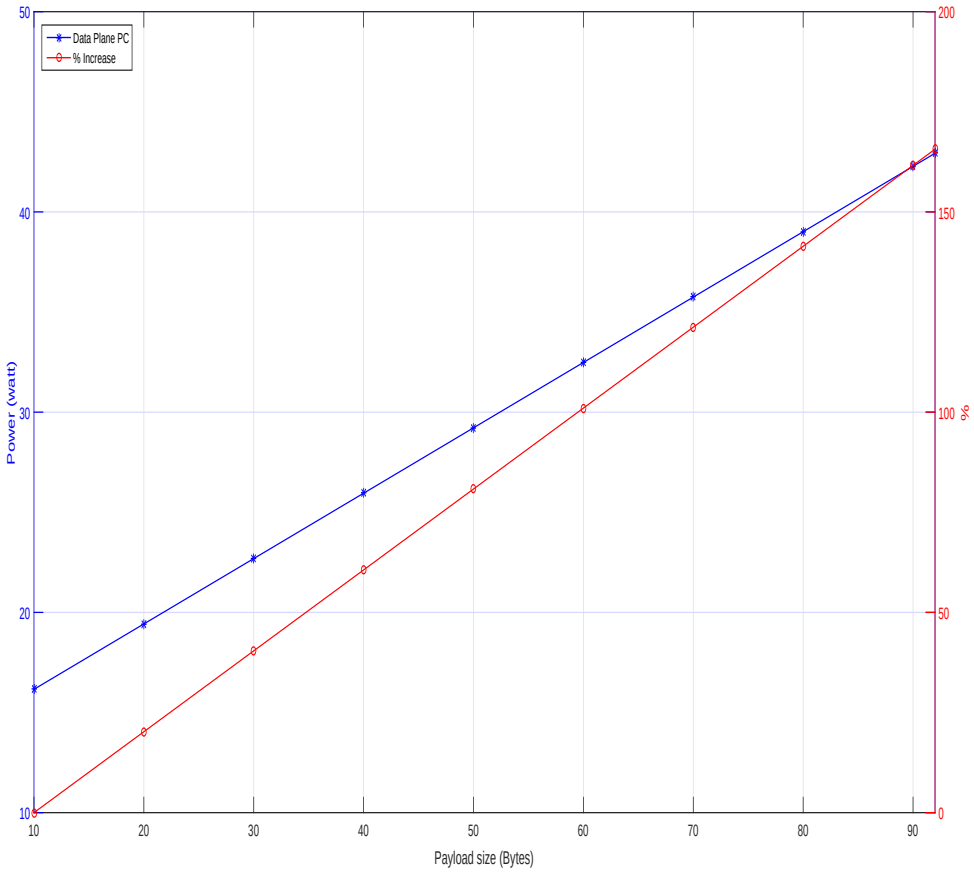

Fig. 5.9 PC of data plane traffic

5.3.4 Total PC

Fig. 5.10 provides the total PC (Data plane and Control plane) of the proposed network scenario in the SNs and SNKs without idle and constant port configuration. As it can be seen from Fig. 5.10, the total PC reduces when the TTI increases and it increases with increasing payload size. Closer inspection of the Fig. 5.10 shows that there is a significant decrease of the total PC when the control plane TTI is increased.

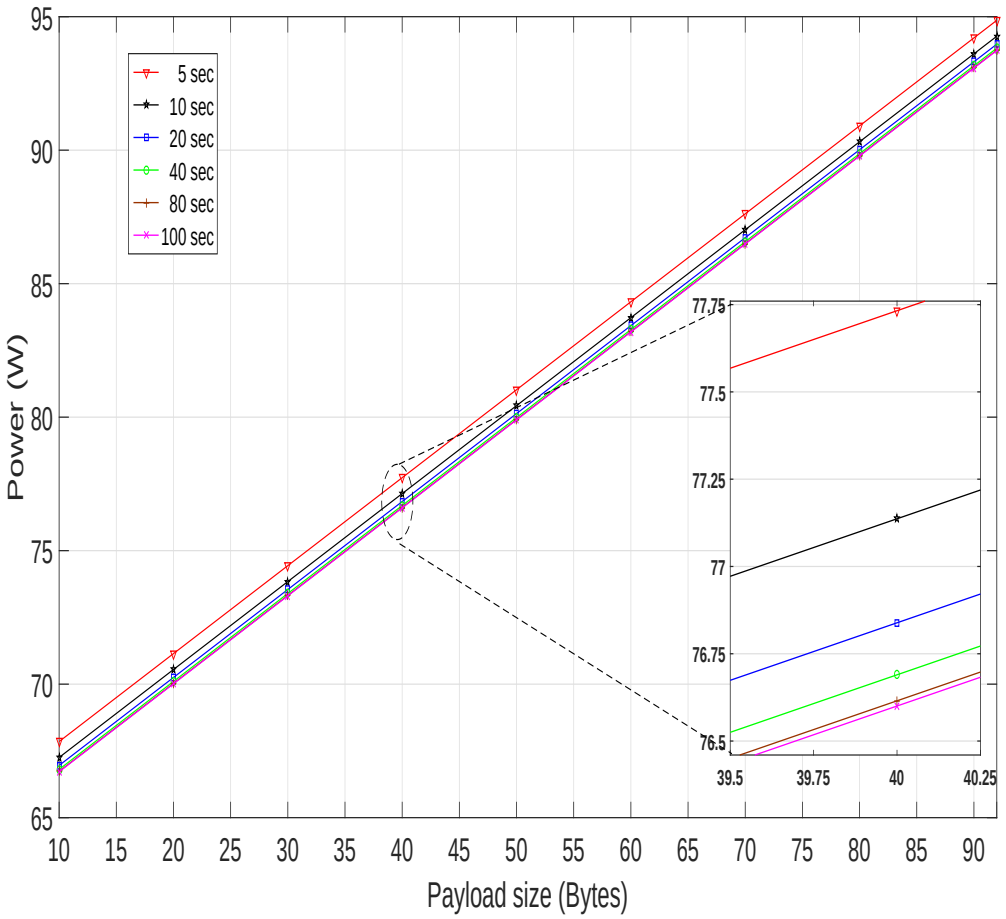

Fig. 5.10 Total PC in Control Plane and Data Plane point of view 1

Fig. 5.11 presents the total PC in the network elements, represented by the PC of the SNs and the SNKs as data plane traffic consumption, as well as the control plane. The PC is represented by control signalling of the network scenario with the PC of the controller application with respect to variation in control plane signalling TTI for different payload sizes starting with 10 Bytes and increasing to 90 Bytes.

Fig. 5.11 shows that there is significant change (decrease) in the total PC when the TTI of control signalling is between 5 and 40 sec. The lower TTI means that for highly supported QoS network needs to provide more network resources to control plane signalling, which in turn is reflected as power consumed in the network element. The overall efficiency of the network can be divided into three parts. The *first* concerns is the PC, the *second* concerns is the ratio of the data plane traffic transmitted between source and destination points to

the control plane signalling, and the *third* is related to NQoS provided to satisfy IoT AQoS needs.

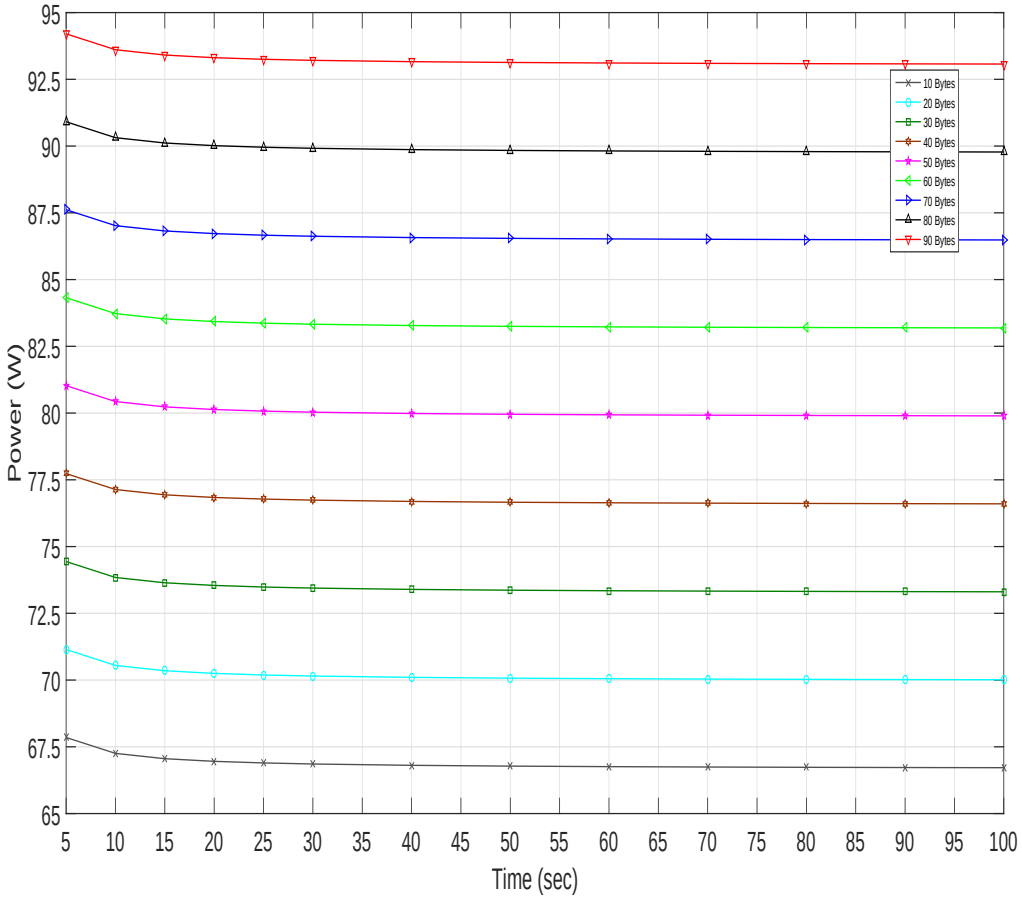

Fig. 5.11 Total PC in Control Plane and Data Plane point of view 2

Furthermore, Fig.5.12 represents a normalized 3D plot of PC with respect to the TTI of control signalling and the payload size of data plane traffic. The idle and constant port configuration power consumptions are not considered and they are only in the SNs and SNKs. This shows that the PC increases with increasing payload size, as well as with decreasing TTI.

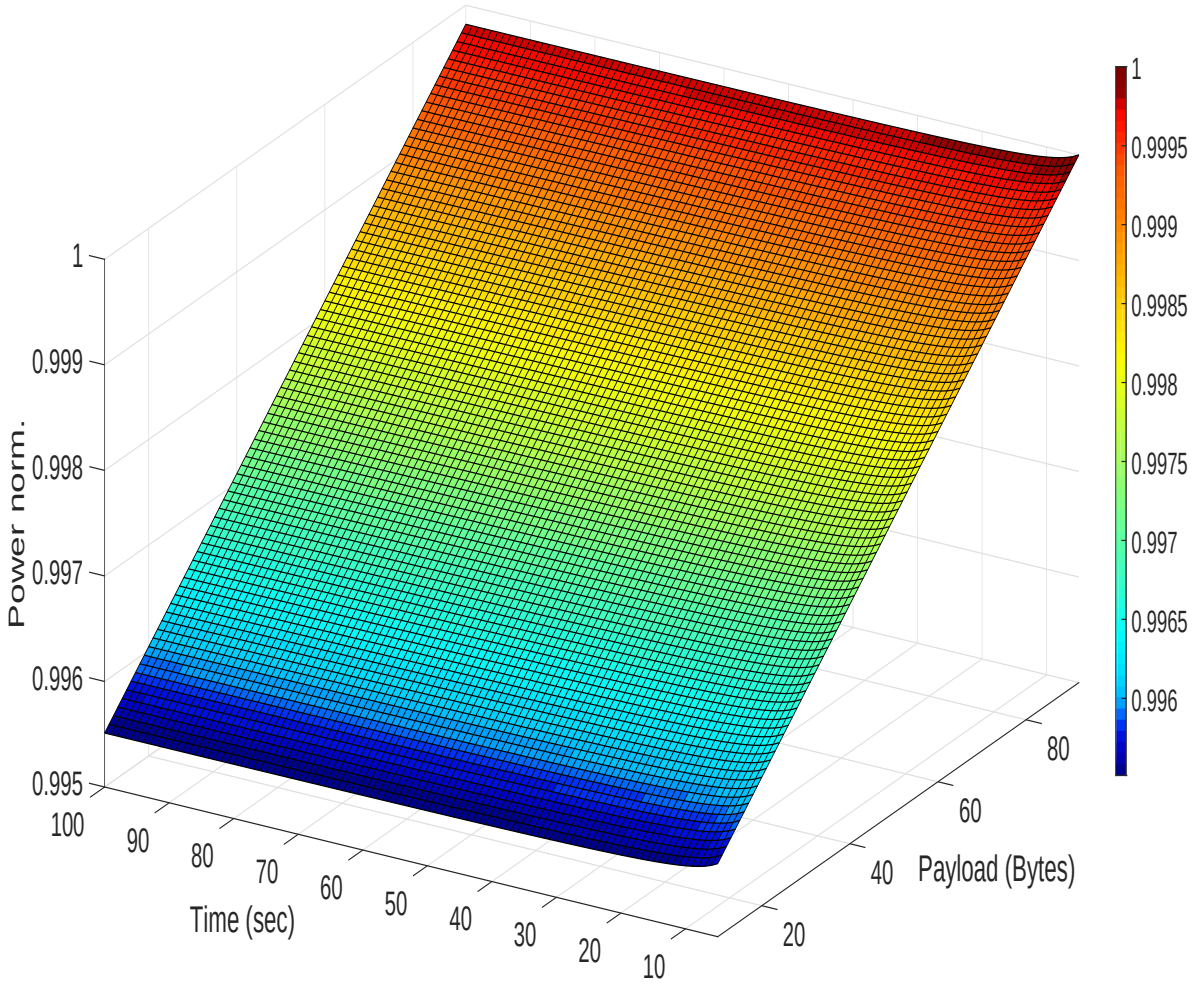

Fig. 5.12 The Total Normalized PC of with respect to TTI and payload size

Fig. 5.13 shows the normalized total PC for 2000 SNs, 16 SNKs and 5 sec TTI setting with respect to payload size (Bytes) and the 802.15.4 PHY layer radio link data Rate (bps). A closer look at this 3D plot shows that the PC increases linearly with the payload size and with the achieved physical layer link rate between SNs and SNKs. This figure is normalised for the maximum achieved power consumption related to maximum payload size and maximum link rate. Here the dominant factor in PC is the achieved link rate; the minimum link rate of 25 kbps gives 18.25% and 18.43% associated with 10 Bytes and 90 Bytes payload sizes respectively, while the maximum link rate of 250 kbps achieves 98.29% and 100% related to 10 Bytes and 90 Bytes payload sizes respectively.

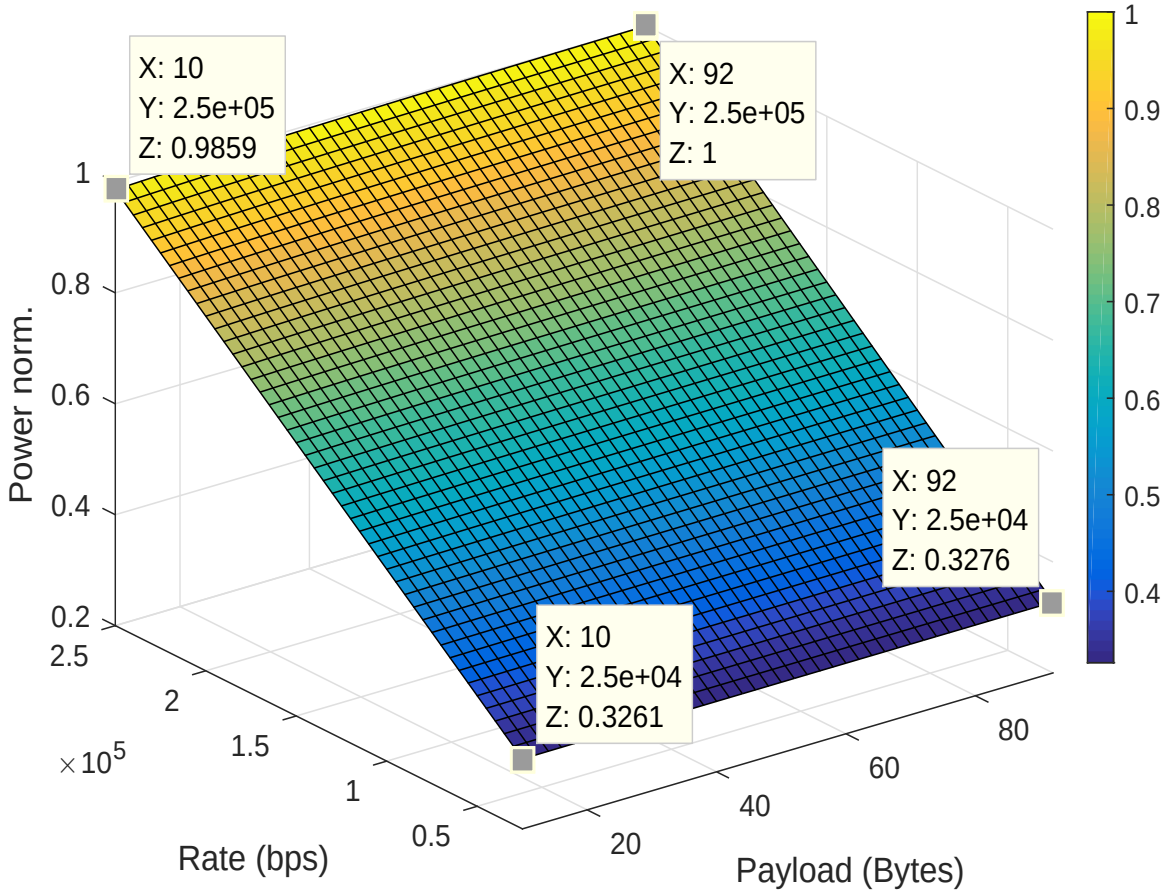

Fig. 5.13 The Total Normalized PC with respect to payload size and data rate

Moreover, the total PC of the Data Plane (DP) from the whole system power is 98%, whereas the Control Plane (CP) spends just 2%, with minimum TTI (5 sec) and maximum payload size of 92 Bytes as shown in Fig. 5.14

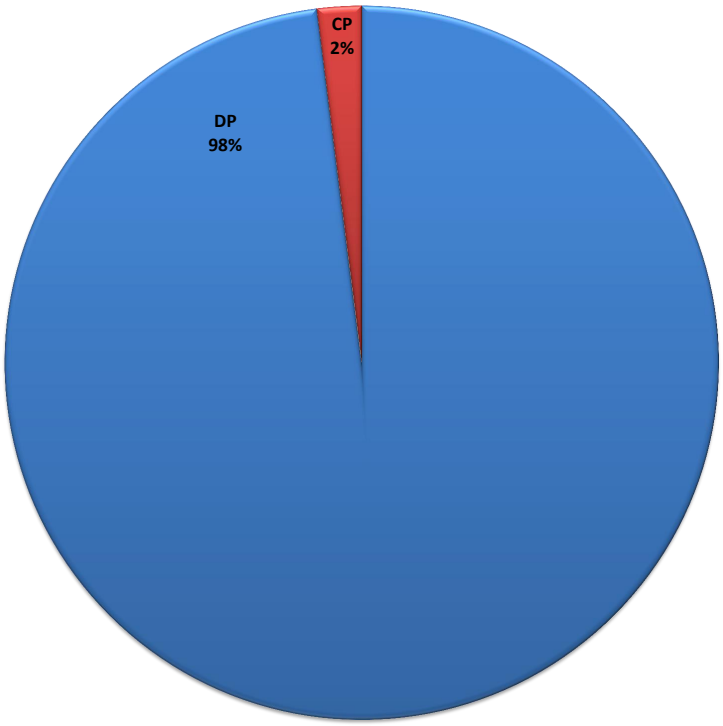

Fig. 5.14 The Total PC for DP and CP

5.4 Summary

A thorough analysis has been done in this chapter to model the PC of a SDN based IoT system. It decomposes all of the element functions of the SDN-WISE structure, which is supporting the IoT application and services of WSN by the SDN. They are working together but according to assorted margins to sustain a high NQoS levels. The architecture of the model of the proposed work is based on [29] for profiling a PC model for SDN in WSN as an SDN-WISE. This model is an essential part for the network to be managed in a flexible manner. Consequently, the proposed PC model for measuring the PC strongly plays an essential role in the offered SDN NQoS for meeting the required AQoS of IoT applications. This chapter casts a mathematical framework in the investigation of the PC model. It is subdivided into two important parts: control signalling and data traffic PCs. This methodology and the associated framework have been based on the power-efficient 802.15.4 in the wireless part and TCP/IP in the wired access technologies for the IoT over a range of traffic levels. A range of parameters have been used to construct the PC of the IoT applications, this done by introducing the SDN-WISE PC model. The propose evaluation processes of the WSN architecture in the SDN-WISE paradigm could be modified depending on the control plane signalling parameters and achieved data traffic metrics. The results indicate that the effectiveness of the additional control signalling are gave a consumption of 98% from the total PC as a Data Plane traffic and 2% as a Control Plane signalling. This figure can be steered in order to achieve the required level in the offered NQoS, such as reducing the TTI of the control signalling in the control plane.

Chapter 6

Conclusions and future work

6.1 Conclusions:

This thesis was focused on management, enhancement, assurance and provision of QoS of PS network as a 5G network.

It's made up of four main chapters. Each chapter provide a specific contribution to support thesis goal as following:

- Chapter 2: In this chapter, an introduction to the fundamentals and principles of chapters 3, 4 and 5 was provided.
- Chapter 3: This chapter has addressed the challenges of heterogeneity by integrating HTC and IoT traffic through their mutual interaction within network elements (nodes and links), in terms of the resultant and distinct E2E NQoS metrics. The motivation for the chapter was based on the fact that the existing LTE-APro PCC rules and procedures do not differentiate between the user type of the terminal devices, which produces a lack of NQoS levels being offered and hence, potentially not meeting the AQoS demands made by the used service. An access WSN gateway has been proposed to provide E2E connectivity for MTC's traffic flow within the licence spectrum of LTE-APro media. An approach of protocol conversion and facilitation of the control of the EPS network resources' QoS level assigned for MTC traffic flows, in the context of PCC functions and rules, has been provided. A policy for traffic flow management that defines MTC traffic flows over the EPS network has been put forward, in order to use a fraction of the available network resources in a seamless manner, accompanied by a new specific group of QCIs, assigned to define the QoS levels of the MTC bearers' connectivity. The allocation of network resources for MTC traffic flows are tuned

based on terminal type needs, i.e. on the level of importance of the traffic type sent by MTD. In addition, The QoE of real time application human users is assured within the perceived quality levels. The simulation results have shown that the proposed policy of traffic flow management within the LTE-APro network infrastructure outperforms the current one in terms of NQoS levels, not only for HTCs traffic flows but also, for those of MTCs. However, in terms of the VoLTE service, it some degradation was encountered with the offered NQoS, due to the use of high rate codec in the application layer and the absence of a specific scheduling procedure to the VoLTE bearer at the radio interface. Nevertheless, the VoLTE service QoE level was retained within the recommended standardisation level.

- Chapter 4: In this chapter, the main challenges in the multiple pools C-RAN architecture are the partition of the network for a required number of BBU pools, their positions and the number of connected RHHs per each pool. In this chapter, an algorithm for partitioning a single network into a required number pools as well as finding the optimal BBU pool positions over the DC-RAN architecture has been proposed. Under this approach the set of RRH positions is considered in terms of a set of feasible locations and the number of BBU pools in a specific network. The multiple pooling based PSO clustering algorithm has been used to solve the RRH pooling configuration problem, with the optimal BBU pool location allocation, after first, determining their optimal number. That is, the BIC criterion have been used to narrow the search problem of identifying the range of the candidate multiple pools numbers in the search for the optimal multiple pools configuration. Subsequently, the measure of spread technique of the RRH numbers among the candidate multiple BBU pool configurations has been successfully used to choose the unique optimal multiple pool configuration for the proposed network. Finally, Voronoi tessellation interaction of the activated main RRHs of DC-RAN has facilitated allocating the pools areas as well as the number of connected RRHs with each BBU pool. It was shown that there was a significant change in the number of active RRHs within each pool area as a result of using the CRE criterion.

- Chapter 5: This chapter casts a mathematical framework in the investigation of the PC model. It's subdivided into two important parts: control signalling and data traffic PCs. This methodology and the associated framework have been based on the power-efficient 802.15.4 in the wireless part and TCP/IP in the wired access technologies for the IoT over a range of traffic levels. A range of parameters have been used to construct

the PC of the IoT applications, this done by introducing the SDN-WISE PC model. The propose evaluation processes of the WSN architecture in the SDN-WISE paradigm could be modified depending on the control plane signalling parameters and achieved data traffic metrics. The results indicate that the effectiveness of the additional control signalling are gave a consumption of 98% from the total PC as a Data Plane traffic and 2% as a Control Plane signalling. This figure can be steered in order to achieve an improve the NQoS, such as reducing the TTI of the control signalling in the control plane.

6.2 Future work:

The proposal for future works is matching the scope of the work that has been done in this thesis as:

- In the context of the heterogeneity of NGN, the key driver will be the use of Network Functions Virtualization (NFV) and SDN in order to set the proposed policy of traffic flow management in the NOS layer as an QoS global engine to drive the control layer elements (controllers) to update the QoS mechanisms in the network elements , such as gateways in the CN. Furthermore, the traffic flow policy management can be set in the COs of the C-RAN network architecture as a local traffic flow policy manger for the data plane traffic apart from CN bearers initiations and setting.

- Regarding the multiple BBU approach, the future work can be employed to support a multiple objective optimisation deployment goals which are supporting different NQoS point of views. Additionally, the proposed PSO multi-polling approach can be built to consider the optimisation goals as an adaptive enhancement of the offered NQoS during the network operation phase to be used in the support of virtual C-RAN, which needs to change the COs deployment and network configuration adaptively according to the radio interfaces traffic loads and AQoS needs/requirements. Finally, the placement of the virtualised BBU pool in the C-RANs based networks, is a crucial issue. The optimal position of the BBU pool can offer enhanced spectral efficiency, received data rates and QoS for the UEs. As the UEs resources assignments entities and set-ups functions are placed far away from the UEs in the pool, the problem of placing the BBU pool becomes a prerequisite to ensure that these functions' signals reach the RRHs without any extra delay. This eternally influences the network performance.

- With respect to the introduced PC model, this model could be used with different optimisations aim such as optimizing the KQI, KPI and energy efficiency. The optimisation coals can be set to improve energy efficiency such as the life time of the terminal network elements with specific energy constraints levels. The PC model can be modified to accommodate any newly introduced or added control signalling, layer or function in order to check their impact from a specific point of view.

References

[1] M. J. Marcus, "5g and" imt for 2020 and beyond"[spectrum policy and regulatory issues]," *IEEE Wireless Communications*, vol. 22, no. 4, pp. 2–3, 2015.

[2] M. Agiwal, A. Roy, and N. Saxena, "Next generation 5g wireless networks: A comprehensive survey," *IEEE Communications Surveys & Tutorials*, vol. 18, no. 3, pp. 1617–1655, 2016.

[3] B. W. Chen, W. Ji, F. Jiang, and S. Rho, "QoE-Enabled Big Video streaming for Large-scale heterogeneous Clients and Networks in Smart Cities," *IEEE Access*, vol. 4, pp. 97–107, 2016.

[4] B. K. J. Al-Shammari, N. Al-Aboody, and H. S. Al-Raweshidy, "Iot traffic management and integration in the qos supported network," *IEEE Internet of Things Journal*, vol. 5, no. 1, pp. 352–370, Feb 2018.

[5] N. F. S. de Sousa, D. A. L. Perez, R. V. Rosa, M. A. Santos, and C. E. Rothenberg, "Network service orchestration: A survey," *arXiv preprint arXiv:1803.06596*, 2018.

[6] ITU Telecommunication Standardization. (2015) FG IMT-2020: Report on Standards Gap Analysis. [Online]. Available: https://www.ietf.org/lib/dt/documents/LIAISON/liaison-2016-02-26-itu-t-sg-13-ietf-ls-on-report-on-standard-gap-analysis-from-itu-t-focus-group-on
pdf

[7] "Series y: Global information infrastructure, internet protocol aspects and next generation networks –future networks: Objectives and design goals," *International Telecommunication Union, Geneva, Switzerland, Recommendation ITU-T Y.3001*, 2011. [Online]. Available: https://www.itu.int/rec/T-REC-Y.3001-201105-I

[8] T. Szigeti and C. Hattingh, *End-to-end qos network design*. Cisco press, 2005.

[9] O. Modeler, "Riverbed Technology," *Inc. http://www. riverbed. com*, 2016.

[10] Chen, H. and Huang, L. and Kumar, S. and Kuo, C.C.J., *Radio Resource Management for Multimedia QoS Support in Wireless Networks*. Springer US, 2012. [Online]. Available: https://books.google.co.uk/books?id=PrwGCAAAQBAJ

[11] S. Yinbiao, P. Lanctot, and F. Jianbin, "Internet of Things: wireless sensor networks," *White Paper, International Electrotechnical Commission, http://www. iec. ch*, 2014.

[12] J. Eckenrode, ""The derivative effect: How financial services can make IoT technology pay off"," 2015. [Online]. Available: https://dupress.deloitte.com/dup-us-en/focus/internet-of-things/iot-in-financial-services-industry.html?coll=11711

[13] F. Ghavimi and H.-H. Chen, "M2M communications in 3GPP LTE/LTE-A networks: architectures, service requirements, challenges, and applications," *IEEE Communications Surveys & Tutorials*, vol. 17, no. 2, pp. 525–549, 2015.

[14] S. N. K. Marwat, T. Pötsch, Y. Zaki, T. Weerawardane, and C. Görg, "Addressing the challenges of E-healthcare in future mobile networks," in *Meeting of the European Network of Universities and Companies in Information and Communication Engineering*. Springer, 2013, pp. 90–99.

[15] M. Khan, R. S. Alhumaima, and H. S. Al-Raweshidy, "Qos-aware dynamic rrh allocation in a self-optimized cloud radio access network with rrh proximity constraint," *IEEE Transactions on Network and Service Management*, vol. 14, no. 3, pp. 730–744, 2017.

[16] H. Ghazzai, E. Yaacoub, M.-S. Alouini, Z. Dawy, and A. Abu-Dayya, "Optimized lte cell planning with varying spatial and temporal user densities," *IEEE Transactions on Vehicular Technology*, vol. 65, no. 3, pp. 1575–1589, 2016.

[17] A. Basta, A. Blenk, K. Hoffmann, H. J. Morper, M. Hoffmann, and W. Kellerer, "Towards a cost optimal design for a 5g mobile core network based on sdn and nfv," *IEEE Transactions on Network and Service Management*, vol. 14, no. 4, pp. 1061–1075, 2017.

[18] M. Khan, Z. H. Fakhri, and H. Al-Raweshidy, "Semi-static cell differentiation and integration with dynamic bbu-rrh mapping in cloud radio access network," *IEEE Transactions on Network and Service Management*, 2017.

[19] C. Pan, M. Elkashlan, J. Wang, J. Yuan, and L. Hanzo, "User-centric c-ran architecture for ultra-dense 5g networks: Challenges and methodologies," *arXiv preprint arXiv:1710.00790*, 2017.

[20] K. Chen and R. Duan, "C-ran: the road towards green ran," *China Mobile Research Institute, White Paper*, 2011.

[21] A. Checko, H. L. Christiansen, Y. Yan, L. Scolari, G. Kardaras, M. S. Berger, and L. Dittmann, "Cloud ran for mobile networks—a technology overview," *IEEE Communications surveys & tutorials*, vol. 17, no. 1, pp. 405–426, 2015.

[22] FUJITSU, "FUJITSU Network Remote Radio Head (RRH) Product Lineup," http://www.fujitsu.com/global/products/network/products/rrh-spec/, 2018, [Online; accessed 20-02-2018].

[23] I. A. Alimi, A. L. Teixeira, and P. P. Monteiro, "Toward an efficient c-ran optical fronthaul for the future networks: A tutorial on technologies, requirements, challenges, and solutions," *IEEE Communications Surveys Tutorials*, vol. 20, no. 1, pp. 708–769, Firstquarter 2018.

[24] (2016, March) C-ran and 5g take transport to new capacity and latency levels: Trends in backhaul, fronthaul, xhaul and mmw. [Online]. Available: http://content.rcrwireless.com/SenzaFili-backhaul-report

[25] Z. H. Fakhri, M. Khan, F. Sabir, and H. Al-Raweshidy, "A resource allocation mechanism for cloud radio access network based on cell differentiation and integration concept," *IEEE Transactions on Network Science and Engineering*, 2017.

[26] S. Watanabe, "A widely applicable bayesian information criterion," *Journal of Machine Learning Research*, vol. 14, no. Mar, pp. 867–897, 2013.

[27] L. Atzori, A. Iera, and G. Morabito, "The internet of things: A survey," *Computer networks*, vol. 54, no. 15, pp. 2787–2805, 2010.

[28] J. Lin, W. Yu, N. Zhang, X. Yang, H. Zhang, and W. Zhao, "A survey on internet of things: Architecture, enabling technologies, security and privacy, and applications," *IEEE Internet of Things Journal*, vol. 4, no. 5, pp. 1125–1142, 2017.

[29] L. Galluccio, S. Milardo, G. Morabito, and S. Palazzo, "SDN-WISE: Design, prototyping and experimentation of a stateful SDN solution for wireless sensor networks," in *2015 IEEE Conference on Computer Communications (INFOCOM)*. IEEE, 2015, pp. 513–521.

[30] S. Bera, S. Misra, and A. V. Vasilakos, "Software-defined networking for internet of things: A survey," *IEEE Internet of Things Journal*, vol. 4, no. 6, pp. 1994–2008, 2017.

[31] I. T. Haque and N. Abu-Ghazaleh, "Wireless software defined networking: A survey and taxonomy," *IEEE Communications Surveys & Tutorials*, vol. 18, no. 4, pp. 2713–2737, 2016.

[32] S. Costanzo, L. Galluccio, G. Morabito, and S. Palazzo, "Software defined wireless networks: Unbridling sdns," in *Software Defined Networking (EWSDN), 2012 European Workshop on*. IEEE, 2012, pp. 1–6.

[33] T. Luo, H.-P. Tan, and T. Q. Quek, "Sensor openflow: Enabling software-defined wireless sensor networks," *IEEE Communications letters*, vol. 16, no. 11, pp. 1896–1899, 2012.

[34] S. Bera, S. Misra, S. K. Roy, and M. S. Obaidat, "Soft-wsn: Software-defined wsn management system for iot applications," *IEEE Systems Journal*, 2016.

[35] K. M. Koumadi, B. Park, and N. Myoung, "Introducing the Latest 3GPP Specifications and their Potential for Future AMI Applications," *KEPCO Journal on Electric Power and Energy*, vol. 2, no. 2, pp. 245–251, 2016.

[36] I. Abdalla and S. Venkatesan, "A QoE preserving M2M-aware hybrid scheduler for LTE uplink," in *Mobile and Wireless Networking (MoWNeT), 2013 International Conference on Selected Topics in*. IEEE, 2013, pp. 127–132.

[37] C. W. Johnson, *LTE in Bullets*. Northampton, England : Chris Johnson, c2012, 2010.

[38] ETSI, "Digital cellular telecommunications system (Phase 2+) (GSM); Universal Mobile Telecommunications System (UMTS); LTE; Policy and charging control architecture," *ETSI TS 123 203 V13.6.0 (2016-03) Technical Specification*, 2016.

[39] M. Chiang and T. Zhang, "Fog and IoT: An overview of research opportunities," *IEEE Internet of Things Journal*, vol. 3, no. 6, pp. 854–864, 2016.

[40] R. Koodli and R. Ravikanth, "One-way loss pattern sample metrics," Tech. Rep., 2002.

[41] G. Almes, S. Kalidindi, M. Zekauskas, and A. Morton, "A one-way delay metric for ip performance metrics (ippm)," Tech. Rep., 2016.

[42] N. Seitz, "ITU-T QoS standards for IP-based networks," *IEEE Communications Magazine*, vol. 41, no. 6, pp. 82–89, 2003.

[43] R. Y. ITU-T, "1541," *Network performance objectives for IP-based services*, 2011.

[44] C. Demichelis and P. Chimento, "Ip packet delay variation metric for ip performance metrics (ippm)," Tech. Rep., 2002.

[45] S. Bradner, "Benchmarking terminology for network interconnection devices," Tech. Rep., 1991.

[46] H. Ekstrom, "QoS control in the 3GPP evolved packet system," *IEEE Communications Magazine*, vol. 47, no. 2, pp. 76–83, 2009.

[47] S. Albasheir and M. Kadoch, "Enhanced control for adaptive resource reservation of guaranteed services in LTE networks," *IEEE Internet of Things Journal*, vol. 3, no. 2, pp. 179–189, 2016.

[48] N. A. Ali, A.-E. M. Taha, and H. S. Hassanein, "Quality of Service in 3GPP R12 LTE-Advanced," *IEEE Communications Magazine*, vol. 51, no. 8, pp. 103–109, 2013.

[49] L. Koroajczuk, "Workshop presentation notes, How to Dimension user traffic in 4G networks," February 2014.

[50] P. Chanclou, A. Pizzinat, F. Le Clech, T.-L. Reedeker, Y. Lagadec, F. Saliou, B. Le Guyader, L. Guillo, Q. Deniel, S. Gosselin *et al.*, "Optical fiber solution for mobile fronthaul to achieve cloud radio access network," in *Future Network and Mobile Summit (FutureNetworkSummit), 2013*. IEEE, 2013, pp. 1–11.

[51] M. Jaber, M. A. Imran, R. Tafazolli, and A. Tukmanov, "5g backhaul challenges and emerging research directions: A survey," *IEEE access*, vol. 4, pp. 1743–1766, 2016.

[52] B. Lahad, M. Ibrahim, and K. Khawam, "A new uplink interference mitigation in hetnets using macro uplink subframe muting," in *Applied Research in Computer Science and Engineering (ICAR), 2015 International Conference on*. IEEE, 2015, pp. 1–6.

[53] O. G. Aliu, A. Imran, M. A. Imran, and B. Evans, "A survey of self organisation in future cellular networks," *IEEE Communications Surveys & Tutorials*, vol. 15, no. 1, pp. 336–361, 2013.

[54] A.-C. G. Anadiotis, G. Morabito, and S. Palazzo, "An sdn-assisted framework for optimal deployment of mapreduce functions in wsns," *IEEE Transactions on Mobile Computing*, vol. 15, no. 9, pp. 2165–2178, 2016.

[55] C. Intanagonwiwat, D. Estrin, R. Govindan, and J. Heidemann, "Impact of network density on data aggregation in wireless sensor networks," in *Distributed Computing Systems, 2002. Proceedings. 22nd International Conference on*. IEEE, 2002, pp. 457–458.

[56] E. Callaway, "Low power consumption features of the ieee 802.15. 4/zigbee lr-wpan standard," *Mini-tutorial, ACM Sensys*, vol. 3, pp. 5–7, 2003.

[57] W. Xiang, N. Wang, and Y. Zhou, "An energy-efficient routing algorithm for software-defined wireless sensor networks," *IEEE Sensors Journal*, vol. 16, no. 20, pp. 7393–7400, 2016.

[58] SDN-WISE. (2018, April) SDN-WISE Core. [Online]. Available: http://sdn-wise.dieei.unict.it/docs/guides/Core.html

[59] P. Di Dio, S. Faraci, L. Galluccio, S. Milardo, G. Morabito, S. Palazzo, and P. Livreri, "Exploiting state information to support qos in software-defined wsns," in *Ad Hoc Networking Workshop (Med-Hoc-Net), 2016 Mediterranean*. IEEE, 2016, pp. 1–7.

[60] R. A. Karam, "Enabling cisco legacy power to support ieee 802.3 af standard power," Jun. 28 2005, uS Patent 6,912,282.

[61] L. Costantino, N. Buonaccorsi, C. Cicconetti, and R. Mambrini, "Performance analysis of an LTE gateway for the IoT," in *World of Wireless, Mobile and Multimedia Networks (WoWMoM), 2012 IEEE International Symposium on a*. IEEE, 2012, pp. 1–6.

[62] A. Lo, Y. W. Law, and M. Jacobsson, "A cellular-centric service architecture for machine-to-machine (M2M) communications," *IEEE wireless communications*, vol. 20, no. 5, pp. 143–151, 2013.

[63] D. Lee, J.-M. Chung, and R. C. Garcia, "Machine-to-Machine communication standardization trends and end-to-end service enhancements through vertical handover technology," in *2012 IEEE 55th International Midwest Symposium on Circuits and Systems (MWSCAS)*. IEEE, 2012, pp. 840–844.

[64] S. Kang, W. Ji, S. Rho, V. A. Padigala, and Y. Chen, "Cooperative mobile video transmission for traffic surveillance in smart cities," *Computers & Electrical Engineering*, vol. 54, pp. 16–25, 2016.

[65] S. N. K. Marwat, Y. Zaki, J. Chen, A. Timm-Giel, and C. Göerg, "A novel machine-to-machine traffic multiplexing in LTE-A system using wireless in-band relaying," in *International Conference on Mobile Networks and Management*. Springer, 2013, pp. 149–158.

[66] J. Zhang, L. Shan, H. Hu, and Y. Yang, "Mobile cellular networks and wireless sensor networks: toward convergence," *IEEE Communications Magazine*, vol. 50, no. 3, pp. 164–169, 2012.

[67] J.-P. Bardyn, T. Melly, O. Seller, and N. Sornin, "IoT: The era of LPWAN is starting now," in *European Solid-State Circuits Conference, ESSCIRC Conference 2016: 42nd*. IEEE, 2016, pp. 25–30.

[68] D. Flore, "3GPP Standards for the Internet of Things," *Qualcomm Technologies Inc.*, 2016.

[69] E. Soltanmohammadi, K. Ghavami, and M. Naraghi-Pour, "A survey of traffic issues in machine-to-machine communications over lte," *IEEE Internet of Things Journal*, vol. 3, no. 6, pp. 865–884, Dec 2016.

[70] R. P. Jover and I. Murynets, "Connection-less communication of IoT devices over LTE mobile networks," in *Sensing, Communication, and Networking (SECON), 2015 12th Annual IEEE International Conference on*. IEEE, 2015, pp. 247–255.

[71] F. Musumeci, C. Bellanzon, N. Carapellese, M. Tornatore, A. Pattavina, and S. Gosselin, "Optimal bbu placement for 5g c-ran deployment over wdm aggregation networks," *Journal of Lightwave Technology*, vol. 34, no. 8, pp. 1963–1970, 2016.

[72] R. Al-obaidi, A. Checko, H. Holm, and H. Christiansen, "Optimizing cloud-ran deployments in real-life scenarios using microwave radio," in *Networks and Communications (EuCNC), 2015 European Conference on*. IEEE, 2015, pp. 159–163.

[73] A. Marotta and L. M. Correia, "A model to evaluate c-ran architectures deployment impact in urban scenarios," in *Broadband Communications for Next Generation Networks and Multimedia Applications (CoBCom), International Conference on*. IEEE, 2016, pp. 1–6.

[74] R. Riggio, D. Harutyunyan, A. Bradai, S. Kuklinski, and T. Ahmed, "Swan: Base-band units placement over reconfigurable wireless front-hauls," in *Network and Service Management (CNSM), 2016 12th International Conference on*. IEEE, 2016, pp. 28–36.

[75] N. Carapellese, M. Tornatore, and A. Pattavina, "Placement of base-band units (bbus) over fixed/mobile converged multi-stage wdm-pons," in *Optical Network Design and Modeling (ONDM), 2013 17th International Conference on*. IEEE, 2013, pp. 246–251.

[76] S. Xu and S. Wang, "Efficient algorithm for baseband unit pool planning in cloud radio access networks," in *Vehicular Technology Conference (VTC Spring), 2016 IEEE 83rd*. IEEE, 2016, pp. 1–5.

[77] N. Carapellese, M. Tornatore, A. Pattavina, and S. Gosselin, "Bbu placement over a wdm aggregation network considering otn and overlay fronthaul transport," in *Optical Communication (ECOC), 2015 European Conference on*. IEEE, 2015, pp. 1–3.

[78] R. Mijumbi, J. Serrat, J.-L. Gorricho, J. Rubio-Loyola, and S. Davy, "Server placement and assignment in virtualized radio access networks," in *Network and Service Management (CNSM), 2015 11th International Conference on*. IEEE, 2015, pp. 398–401.

[79] S. Nanba, N. Agata, N. Nishi, and K. Nishimura, "Geographical constraint-based optimization framework for c-ran design," *Journal of Optical Communications and Networking*, vol. 8, no. 12, pp. B61–B69, 2016.

[80] P. Ferrari, A. Flammini, and E. Sisinni, "New architecture for a wireless smart sensor based on a software-defined radio," *IEEE Transactions on Instrumentation and Measurement*, vol. 60, no. 6, pp. 2133–2141, 2011.

[81] H. Fotouhi, M. Vahabi, A. Ray, and M. Björkman, "Sdn-tap: an sdn-based traffic aware protocol for wireless sensor networks," in *e-Health Networking, Applications and Services (Healthcom), 2016 IEEE 18th International Conference on*. IEEE, 2016, pp. 1–6.

[82] D. Zeng, P. Li, S. Guo, T. Miyazaki, J. Hu, and Y. Xiang, "Energy minimization in multi-task software-defined sensor networks," *IEEE transactions on computers*, vol. 64, no. 11, pp. 3128–3139, 2015.

[83] T. Miyazaki, S. Yamaguchi, K. Kobayashi, J. Kitamichi, S. Guo, T. Tsukahara, and T. Hayashi, "A software defined wireless sensor network," in *Computing, Networking and Communications (ICNC), 2014 International Conference on*. IEEE, 2014, pp. 847–852.

[84] F. Kaup, S. Melnikowitsch, and D. Hausheer, "Measuring and modeling the power consumption of openflow switches," in *Network and Service Management (CNSM), 2014 10th International Conference on*. IEEE, 2014, pp. 181–186.

[85] X. An, F. Pianese, I. Widjaja, and U. Günay Acer, "DMME: A distributed LTE MME," *Bell Labs Technical Journal*, vol. 17, no. 2, pp. 97–120, 2012.

[86] G. Crosby and F. Vafa, "A novel dual mode gateway for wireless sensor network and LTE-A network convergence," *INTERNATIONAL JOURNAL OF ENGINEERING RESEARCH AND INNOVATION*, vol. 5, no. 2, 2013.

[87] G. Horváth, "End-to-End QoS management across LTE networks," in *Software, Telecommunications and Computer Networks (SoftCOM), 2013 21st International Conference on*. IEEE, 2013, pp. 1–6.

[88] T. Innovations, "Lte in a Nutshell:Protocol Architecture," *White paper*, 2010.

[89] A. M. Ghaleb, E. Yaacoub, and D. Chieng, "Physically separated uplink and downlink transmissions in LTE HetNets based on CoMP concepts," in *Frontiers of Communications, Networks and Applications (ICFCNA 2014-Malaysia), International Conference on*. IET, 2014, pp. 1–6.

[90] H. Holma and A. Toskala, *WCDMA for UMTS: HSPA evolution and LTE*. John Wiley & Sons, 2010.

[91] Cisco. (2016) Voice Over IP - Per Call Bandwidth Consumption. [Online]. Available: http://www.cisco.com/c/en/us/support/docs/voice/voice-quality/7934-bwidth-consume.html

[92] S. J. M. Baygi, M. Mokhtari *et al.*, "Evaluation performance of protocols LEACH, 802.15. 4 and CBRP, using analysis of QoS in WSNs," *Wireless Sensor Network*, vol. 6, no. 10, p. 221, 2014.

[93] S. O. Dr. Robert. (2014) Lectures: CSCI 4151 Systems Simulation Class. [Online]. Available: http://www.robertowor.com/csci4151/lecture5.htm

[94] N. Ince and A. Bragg, *Recent Advances in Modeling and Simulation Tools for Communication Networks and Services*. Springer US, 2007. [Online]. Available: https://books.google.co.uk/books?id=pJSqZZmc9_oC

[95] Riverbed_Technology. (2017) "verifying statistical validity of discrete event simulations". [Online]. Available: https://enterprise14.opnet.com/4dcgi/CL_SessionDetail?ViewCL_SessionID=3172,White_Paper_from_OPNET%5cVerifying_Statistical_Validity_DES.pdf

[96] *OpNet Modeling Concepts*, 2007. [Online]. Available: http://suraj.lums.edu.pk/~te/simandmod/Opnet/07%20Simulation%20Design.pdf

[97] ROHDE&SCHWARZ. (2017) 1MA272: Testing LTE-A Releases 11 and 12. [Online]. Available: https://www.rohde-schwarz.com/us/applications/testing-lte-a-releases-11-and-12-application-note_56280-307009.html

[98] 3GPP TS 36.213 V14.2.0 (2017-03). [Online]. Available: https://portal.3gpp.org/desktopmodules/Specifications/SpecificationDetails.aspx?specificationId=2427

[99] A. Sethi and V. Hnatyshin, *The Practical OPNET User Guide for Computer Network Simulation*. Taylor & Francis, 2012. [Online]. Available: https://books.google.co.uk/books?id=3E3wqbSoHQQC

[100] AT&T, Orange, Telefonica, TeliaSonera, Verizon, Vodafone, Alcatel-Lucent, Ericsson, Nokia Siemens Networks, Nokia, Samsung and Sony Ericsson, "One Voice; Voice over IMS profile," vol. 1. 0. 0, 2009-11.

[101] "Technical Specification Group Services and System Aspects; Policy and charging control architecture (Release 10)," *3GPP TS 23.203*, vol. 10.6.0, March 2012.

[102] M. Tabany and C. Guy, "An End-to-End QoS performance evaluation of VoLTE in 4G E-UTRAN-based wireless networks," in *the 10th International Conference on Wireless and Mobile Communications*, 2014.

[103] Cisco, "Cisco Networking Academy Program: IP Telephony v1.0," 2005. [Online]. Available: http://www.hh.se/download/18.70cf2e49129168da015800094781/1341267715838/7_6_Jitter.pdf

[104] S. A. Ahson and M. Ilyas, *VoIP handbook: applications, technologies, reliability, and security*. CRC Press, 2008.

[105] ITU. (2015-06-29) G.107 : The E-model: a computational model for use in transmission planning. [Online]. Available: https://www.itu.int/rec/T-REC-G.107-201506-I/en

[106] A. Clark, G. Hunt, and M. Kastner, "RTCP XR Report Block for QoE Metrics Reporting," 2011.

[107] A. D. Clark, P. D. F. Iee *et al.*, "Modeling the effects of burst packet loss and recency on subjective voice quality," 2001.

[108] B. Belmudez, *Audiovisual Quality Assessment and Prediction for Videotelephony*, ser. T-Labs Series in Telecommunication Services. Springer International Publishing, 2014. [Online]. Available: https://books.google.co.uk/books?id=ULTzBQAAQBAJ

[109] I. GSMA, "IMS Profile for Voice and SMS," 92.

[110] China Mobile, "VoLTE White Paper," 2013.

[111] V. Spirent, "Deployment and the Radio Access Network," *The LTE User Equipment Perspective, White Paper*, 2012.

[112] V. Kachitvichyanukul, "Comparison of three evolutionary algorithms: Ga, pso, and de," *Industrial Engineering and Management Systems*, vol. 11, no. 3, pp. 215–223, 2012.

[113] R. Hassan, B. Cohanim, O. De Weck, and G. Venter, "A comparison of particle swarm optimization and the genetic algorithm," in *46th AIAA/ASME/ASCE/AHS/ASC structures, structural dynamics and materials conference*, 2005, p. 1897.

[114] K. Jahanbin, F. Rahmanian, H. Rezaie, Y. Farhang, and A. Afroozeh, "K-means optimization clustering algorithm based on hybrid pso/ga optimization and cs validity index."

[115] H. J. Son and S. Shin, "Fronthaul size: Calculation of maximum distance between rrh and bbu," *Netmanias Tech-Blog*, 2014.

[116] H. J. Son and M. M. Do, "Mobile network architecture for 5g era—new c-ran architecture and distributed 5g core," *NetManias Tech Blog, Oct. 6, 2015.*, 2015.

[117] J. Ding, V. Tarokh, and Y. Yang, "Bridging aic and bic: a new criterion for autoregression," *IEEE Transactions on Information Theory*, 2017.

[118] J. H. Creighton, *A first course in probability models and statistical inference*. Springer Science & Business Media, 2012.

[119] F. Aurenhammer, R. Klein, and D.-T. Lee, *Voronoi diagrams and Delaunay triangulations*. World Scientific Publishing Company, 2013.

[120] Embit. (2018, June) EMB-Z2530PA-EVK. [Online]. Available: http://www.embit.eu/?s=Z2530PA

[121] A. Carroll, G. Heiser *et al.*, "An analysis of power consumption in a smartphone." in *USENIX annual technical conference*, vol. 14. Boston, MA, 2010, pp. 21–21.

[122] V. Sivaraman, A. Vishwanath, Z. Zhao, and C. Russell, "Profiling per-packet and per-byte energy consumption in the netfpga gigabit router," in *Computer Communications Workshops (INFOCOM WKSHPS), 2011 IEEE Conference on*. IEEE, 2011, pp. 331–336.

[123] F. Farouk, R. Rizk, and F. W. Zaki, "Multi-level stable and energy-efficient clustering protocol in heterogeneous wireless sensor networks," *IET Wireless Sensor Systems*, vol. 4, no. 4, pp. 159–169, 2014.

[124] Texas Instruments Incorporated. (2013, apr) AN-1540 Power Measurement of Ethernet Physical Layer Products. [Online]. Available: http://www.ti.com/